Order Number 9029969

Aspects of helicity in turbulent flows

Polifke, Wolfgang Herbert, Ph.D.

City University of New York, 1990

U·M·I
300 N. Zeeb Rd.
Ann Arbor, MI 48106

H

ASPECTS OF HELICITY IN TURBULENT FLOWS

by

WOLFGANG POLIFKE

A dissertation submitted to the Graduate Faculty in Physics in partial fulfillment of the requirements for the degree of Doctor of Philosophy, The City University of New York.

1990

This manuscript has been read and accepted for the Graduate Faculty in Physics in satisfaction of the dissertation requirement for the degree of Doctor of Philosophy.

4/17/90
Date

Chair of Examining Committee

4/23/90
Date

Executive Officer

Supervisory Committee

The City University of New York

Abstract

ASPECTS OF HELICITY IN TURBULENT FLOWS

by

Wolfgang Polifke

Adviser: Professor Andreas Acrivos

Helicity, the scalar product of velocity and vorticity, is a quantity of great potential significance for our understanding of turbulent flows, as it possesses a number of intriguing properties related to the nonlinear dynamics and the structure of turbulent flows. In this study we investigate several aspects of helicity via direct numerical simulations of decaying and quasi-stationary turbulent flows: The influence of helicity on the energy transfer and the nonlinearity, the statistics and dynamical significance of helicity fluctuations, and the relation of helicity to the local 'entangledness' of vortex lines.

A new initialization and forcing procedure has been developed, which allows to control the mean helicity in numerical simulations of turbulence. It is observed in agreement with earlier work by Andre & Lesieur (J. Fluid Mech. **81**, 1977), that strong mean helicity impedes the transfer of energy towards smaller scales, depresses the nonlinearity of a turbulent flow, and reduces dissipation in decaying turbulence.

A random-phase or quasi-Gaussian approximations (QGA) is employed to gauge the fluctuations of helicity observed in simulations of turbulent flows. It is shown that the QGA is compatible with Kolmogorov-type scaling arguments supplemented by elementary statistical considerations. Sweeping effects on helicity fluctuations are discussed. In decay-

ing and stationary flows with small mean helicity it is found that the fluctuations of the helicity of the large scales are well described by the QGA, and as such not strong enough to directly influence the energy transfer. No evidence of an inverse cascade of mean-square helicity (Levich & Tsinober, Phys. Lett. A **93**, 1983) was found. The helicity of the small scales is observed to fluctuate anomalously, i.e. stronger than Gaussian, which indicates the presence of small scale phase coherence. However, the nature of the observed fluctuations suggests that the adiabatic invariance of helicity fluctuations at large Reynolds numbers is not the cause of the phase coherence (Levich, Phys. Rep. **151**,1987, and Levich & Shtilman, Phys. Lett. A **126**, 1988). The mechanism of the depression of nonlinearity in isotropic turbulence (Kraichnan & Panda, Phys. Fluids **31**, 778, 1988) is investigated. It is found that the main source of the depression in non-helical flows is a tendency of the Lamb vector to develop a significant potential component. The possibility of probing the local structure or 'entangledness' of the vorticity field of turbulent flows with an appropriately defined 'relative helicity' (Levich, Phys. Rep. **151**, 1987) is discussed. Preliminary numerical results show a correlation of entangledness with turbulent activity.

Acknowledgments

I am indebted to Evgeny Levich, who played a central role in the development of many of the ideas and concepts that are scrutinized in this dissertation. Indeed, he initiated this work, and much of what is investigated here has been the subject of earlier studies by Evgeny, or has been brought to my attention by him. Thanks also for spirited discussions and clarifying comments. Financial support was provided by D.O.E. grant No. NE-FG0288ER13837. Many thanks to Leonid Shtilman, with whom I collaborated closely during the first year of my thesis work. Leonid taught me the tricks of the supercomputing trade, and repeatedly lured me with free dinner on late-night 'bug hunts'. We stayed in contact even after Leonid left the Levich Institute, and I greatly appreciate his help in putting the finishing touches on this work. I feel that I have profited enormously from my stay at the Center for Turbulence Research at Stanford/NASA Ames. I am grateful to Parviz Moin for making it possible, and to Mike Rogers, Bob Moser, Alan Wray and Bob Rogallo for their expert help and their willingness to put up with my numerous questions. Mark Nelkin, Alexander Frenkel and Keith Moffatt contributed greatly through discussions and very detailed and helpful comments on draft versions of this thesis.

The members (past and present) of the Levich Institute deserve special mention for making this place so supportive, inspiring and fun (sic). I am especially grateful to the Institute's Director, Andreas Acrivos, whose help and encouragement were invaluable in completing this work.

I also want to thank Drs.-to-be Marianne Sommer and Martin Muschol, who joined me on the long journey to New York and through Graduate School. Without them it would have been a lot harder. Very special thanks to Birgitte and my family for their love, support and understanding.

Contents

List of Figures

List of Tables

Chapter 1

Introduction

Turbulence, i.e. temporally and spatially irregular flow of fluids, is ubiquitous in nature and technology. It may be found in fields of science and engineering as diverse as cardiovascular medicine and astrophysics, aerodynamics and chemical engineering. The incompressible Navier-Stokes equation (NSE),

$$\frac{\partial}{\partial t}\vec{v} + (\vec{v}\cdot\nabla)\vec{v} = -\frac{1}{\rho}\nabla p + \nu\nabla^2\vec{v}, \tag{1.1}$$

$$\nabla\cdot\vec{v} = 0,$$

is believed to adequately describe many features of turbulent flows. Here $\vec{v}(\vec{x},t)$ is the Eulerian velocity field, $p(\vec{x},t)$ the pressure, ν the kinematic molecular viscosity and ρ the density of the fluid. The only dimensionless parameter is the Reynolds number $R = UL/\nu$, where L is the typical size of the largest scales of the flow and U the typical velocity of those scales. Simple dimensional reasoning yields

$$\frac{|(\vec{v}\cdot\nabla)\vec{v}|}{|\nu\nabla^2\vec{v}|} \sim R, \tag{1.2}$$

i.e. the Reynolds number is a measure of the nonlinearity of a flow. Reynolds numbers of fully turbulent flows are very large; values of order 10^6 and much greater are not uncommon in nature.

Although the Navier-Stokes equation has been known since early in the last century, and O. Reynolds began his pioneering studies in turbulence more than 100 years ago, one may certainly not claim that the problem of turbulence has been solved; there is not even

consensus among turbulence researchers what would constitute such a solution. Nevertheless, there is great activity in the field and impressive advances have been made. The mere volume of the work of Monin & Yaglom (1975), where many of the results of modern turbulence research are compiled, may testify to this statement. More introductory and accessible texts on the subject are Batchelor (1953), Tennekes & Lumley (1972), Orszag (1977), Landahl & Mollo-Christensen (1986), Landau & Lifshitz (1987) and Stanišić (1988).

Fully developed turbulent flows extend over a very wide range of scales. Correspondingly, the number of active degrees of freedom is tremendously large; indeed it scales as the 9/4th power of the Reynolds number. It was thus suggested by O. Reynolds and G.I. Taylor that statistical methods should provide an adequate description of turbulent flows. Why has this approach met only with limited success ?

Firstly, the well known 'closure problem' - caused by the nonlinear nature of the Navier-Stokes equation - makes it impossible to obtain closed equations of motion for mean quantities and correlation functions without invoking additional assumptions and approximations. However, devising a sound closure model from first principles has proven to be a very difficult problem, because the nonlinearities in the NSE are very strong and they continuously involve many degrees of freedom from a wide range of scales. Furthermore, turbulence is strongly dissipative. Therefore, many powerful methods from statistical mechanics are not applicable to turbulence. Arguably the most successful attempt in this direction is Kraichnan's (1959,1977) 'Direct Interaction Approximation', which employs renormalized perturbation techniques borrowed from quantum field theory, and its various derivatives, e.g. Orszag's (1970) 'Eddy Damped Quasi-Normal Markovian' model. Unfortunately, it is very hard to apply these approximation schemes to 'real', i.e. inhomogeneous, flows.

Another shortcoming of statistical descriptions of turbulent flows in terms of low-order moments is the inability of these methods to capture the intermittent structure of the small scales of turbulence. Since Landau's remark concerning the intermittent distribution of dissipation, and the resulting corrections to the power-law of the inertial range energy spectrum (Landau & Lifshitz, 1987), much effort has been devoted to experimental and theoretical investigations of the (multi-) fractal structure of turbulence. We refer to Meneveau & Sreenivasan (1987) and references therein.

Furthermore, mean quantities (mean velocity, mean rate of dissipation, mean heat flux, etc.), and their higher order equivalents, e.g. the correlation functions, are inappropriate for the description of some of the most intriguing aspects of turbulent flows, e.g. their spatial structure. For example, in the pioneering study by Kline *et al.* (1967) the near-wall region of a turbulent boundary layer was investigated with flow-visualization techniques. It was found that low-speed streaks of fairly regular spanwise spacing exist, which begin to oscillate intermittently and break up in a violent 'burst'. Remarkably, about 70 % of the total turbulence production is associated with the bursts (Kim *et al.* ,1971).

It is now commonly accepted that many turbulent flows possess *structure*, see for example Cantwell (1981) and Tsinober & Levich (1983b), where a wide variety of experimental observations is compiled. It is also widely believed that 'coherent structures' are dynamically significant. Unfortunately, there is little agreement as to what the adequate conceptual or mathematical description of such structures should be.

For example, Lumley (1967) has suggested to identify coherent structures with a set of optimal orthogonal eigenfunctions. Lumley's eigenfunctions are optimal in the sense that a finite mode reconstruction of the turbulent velocity field based on them retains more of the kinetic energy than any other finite mode reconstruction of equal order. The eigenfunctions are obtained through a technique known as 'proper orthogonal decomposition', where one maximizes the average projection on the turbulent field of each eigenfunction. Other authors (see Cantwell, 1981) have attempted to gain insight into the organized motion of large eddies by measuring long-time-averaged spatial correlation functions. Alternatively, Hussain (1985) has developed a technique of successive conditional averaging whereby one 'educes' vortical coherent structures from a fluctuating background field. Yet other methods based on 'conditional sampling' and 'stochastic estimation' are discussed in Adrian (1988).

A common feature of many of the above studies is that emphasis is put on defining, describing or detecting 'structures'. It is not understood whether structures are merely a result of 3- dimensional instabilities of a large scale mean flow, or whether they are universal and intrinsic to all turbulent flows, i.e. also homogeneous and isotropic ones. Attempts to predict the appearance of structures from first principles, i.e. the Navier-Stokes equation, have in general not been successful.

This is not quite so in two dimensional turbulence, where the vorticity $\vec{\omega} = \nabla \times \vec{v}$ is conserved by the nonlinear terms of the 2-D Navier-Stokes equation. It follows that there exists a second inviscid integral invariant besides the energy $E = 1/2 \int_V v^2 d\vec{x}$, i.e. the enstrophy $\Omega = 1/2 \int_V \omega^2 d\vec{x}$. The conservation of enstropy by the inviscid terms of the two dimensional NSE is understood to be at least partially responsible for the overall structure of 2-D turbulence (Santangelo *et al.* , 1989, and references therein). Most intriguing, in forced 2-D turbulence, the inviscid conservation of enstrophy leads to an 'inverse cascade' of energy (Kraichnan, 1967, Frisch & Sulem, 1984), i.e. a transfer of energy towards larger scales.

In three dimensions, there also exists another inviscid integral invariant besides the energy: the helicity $H = \int \vec{v} \cdot \vec{\omega} \, d\vec{x}$. Levich & Tsinober (1983a,1983b), Levich (1987) and Moffatt (1985) have proposed scenarios of turbulent flows, where helicity determines (or is at least intimately linked to) a universal structure of 3-dimensional turbulence. Before we outline these scenarios, let us review basic properties of helicity and some of the earlier work on its possible significance to turbulence.

1.1 Properties of Helicity

Helicity possesses a number of intriguing properties and has been the subject of a series of theoretical, numerical and experimental investigations. The first reference to helicity in the context of turbulence was made by Betchov (1961). He considered the general form of the two point velocity correlators in 'semi-isotropic' turbulence, i.e. turbulence that is invariant under rotations but not necessarily under reflections:

$$\langle v_i(\vec{x}) v_j(\vec{x} + \vec{r}) \rangle = \langle v^2 \rangle \left(\frac{b_{rr}(r) - b_{tt}(r)}{r^2} r_i r_j + b_{tt} \delta_{ij} + \epsilon_{ijk} g(r) r_k \right). \tag{1.3}$$

The scalar functions b_{rr} and b_{tt} are the well-known longitudinal and transversal correlation functions. The last term on the r.h.s is not invariant under reflections (it is antisymmetric in i, j) and related to the average of the helicity density $\gamma(\vec{x}) = \vec{v}(\vec{x}) \cdot \vec{\omega}(\vec{x})$ by

$$\langle \gamma(\vec{x}) \rangle = -6g(0). \tag{1.4}$$

Obviously, helicity is a pseudo-scalar fundamentally related to the symmetry properties of a turbulent flow. To quote Betchov (1961), one may think of the contents of a box of nails after

vigorous mixing as an example of an isotropic medium. A box of ordinary screws would then serve as an example of a helical or 'semi-isotropic' medium. Unfortunately, Betchov omitted some terms in the general expression for the semi-isotropic third order correlation functions and erroneously concluded that there is no nonlinear transfer of helicity (Equations (2) and (8) in his paper). (Note also that it has become customary to refer to both 'semi-isotropic' and 'isotropic' flows simply as 'isotropic'. Therefore, we shall in the following use the former only when necessary.)

Moreau (1961) and independently Moffatt (1969) showed that the total helicity $H = \int_D \vec{v} \cdot \vec{\omega} d\vec{x}$ of a localized vortex tangle is a measure of the degree of 'knottedness' of the vortex lines. (It is essential here that the vorticity distribution is localized, i.e. the vorticity $\vec{\omega}$ at the surface ∂D of the domain D either vanishes or is tangential to the surface.) In inviscid flows with conservative body forces the vortex lines are 'frozen' in the fluid, and consequently their linkages are conserved. It follows that helicity is an inviscid invariant of the Navier-Stokes equations. This may also be seen directly by considering the helicity balance equation for a material volume V in the case $\nu = 0$:

$$\frac{dH}{dt} = \int_{\partial V} (\frac{v^2}{2} - \frac{p}{\rho}) \vec{\omega} \cdot \hat{n} \, dA + \nu \int_V (\vec{v} \cdot \nabla^2 \vec{\omega} + \vec{\omega} \cdot \nabla^2 \vec{v}) \, d\vec{x}. \tag{1.5}$$

The integral over the surface vanishes because by assumption no vortex lines penetrate the surface. The connection of helicity with the topology of the vorticity field rests on a sound mathematical footing, as the helicity may be indentified with the so-called 'asymptotic Hopf - invariant' (see Arnol'd, 1974, and the review article by Moffatt, 1981).

In a series of papers Frisch and his collaborators and Kraichnan investigated whether helicity imposes - in close analogy with the role of enstrophy in two dimensions - constraints on the dynamics of a turbulent flow, in particular the energy cascade. Using simple phenomenological and dimensional arguments, Brissaud *et al.* (1973) suggested the possibility of a pure helicity cascade and the resulting modification of the power-law exponent of the energy spectrum in a Kolmogorov-type inertial range. It was also speculated that simultaneous injection of energy and helicity at intermediate wave numbers might lead to transfer of helicity to larger wave numbers and transfer of energy to smaller wave numbers, i.e. an inverse cascade of energy. However, Kraichnan (1973) discussed the absolute equilibrium statistics of a truncated (in k-space) model of 3-D helical turbulence and argued that 'the

inertial range energy cascade in isotropic turbulence driven by helical input should not differ asymptotically from that of non-helical turbulence'. Note that this method, applied to a truncated model of 2-D turbulence suggested the existence of an inverse cascade of energy in two dimension (Kraichnan 1967). Kraichnan (1973) also investigated analytically the interaction of two helical waves and concluded that the presence of mean helicity in a turbulent flow should inhibit the energy transfer to the small scales. There is a simple argument credited to S. Patterson and W.V. Malkus in support of this conclusion: if the total helicity H is large, the velocity $\vec{v}$ and the vorticity $\vec{\omega}$ will tend to align, consequently the nonlinear term $\vec{v} \times \vec{\omega}$ responsible for the energy transfer will be small.

Numerical simulations of a Markovian variant of Orszag's (1970) eddy-damped quasi-normal theory essentially vindicated Kraichnan's arguments (Frisch *et al.* ,1975 and André & Lesieur, 1977). It was observed that simultaneous injection of energy and helicity leads to a cascade of both energy and helicity to large wave numbers. With increasing wave numbers the normalized helicity (see Section 3.1 for definitions) tends to zero and helicity is carried along locally and linearly with the energy cascade like a passive scalar.

The simultaneous cascade of energy and helicity towards smaller scales is possible because the energy imposes only an upper bound on the magnitude of the helicity spectrum, i.e. $|H(k)| \leq 2kE(k)$, whereas the enstrophy spectrum $\Omega(k)$ is uniquely determined by the energy spectrum, $\Omega(k) = k^2 E(k)$. One might argue qualitatively that the constraints in the 2-D case are more severe because the (global) conservation of enstrophy is really the consequence of a *local* conservation law, i.e. in 2-dimensional Euler flows the vorticity of each fluid element is conserved. There is no such local conservation of the energy density or the helicity density γ (Note that 'linkage properties' cannot be defined locally). Consequently, when investigating the relation of helicity to the dynamics or the structure of three-dimensional flows, one should not expect to find close analogies with the situation in two dimensions.

It was also confirmed by André & Lesieur (1977) that the presence of significant mean helicity reduces the cascade of energy to the small scales, and that viscosity can lead to creation of total helicity. The latter was expected because the viscous term in the helicity balance equation (1.5) is of indefinite sign. The link between mean helicity and the nonlinear

transfer of energy can play an important role in atmospheric turbulence, i.e. it may stabilize certain types of storms (Lilly, 1986), and has motivated the inclusion of helicity as an additional subgrid parameter in large eddy simulations (Lautenschlager *et al.* , 1987).

1.2 Topology, Helicity and the Structure of Turbulence

The investigations discussed in the previous section indicate that the constraints imposed by the inviscid invariance of helicity are of a different nature than those imposed by the invariance of enstrophy in the two dimensional case. In this section we will discuss further work on the possible connection between the dynamics and structure of turbulent flows and helicity, stimulated by the fact that helicity is closely related to the topology of the vorticity field.

In particular, Levich (1983) argued for the existence of 'topological solitons' of non-zero helicity in turbulent flows. The argument is essentially based on the observation that a localized vortex structure of nonzero helicity (i.e. with linked vortex lines) can only be represented by multi-valued Clebsch-potentials (Lamb, 1931). In this representation, there are no non-singular transitions from one state of linkage to another; this presumably endows linked vortex tangles with great dynamical stability.

This concept was extended in Levich & Tsinober (1983a), where it was suggested that in a turbulent flow helical solitons, i.e. entangled vortex structures with coherent helicity, should exist *on all scales*. The volume-integral $I = \int_V \langle \gamma(\vec{x})\gamma(\vec{x}+\vec{r})\rangle d\vec{r}$ over the two-point correlation function of the helicity density was found to be an inviscid invariant ('I-invariant'), which defines a length scale $\mathcal{L} = I/\tilde{E}^2$ intrinsic to turbulent flows in the sense that it does not depend on external length scales in an obvious way. Because I is conserved by the nonlinear terms of the NSE, it was argued to be subject to an upscale cascade, much like the inverse cascade of energy in two dimensions. It was concluded that
(1) 'Typical realizations of (homogeneous and isotropic) turbulent flow generally should have violated global reflectional symmetry and have, consequently, vastly complicated topological structures.'
(2) 'The existence of inverse cascades (in homogeneous turbulence the cascade of I) forms the basis for the birth and existence of organized structures and thus the tendency for

self-organization in three-dimensional turbulence.'

In Levich & Tsinober (1983b) possible implications for the fractal structure of turbulent flows and for renormalized perturbation group approaches were discussed. The central idea is that a hierarchy of helical fluctuations (structures) in the turbulent flow field organizes the geometry of the fractal. These fluctuations serve as a mechanism of long-range order in turbulence, inhibiting the cascade of energy to the small scales. Confronted with new experimental and numerical evidence (see below), it was later acknowledged that coherent structures and helicity fluctuations are not necessarily long-lived (Levich, 1987). Levich & Shtilman (1988) argued further that in a decaying fully developed turbulent flow the inviscid conservation of I during the decay process strongly favors the build-up of phase coherence, which accounts for the presence of strong fluctuations of helicity and large-scale helical structures. Phase coherence might also lead to an increase in the correlation length of helicity density fluctuations in physical space. It was suggested (Levich & Shtilman,1988, Kit *et al.* , 1988) that this might in turn result in a spontaneous breaking of reflexional symmetry. A more detailed discussion of these concepts is given in Chapter 4.

Moffatt (1985) arrived at a somewhat similar scenario, although from a very different starting point. He considered - exploiting the well-know analogy between the Euler equations for steady flow and the equations of magnetostatic equilibrium in a perfectly conducting fluid - the topology of the velocity field of steady Euler flows. Using the technique of 'magnetic relaxation' (Arnol'd, 1974), Moffatt demonstrated the existence of steady Euler flows that are 'topologically accessible' from velocity fields $\vec{v}_0(\vec{x})$ with *arbitrarily* prescribed topology. In particular, if the streamlines of $\vec{v}_0(\vec{x})$ are ergodic, the corresponding steady Euler flow contains 'blobs' of maximal helicity (i.e. the velocity is parallel or anti-parallel to the vorticity), separated by regular surfaces. Viscous effects aside, steady Euler flows may be regarded as (unstable) fixed points in the phase space of the Navier-Stokes equation, and one may assume that a turbulent flow evolves in the neighborhood of an Euler flow (or a succession of Euler flows). This implies that coherent structures in turbulence should be identified with the helical 'blobs', whereas strong turbulent activity and dissipation is confined to the surfaces (vortex sheets) that separate the helical regions. The vortex sheets are subject to Kelvin-Helmholtz instability, which can in principle lead to a $k^{-5/3}$ inertial

range.

Levich (1987) notes that Moffatt's scenario should be endowed with a self-similar structure, arguing that regions of positive and negative helicity will form a self-similar hierarchy on all scales throughout the inertial range. The vortex sheets that separate the helical fluctuations are then convoluted on all scales, i.e. they form a fractal.

1.3 Numerical and Experimental Results

What is the experimental and numerical evidence in regard to the above speculations concerning the (helical) structure of turbulence? A wide variety of experimental observations of coherent structures in turbulent flows is reviewed by Tsinober & Levich (1983b), with the conclusion that three-dimensional coherent structures typically possess coherent helicity. However, the authors emphasize that most of the reviewed experiments were performed at transitional or rather low Reynolds number. They allow for the possibility that the observed coherent structures are the results of three-dimensional instabilities and will not survive in fully developed turbulence. It is acknowledged that so far there is no experimental evidence of helical coherent structures in homogeneous, isotropic turbulence.

In Levich & Tzvetkov (1985) it is reported that the concepts of helicity fluctuations and in particular the inverse cascade of the I-invariant may be fruitfully applied to a large class of mesoscale atmospheric phenomena. Lilly (1986), on the other hand, investigates the effects of (mean) helicity on the energy transfer and viscous dissipation in rotating convective storms without invoking the concept of an inverse cascade. He identifies a mechanism of helicity creation (vortices coinciding with updraft) that is clearly a consequence of the very special boundary and forcing conditions of the storm types under consideration.

Moffatt (1985) has remarked that a crucial test of the ideas concerning the importance of helicity in the organization of coherent structures would be to check whether high normalized helicity density $h = |\vec{v} \cdot \vec{\omega}|/(|v||\omega|)$ correlates with high dissipation in a turbulent flow. Pelz *et al.* (1985) and Shtilman *et al.* (1985) investigated the statistics of the normalized helicity density in direct numerical simulations of channel flow and Taylor-Green vortex flow. In presumed support of the above concepts, it was observed that in regions of low dissipation the velocity and vorticity vector indeed have a tendency to align. Direct

numerical simulations of isotropic decaying turbulence (Pelz *et al.* 1986) 'exhibit clearly that much of the flow evolves in orientation to a state in which the velocity vector is nearly aligned with the vorticity vector'. It was reported, though, that the tendency to align is not as strong as in the Taylor-Green case, and no quantitative results concerning the correlation with dissipation are given. Numerical simulations of homogeneous flows and fully developed turbulent channel flows at significantly higher resolution than the earlier computations by Pelz and Shtilman were performed by Kerr (1987) and Rogers & Moin (1987). Investigating the statistics of the (normalized) helicity density, the authors came to the conclusion that isotropic flows are only slightly helical, that the presence of mean strain suppresses helical behavior, and that there is *no* correlation between normalized helicity density and viscous dissipation of turbulent kinetic energy. However, it had been realized in the meantime that the (normalized) helicity density γ (or h) is not adequate to characterize fluctuations of helicity; see the review by Levich (1987) and also the work by Speziale (1987), who pointed out that h is not Galilean invariant. In order to circumvent the problem of Galilean invariance, Levich & Shtilman (1988) concentrated in their analysis of high resolution DNS of decaying isotropic non-helical turbulence on Fourier space quantities. It was reported that the helicity spectrum $H(k)$ and the normalized helicity density h of Fourier transformed wave-packets ('filtered fields') display large fluctuations. The authors conclude that these fluctuations are remnants of the phase correlations generally favored by turbulent dynamics.

Kit *et al.* (1987) have attempted to measure directly the helicity density in a turbulent flow behind a grid. Remarkably, they observed that the decaying flow develops significant mean helicity, i.e. histograms of h (the cosine of the angle θ between the velocity and the vorticity) are skewed This occured although the experiments were performed under reflexionally symmetric boundary conditions. Note however, that the experimental inaccuracy in the determination of the vorticity is rather large; isotropy relations for velocity derivatives are satisfied only within about 30%. Wallace & Balint (1990) have recently conducted similar experiments in a variety of turbulent flows. Althought their measurements do not seem to be more precise than those of Kit *et al.* , the agreement with the numerical simulations by Rogers & Moin (1987) is surprisingly good. In particular, no significant correlations with dissipation have been observed. Wallace & Balint also report that the normalized helicity

density is not always large within three dimensional coherent structures. For example, in turbulent shear flow the velocity and vorticity vectors tend to be aligned in regions where organized vortices have axes at least partially aligned with the mean flow. The opposite is true if the vorticity vector is nearly orthogonal to the mean flow, i.e. near the walls. It is also argued that experimentally observed asymmetries in the distribution of h can be easily explained by residual and spurious values of mean vorticity and velocity, which are caused by probe misalignment. Correcting numerically for probe misalignment yields histograms of h that are nearly flat. These findings are not undisputed: Dracos *et al.* (1990) claim that observed mean helicity is not caused by experimental inaccuracies – and their measurements seem to be the most precise to date (isotropy relations for velocity derivatives are satisfied within about 15%). Dracos *et al.* (1990) present plots of helicity spectra that clearly display broken reflexional symmetry, i.e. non-zero mean helicity at the large scales of a turbulent flow behind a grid. Clearly, presently available experimental evidence concerning the role of helicity in turbulent flows is still ambiguous, and more work is needed in this area before definite conclusions may be made.

1.4 Outline of the Thesis

In the previous Sections we have outlined several facets of the role of helicity in turbulence. In this work, we have concerned ourselves mainly with three problems: the influence of helicity on the energy transfer and the nonlinear terms of the NSE, the statistics of helicity fluctuations, and the possibility of using 'relative helicity' (see below) as a measure of the local 'entangledness' of vorticity field lines.

As our analysis rests heavily on results obtained by direct numerical simulation of turbulent flows, we have devoted the next chapter to a discussion of purely computational questions. In particular, we shall outline the overall structure of a 'pseudospectral' algorithm, and discuss its most essential elements, i.e. the Fourier transform routines, the dealiasing scheme and the time-stepping scheme.

The influence of mean helicity on decaying and quasi-stationary homogeneous turbulence is investigated in the third chapter. In the simulations reported there we employ a new initialization procedure which allows to control both the energy and the helicity spectrum

of the initial flow field. The initialization procedure may also be modified to provide a (helical) random forcing for simulations of quasi-stationary homogeneous turbulence. In good agreement with the results of André & Lesieur (1977) it is observed that strong mean helicity impedes the transfer of energy towards smaller scales, depresses the mean-square nonlinear term and inhibits the buildup of enstrophy and reduces dissipation in decaying flows. The results for forced helical flows are similar.

The statistics of helicity fluctuations in decaying and stationary turbulence are the subject of Chapter 4. It is found that in simulations with vanishing mean helicity the fluctuations of the average helicity $\bar{H}$ and the helicity spectral density $H(k)$ at small wave numbers are surprisingly well described by a simple quasi-Gaussian or random-phase approximation. There is no evidence of a build-up of phase coherence at large scales. This indicates that at moderate Reynolds number spontaneous fluctuations of helicity are not large enough to directly influence the energy transfer. We did observe significant deviations from the quasi-Gaussian approximation for the helicity fluctuations at the small scales; suggesting the presence of phase-coherence. However, the nature of the observed fluctuations indicates that the adiabatic invariance of I is not the cause of the phase coherence. It is also shown that the quasi-Gaussian approximation is equivalent to Kolmogorov-type similarity arguments supplemented with elementary probability theory. Possible modifications of this approximation due to sweeping effects are discussed.

The work presented in Chapter 5 was motivated by a paper by Kraichnan & Panda (1988), where it was observed that simulations of decaying isotropic turbulence exhibit depression of the mean-square nonlinear term to 57 % of the value of a Gaussianly distributed velocity field. Kraichnan & Panda argued that a slight increase in the mean-square helicity density observed in the simulations may not be specifically associated with the depression of nonlinearity. Indeed, we have found that the Fourier transform of the nonlinear term exhibits a peculiar structure, which seems to be the major cause of the depression.

We conclude with some work related to the topological properties of helicity. As mentioned above, the total helicity $H = \int_V \vec{v} \cdot \vec{\omega} dV$ of a *localized* vorticity distribution ($\vec{\omega} \cdot \hat{n}|_{\partial D} = 0$) can be associated with the knottedness of the vortex lines. However, no absolute measure of topological complexity exists for open field structures. Berger & Field

(1984) have demonstrated that the difference between the total helicity of the vorticity field $\vec{\omega}$ and that of a suitable reference field $\vec{\omega}'$ can provide a topologically meaningful and gauge-invariant relative measure of the entangledness of the vortex lines in an open subdomain D. We discuss the properties of a related measure of local 'entangledness', the relative helicity $H_R = \int_D \vec{v} \cdot (\vec{\omega} - \vec{\omega}')dV$ (Levich, 1987). In an analysis of vorticity fields obtained from direct numerical simulations of homogeneous turbulent flows it is found that the vorticity field shows indeed a more complex structure in regions of high relative helicity. Also, statistical correlations between relative helicity and turbulent activity have been observed. Implications for the above mentioned scenarios of coherent structures in turbulence are discussed briefly.

Studies of the turbulence in strongly interacting systems come across a number of generally known difficulties. Therefore it is important to overcome some of these difficulties.

R. Z. Sagdeev, Theory of Strong Turbulence and Topological Solitons (1986)

If this discourse appears to be too long to be read at one sitting, it may be split into six parts.

René Descartes, Discourse on Method (1637)

Chapter 2

Numerical Details

In performing numerical work or storing and processing experimental data, computers have become indispensable for both theoretical analysis and laboratory experiment in the 40-odd years since the development of the first 'electronic brain'. More than that, computers have enriched the scientific arsenal with a conceptually new and powerful tool: the computer simulation. The possibility of exploring the behavior of a system by numerical simulation has led to true breakthroughs and fascinating discoveries. This is especially so for nonlinear phenomena, which are generally unyielding to traditional methods of analysis. Furthermore, numerical simulations have spawned new branches of mathematics and analysis, and they have opened new perspectives in interpreting experimental observations.

This study, too, is based to a large extent on results obtained from computer simulations, i.e. direct numerical simulations (DNS) of homogeneous isotropic turbulent flows. However, we were not concerned with the development of a new computational algorithm. The structure of the simulation program used in this study was outlined by Orszag (1971) in its essential elements almost 20 years ago. Although the algorithm has been improved in some aspects - most notably see the work of Rogallo (1984) - one is certainly justified in asserting that the advances in the direct numerical simulation of homogeneous isotropic turbulent flows are mostly due to improvements in computer technology. This is because turbulence is a phenomenon that involves a wide range of scales, i.e. a large number of degrees of freedom. The goal of direct numerical simulations is to faithfully represent all relevant degrees of freedom, without making use of any turbulence model or 'subgrid model', as they are called in numericists' parlance. To simulate developed turbulent flows requires tremendous

amounts of computer memory, and the development of better algorithms cannot overcome this fundamental obstacle. The amount of memory available on modern supercomputers allows direct numerical simulation of homogeneous turbulent flows at Reynolds numbers of about 500 with relative ease. These simulations reproduce correctly many of the low-order single-point statistical characteristics of moderately turbulent laboratory flows.

Unfortunately, according to Landau (Landau & Lifshitz, 1987) the number of relevant degrees of freedom is proportional to the 9/4th power of the Reynolds number. This implies that however spectacular advances in computer technology will be, the range of Reynolds numbers accessible to direct numerical simulations will remain rather limited. It would be completely wrong though to conclude that numerical turbulence research has entered a dead end. On the contrary, in the interplay with subgrid modeling, laboratory experiments and theory, direct numerical simulations have led to a wealth of new and exciting results, see for example Rogallo & Moin (1984), Aref (1985) and Moin (1987,1988). DNS are indispensable inasmuch as they yield data that are simply not available from laboratory experiments. Most advantageous, they provide detailed information about the dynamics in momentum space, which is appropriate for the formulation of most modern analytical theories of turbulence. Let us turn our attention now to some of the details of the program used in this study.

2.1 The Pseudospectral Method

It is standard practice to model statistically homogeneous turbulence as 'flow in a periodic box', i.e. one solves the Navier-Stokes equation in a cubic computational domain of side length L with the boundary condition

$$\vec{v}(0, x_2, x_3) = \vec{v}(L, x_2, x_3), \tag{2.1}$$

and similarly for the x_2 , x_3 direction. The boundary conditions make the problem ideally suited for a class of numerical approximation schemes known as 'Galerkin methods' or 'spectral methods'. Extensive references may be found in the recent monograph by Canuto *et al.* (1988), we also want to draw attention to articles by Orszag (1971), Patterson & Orszag (1971) and Rogallo (1984). These methods, which are extensively used for numerical

simulations of flows with simple boundaries, are generally applicable to partial differential equations of the type

$$\frac{\partial a(x,t)}{\partial t} = f(a(x,t),x,t), \tag{2.2}$$

with suitable boundary and smoothness conditions. The method is based on a truncated series expansion of the solution $a(x,t)$ in a set of orthogonal functions $\{g_n(x)\}$, $(g_n, g_m) = \delta_{n,m}$, i.e.

$$a(x,t) = \sum_{n=1}^{N} \tilde{a}_n(t) g_n(x). \tag{2.3}$$

Forming the inner product of the partial differential equation (2.2) with one of the basis functions g_n yields a system of ordinary (coupled, nonlinear) differential equations for the expansion coefficients $\tilde{a}_n(t)$:

$$\frac{d}{dt}\tilde{a}_n(t) = (g_n \ , \ f(\sum_{m=1}^{N} \tilde{a}_m(t) g_m)). \tag{2.4}$$

Ideally, if N is sufficiently large, one can achieve what is called 'spectral accuracy', i.e. the magnitude of neglected terms $\tilde{a}_n g_n$, $n > N$, decays faster than any power of n. This property makes spectral methods in principle superior to finite difference schemes.

For the flow in a periodic box, we expand the velocity field $\vec{v}(\vec{x},t)$ in a discrete Fourier series

$$\vec{v}(\vec{x},t) = \sum_{\|\vec{k}\|<K} \vec{v}(\vec{k},t) \exp\{i\vec{k}\cdot\vec{x}\}, \tag{2.5}$$

where $\|\vec{k}\| < K$ means $|k_i| < K$, $i = 1,2,3$, $K = N/2 - 1$, and N is equal to the number of grid points in one direction.

It is computationally advantageous to work with the rotational form of the NSE :

$$\frac{\partial}{\partial t}\vec{v}(\vec{x},t) = \vec{\lambda}(\vec{x},t) - \nabla\tilde{p}(\vec{x},t) + \nu\nabla^2\vec{v}(\vec{x},t). \tag{2.6}$$

$\vec{\lambda} = \vec{v} \times \vec{\omega}$ is the Lamb vector, $\tilde{p} = p + \frac{1}{2}|\vec{v}|^2$ the kinematic pressure.

One obtains for the Galerkin approximation of (2.6)

$$\frac{d}{dt}v_i(\vec{k},t) = \epsilon_{ijk} \sum_{\vec{p}+\vec{q}=\vec{k}} v_j(\vec{p},t)\omega_k(\vec{q},t) - ik_i\tilde{p}(\vec{k},t) - \nu k^2 v_i(\vec{x},t). \tag{2.7}$$

However, computing the Galerkin approximation in this form is not feasible even for only moderately large N. The difficulty stems from the nonlinear term of the NSE: A direct evaluation of the convolution sum $\sum_{\vec{q}+\vec{p}=\vec{k}}$ requires $\mathcal{O}(N^6)$ operations, which is grossly inefficient. As a consequence, Galerkin methods could not be used for high resolution fluid dynamics simulations until Orszag (1971) devised an approximate and very efficient 'pseudospectral' method for evaluating the nonlinear terms in (2.7). A pseudospectral approximation $\tilde{\vec{\lambda}}(\vec{k},t)$ to the convolution sum is obtained by applying a discrete backward Fourier transform to $\vec{v}(\vec{k},t)$ and $\vec{\omega}(\vec{k},t) = i\vec{k} \times \vec{v}(\vec{k},t)$, forming the cross-product $\vec{\lambda}(\vec{x},t)$ in physical space by simple multiplication, and then transforming the Lamb vector into Fourier space.

In a pseudospectral simulation the bulk of the computational work will be spent on transforming back and forth between physical and Fourier space. Fortunately, the Fast Fourier Transform (FFT) algorithm developed by Cooley & Tukey (see Press *et al.* , 1986) provides a very efficient and accurate method of performing discrete Fourier transforms. The number of required operations is of order $N \log_2 N$ compared to N^2 for straightforward transformation. The FFT algorithm is available in many different implementations. The performance of these routines is strongly machine and compiler dependent, and efforts in upgrading code performance are best spent in increasing the efficiency of the Fourier transforms. Some details pertaining to code optimization are discussed in Section 2.2.

Although not obvious on first sight, the pseudospectral procedure is not exact, i.e. $\tilde{\lambda}(\vec{k},t)$ is not equal to the convolution sum in (2.7) (Therefore the '~' on $\tilde{\vec{\lambda}}$). However, techniques have been developed to control and eliminate the errors incurred by this approximation, which are known as 'alias-errors'. This will be discussed in more detail in Section 2.3.

We obtain for the pseudospectral approximation of the rotational form of the Navier-Stokes equation

$$\frac{\partial}{\partial t} v_i(\vec{k},t) = -\nu k^2 v_i(\vec{k},t) + P_{ij}(\vec{k})\tilde{\lambda}_j(\vec{k},t). \tag{2.8}$$

Here the pressure term has been eliminated by use of the projection operator $P_{ij}(\vec{k})$:

$$P_{ij}(\vec{k}) = \delta_{ij} - \frac{k_i k_j}{k^2} . \tag{2.9}$$

The algorithm employed for time advancing (2.8) will be discussed in the last section of this chapter.

2.2 Code Optimization

It was mentioned above that DNS of turbulent flows require large amounts of computer memory. Experience has shown that at least 64^3 grid points or about 2 million words of memory are required to correctly reproduce the single point statistical properties of homogeneous turbulent flows. Until the mid-1980's, there was no computer available with a core memory large enough to contain this amount of data. Therefore, simulations were generally written 'out-of-core', i.e. while the complete set of simulation data is stored on disk, a (small) portion of the data is loaded into core memory and processed by the CPU. The results are then written back to disk, and the next batch of data is loaded into the core. Although straightforward in principle, there are serious drawbacks associated with out-of-core code. Firstly, the constant transfer of data incurs large Input/Output overhead and significantly decreases real time performance, especially so if there is no solid state disk with fast I/O available. Secondly, in practice it is necessary to synchronize the data transfer with the computational work, i.e. while one batch of data is retrieved from disk, another set is being processed in the CPU, while yet another batch of data is being written to disk. One may imagine that this is a cumbersome thing to do. Thirdly, often there are interdependencies among the variables which do not allow the piecemeal processing necessitated by the out-of-core approach.

These difficulties provided the motivation for developing the CRAY-2, whose core memory is big enough to handle even a 128^3 simulation quite comfortably. This machine was installed at the Livermore computer center (NMFECC) in 1986, where we performed most of our computations. It seemed advantageous to develop an in-core program for the direct numerical simulation of homogeneous turbulence. However, the CRAY-2 possesses like most supercomputers a number of idiosyncrasies, which the program - especially the FFTs - had to be adapted to.

The code used in this study is derived from an in-core version – written by Richard Pelz – of Steven A. Orszag's BIGBOX program. Pelz' program made use of the FFT99 Fast Fourier Transform package by Bruce Temperton, which is available in Cray Assembler Language (CAL) for the CRAY-XMP. However, no CAL version of FFT99 exists for the CRAY-2, which has an assembler language different from other CRAY computers. We therefore decided to

use the VCFT routines developed by Buneman (1989). This is a complex-to-complex FFT routine based on the Cooley-Tukey algorithm for transforms of length N, where N is a power of 2. It is optimized for use on the CRAY-2, fully vectorizing and allows multitasking. Straightforward replacement of a FORTRAN version of FFT99 by VCFT decreased the CPU time required for one three-dimensional 64^3 FFT from about 600 milliseconds to 180 milliseconds.

It was possible to further decrease the time required for the Fourier transforms. Unlike FFT99, VCFT does not have special provisions for real-to-complex transforms. We decided to follow the procedure outlined in Canuto *et al.* (1988) : define a complex variable $w(x)$

$$w(x) = u(x) + iv(x), \tag{2.10}$$

where $u(x), v(x)$ are purely real functions. After transforming $w(x)$to Fourier space, one may extract the values of $u(k)$ and $v(k)$ by exploiting the complex conjugate symmetry $u(-k) = u^*(k)$, i.e.

$$u(k) = \frac{1}{2}(w(k) + w^*(-k)), \tag{2.11}$$

and similarly for $v(k)$. One obtains 2 real-to-complex transforms for the cost of one complex-to-complex.

Furthermore, as emphasized by Buneman (1989), the CRAY-2 is 'allergic' to even strides. The 'stride' is the number of words between vector elements. Strides with high 'evenness' (the degree of evenness of a number n is the highest power of 2 in the factorization of n) do not cycle through all of the CRAY-2's memory banks. This means that the number of effectively available banks decreases, bank and section line conflicts increase, and performance degrades. Note that the stride of vectors of type COMPLEX is at least two in FORTRAN. One is therefore advised to eliminate the data type COMPLEX altogether. This is done by storing the real and imaginary parts of complex variables as REAL variables, and doing all complex arithmetic explicitly. All even strides may now be eliminated by patching arrays to dimensions $(N+1, N+1, N)$, where the $(N+1)$th rows are left blank.

These additional modifications further decrease the CPU requirements for one 64^3 FFT to less than 80 milliseconds. The total time required for one time step of the simulation program is less than 1 second of CPU time.

2.3 Alias Errors

As mentioned above, the pseudospectral method of evaluating convolution sums suffers from so-called 'alias errors'. In this section we shall discuss briefly what the source of these errors is and how one can control or eliminate them.

Consider the Dirac δ - function and one of its frequently encountered representations :

$$\delta(k-p) = \frac{1}{2\pi}\int_{-\infty}^{+\infty} dx\, e^{-ix(p-k)}, \tag{2.12}$$

It would seem that the corresponding representation of a Kronecker delta $\delta(k-p)$ in the case of a periodic domain $[0,2\pi]$with a finite number N of discrete modes x_i could be obtained by replacing

$$\frac{1}{2\pi}\int dx \; arrow \frac{1}{N}\sum_{x_i}. \tag{2.13}$$

However,

$$\frac{1}{N}\sum_{x_i} e^{-ix(p-k)} = \delta(k-p+\frac{2\pi}{N}n);\; n \in \mathcal{Z}. \tag{2.14}$$

The terms with $n \neq 0$ on the r.h.s. of (2.14) are the source of the alias errors. Namely, one may show by considering the discrete version of the convolution theorem that for the NSE

$$\begin{aligned}
\tilde{\lambda}_i(\vec{k}) &= \epsilon_{ijk}\sum_{\vec{p}+\vec{q}=\vec{k}} v_j(\vec{p})\omega_k(\vec{q}) \\
&+ \epsilon_{ijk}\sum_{\vec{p}+\vec{q}=\vec{k}\pm N\hat{e}_i} v_j(\vec{p})\omega_k(\vec{q}) \\
&+ \epsilon_{ijk}\sum_{\vec{p}+\vec{q}=\vec{k}\pm N\hat{e}_i\pm N\hat{e}_j} v_j(\vec{p})\omega_k(\vec{q}) \\
&+ \epsilon_{ijk}\sum_{\vec{p}+\vec{q}=\vec{k}\pm N\hat{e}_1\pm N\hat{e}_2\pm N\hat{e}_3} v_j(\vec{p})\omega_k(\vec{q}).
\end{aligned} \tag{2.15}$$

Here $\tilde{\lambda}_i(\vec{k})$ is the pseudospectral approximation to the Galerkin representation $\epsilon_{ijk}\sum_{\vec{p}+\vec{q}=\vec{k}} v_j(\vec{p})\omega_k(\vec{q})$ of the Lamb vector. The $\hat{e}_i$, i=1,2,3, are the unit vectors in Fourier space. The second, third and fourth term on the r.h.s are the alias terms of first, second and third order, respectively.

Alias errors occur in general when one attempts to discretize with insufficient resolution (see Fig. 2.1 and the discussion in Canuto *et al.* , 1988), or when an operation on a set

of data of a given wave number range produces data that spread over a wider range of wave numbers. Forming the cross product of velocity and vorticity is an example of such an operation. Some of the high wave number components are then 'aliased' back into the range of resolved wave numbers by the discrete transform (see Fig. 2.2).

The most straigntforward way of eliminating alias errors ('dealiasing') is known as the '2/3 - rule' . Here one truncates the range of active modes in the simulation to the region

$$|\vec{k}| < 2/3K, \tag{2.16}$$

by setting all $\vec{v}(\vec{k})$, $\tilde{\vec{\lambda}}(\vec{k})$ outside of the domain (2.16) explicitly to zero. One may convince oneself that after the truncation no alias terms can spuriously contribute to the active region (2.16), see also Fig 2.2. However, the '2/3 - rule' is expensive. It reduces the resolution of the simulation, i.e. the maximum wave number of the active modes, by a factor of two thirds.

Other, more efficient and more complicated dealiasing methods are discussed in great detail by Canuto *et al.* (1988). We decided to use a simple truncation method that eliminates all second and third order alias errors and does not reduce the maximum wave number of the simulation. In this truncation scheme (Patterson & Orszag, 1971) the active region has the shape of an 'octodecahedron' , i.e. a 18 - sided polyhedron :

$$|k_i| < K, \tag{2.17}$$

$$|k_i \pm k_j| < K \ , \ i,j = 1,2,3.$$

We are convinced that this truncation scheme suffices to control alias errors. See also the discussion in Canuto *et al.* (1988), where it is emphasized that alias errors even in fully aliased pseudospectral simulations are not likely to create significant inaccuracies if all scales are well resolved.

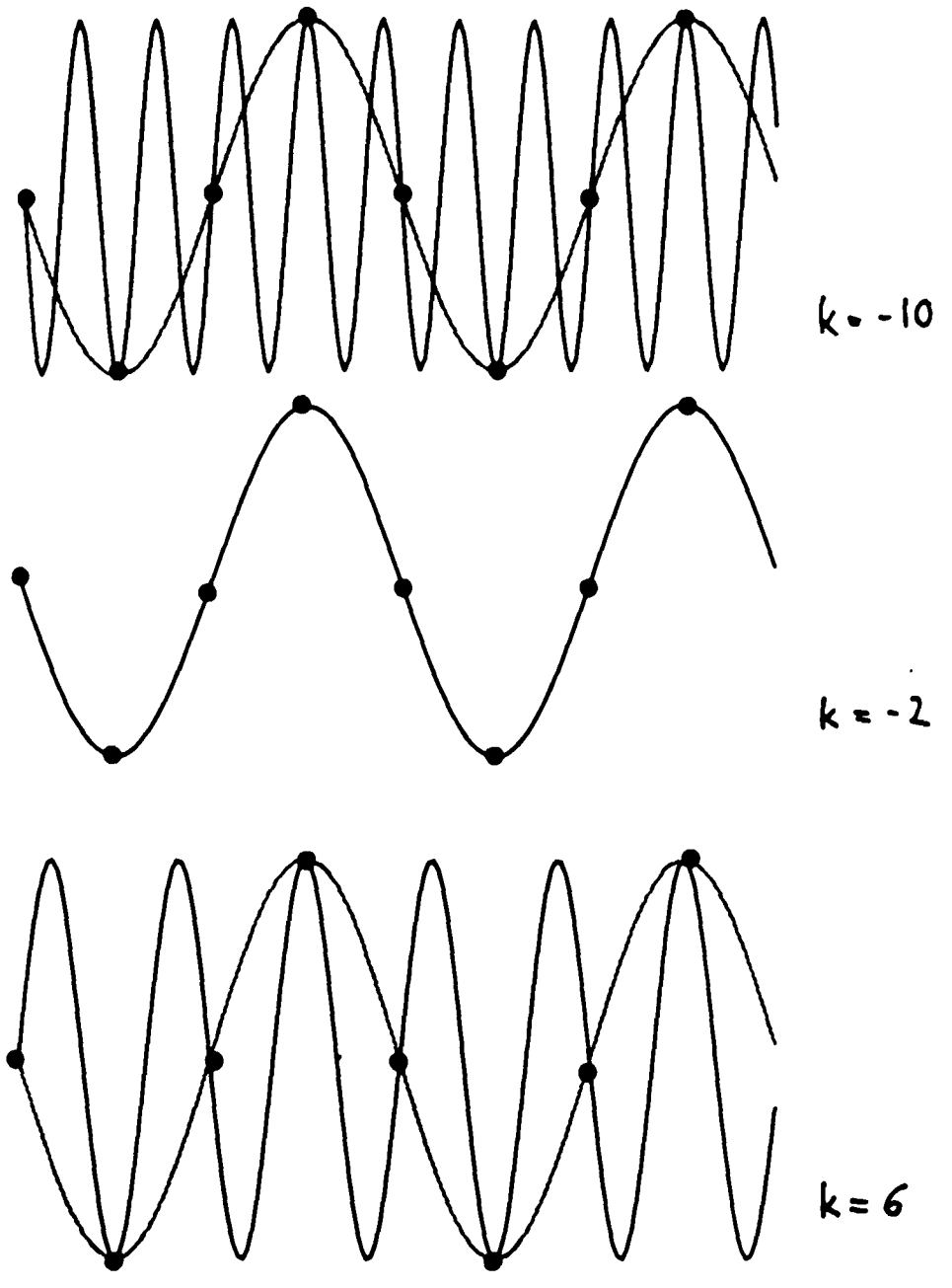

Figure 2.1: Three sine waves which have the same $k = -2$ interpretation on an eight point grid. The nodal values are denoted by the filled circles. The actual sine waves are denoted by the solid curves. Both the $k = 6$ and the $k = -10$ waves are misinterpreted as a $k = -2$ wave (from Canuto *et al.* , 1988).

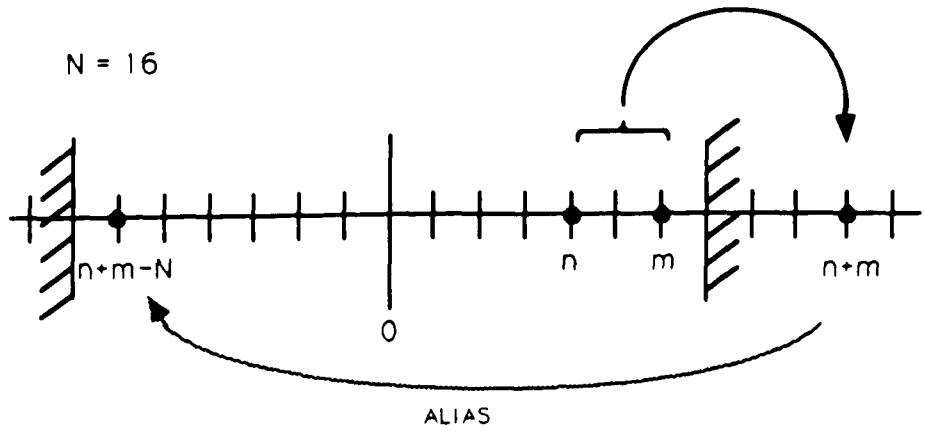

Figure 2.2: Product of modes with wave numbers n and m can produce the aliased mode at $n + m - N$ rather than at the correct wave number $n + m$ (from Rogallo, 1984).

2.4 The Time Stepping Scheme

In this study we employed and analyzed a time-stepping scheme that until now had not been used for simulations of homogeneous turbulence. A second order scheme commonly used for time advancing the Navier Stokes Equation in Fourier space (2.8) is the 'stabilized leap-frog Crank-Nicolson' (simply 'leap-frog' in the following) :

$$v_i^{(n+1)}(\vec{k}) = \frac{(1 - \nu k^2 \delta t) v_i^{(n-1)}(\vec{k}) + 2\delta t P_{ij}(\vec{k}) \tilde{\lambda}_j^{(n)}(\vec{k})}{1 + \nu k^2 \delta t}. \tag{2.18}$$

Other authors favor second or third order Runge-Kutta methods (see, e.g., Rogallo & Moin, 1984). We used a scheme (Frisch *et al.* ,1986) that can be obtained from the exact relation

$$v_i(\vec{k}, t + \delta t) = e^{-2\nu k^2 \delta t} v_i(\vec{k}, t - \delta t) + \int_{t-\delta t}^{t+\delta t} e^{-2\nu k^2 (t+\delta t-\tau)} \; P_{ij}(\vec{k}) \tilde{\lambda}_j(\vec{k}, \tau) d\tau \tag{2.19}$$

by pulling the nonlinear term $P_{ij}(\vec{k})\tilde{\lambda}_j$ out of the integral at time t:

$$v_i^{(n+1)}(\vec{k}) = e^{-2\nu k^2 \delta t} \; v_i^{(n-1)}(\vec{k}) + \frac{1 - e^{-2\nu k^2 \delta t}}{\nu k^2} P_{ij}(\vec{k}) \tilde{\lambda}_j^{(n)}(\vec{k}). \tag{2.20}$$

This scheme - called the 'slave-frog' - is also second order in time and reduces analytically to the leap frog for $\nu k^2 \delta t \to 0$. The distinct feature of the slave-frog is that it is able to reproduce what has been called 'slaved' behavior (Frisch *et al.* , 1986). Namely, if $\nu k^2 T \gg 1$, where T is the typical time scale of the nonlinear term, then to leading order in $1/(\nu k^2 T)$

$$v_i(k,t) \sim \frac{P_{ij}(\vec{k})\lambda_j(\vec{k})}{\nu k^2}. \tag{2.21}$$

Can we expect to encounter such slaved behavior in turbulence? Let us consider the influence of the large scales of size L and typical velocity U on the small scale end of the inertial range, $k \sim k_D$. Scaling arguments for fully developed turbulence imply that

$$\nu k_D^2 T_0 \sim \nu\sqrt{\epsilon/\nu^3}\frac{L}{U} = \sqrt{2\Omega}\frac{L}{U} \sim \sqrt{2}\frac{L}{\lambda}, \tag{2.22}$$

where λ is the Taylor microscale and Ω is the enstrophy. This shows that for the scales of velocity and vorticity being well separated, i.e. $L \gg \lambda$, the interaction of the dissipating modes with the energy containing modes becomes very stiff, i.e. the high-k modes are slaved. Such non-local interactions between small and large scales - although neglected in the Kolmogorov scenario - must not be neglected in the study of advection effects, higher order moments, intermittency and coherent structures. See also the work by Domaradzki (1988) on the nonlocal nature of the nonlinear interactions. However, one must realize that so far no clear separation of the scales of velocity and vorticity has been achieved in DNS of homogeneous turbulence. Typically, the ratio of the integral scale to the Taylor microscale $L/\lambda \approx 2-3$. Therefore, drastic differences between the leap-frog and the slave- frog should not be expected.

In the absence of useful analytical results concerning the precision of time stepping schemes, the best one can do is to carefully analyze data obtained from simulations with different time stepping schemes. We take a velocity field from a developed simulation of decaying turbulence at some time t_0, and perform with both the slave-frog and the leap-frog several continuation runs - with different time steps δt - up to a final time t_f, when we compare velocity fields $\vec{v}_0(\vec{x},t_f)$ (obtained by continuing with a very small time step δt_0) and $\vec{v}'(\vec{x},t_f)$ (obtained by continuing with a larger time step $\delta t'$). Define then the relative

shell-averaged difference $\rho(k)$

$$\rho(k) = \left\langle \frac{|\vec{v}_0(\vec{k}, t_f) - \vec{v}'(\vec{k}, t_f)|}{|\vec{v}_0(\vec{k}, t_f)|} \right\rangle_{S(k)} \tag{2.23}$$

where the average $\langle ... \rangle_{S(k)}$ over the shell in k-space is obtained by dividing with the number of modes in one shell. Figure 2.3 shows the relative time-stepping error $\rho(k)$ per time step $\delta t' = 0.01$. The reference time step was $\delta t_0 = 0.0025$. In agreement with the above analysis we observe that the relative error $\rho(k)$ increases dramatically with k. At the high-k end of the wave number range the relative error is several orders of magnitude larger than the error observable for the large scales and for global quantities (like the average energy $\bar{E}$, integral scale L, etc.). There is a simple explanation for this 'cascade' of time-stepping errors: An absolute error $\Delta(k_l) = \langle |\vec{v}(\vec{k}) - \vec{v}'(\vec{k})| \rangle_{S(k_l)}$ introduced by the time-stepping in a low-k shell introduces through the nonlinear interactions an absolute error $\mathcal{O}(\Delta(k_l)^2)$, which will result in a *relative* error orders of magnitude greater than $\rho(k_l)$, because the typical amplitude of high-k modes is orders of magnitude less than $|\vec{v}(\vec{k}_l)|$. Figure 2.3 also allows a comparison of the slave-frog (solid line) and the leap-frog (dotted line). We see that the slave-frog scheme is equivalent to the leap-frog scheme for small wave numbers (remember that the schemes converge analytically for $\nu k^2 \delta t \to 0$). For large wave numbers the slave-frog is only marginally better, certainly not enough to allow an increase of the time step in a simulation. We may expect that this advantage will become more significant in simulations with higher Reynolds number, i.e. better separation of the scales of velocity and vorticity. The slave-frog does not require more memory or CPU time than the leap-frog, we therefore promote the slave-frog as the preferable second-order time-stepping scheme for the NSE. However, we must also note that third-order Runge Kutta schemes are for presently achievable Reynolds numbers superior to the slave-frog.

But the Demon of the Second Kind continued to operate at a speed of three hundred million facts per second and mile after mile of tape coiled out and gradually buried the Ph.D. pirate ...

Stanislaw Lem, The Cyberiad (1967)

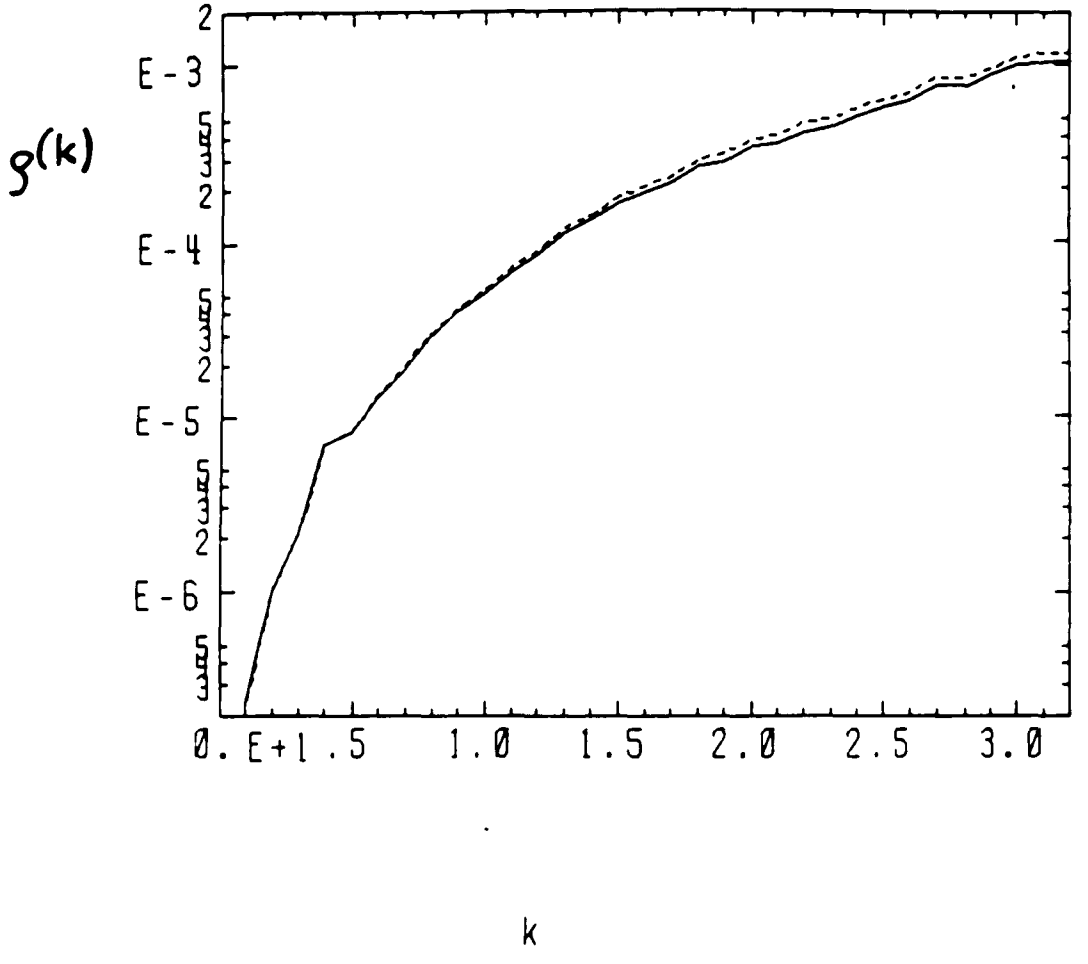

Figure 2.3: Relative error $\rho(k)$ per time step $\delta t' = 0.01$ as a function of wave number. Solid line — slave frog, dotted line — leap frog

Chapter 3

The Influence of Mean Helicity on the Energy Transfer in Isotropic Turbulence

In this chapter we shall investigate by direct numerical simulation the influence of mean helicity on the energy transfer in homogeneous isotropic turbulence. To begin, we will establish in the first section the notation used throughout this thesis. We feel that this is necessary because so far no standard terminology pertaining to helicity has been established. Inconsistent and conflicting definitions are in use, which has repeatedly lead to confusion and misunderstandings. In Section 3.2 we will discuss in detail the initialization scheme that allows us to create initial fields for simulations of decaying flows with arbitrary helicity. With just a few modifications, this scheme may also be used to provide a (helical) Gaussian stirring force for simulations of quasi-stationary turbulence. In Section 3.3 we present numerical results from simulations of decaying turbulence, the quasi-stationary case is discussed in the fourth Section.

3.1 Definitions

The fundamental dynamical variable is the velocity $\vec{v}(\vec{x})$ and its Fourier transform

$$\vec{v}(\vec{k}) = \frac{1}{V}\int_V d\vec{x}\ \vec{v}(\vec{x})\exp\{-i\vec{k}\cdot\vec{x}\}\ ,\ k_i = \frac{2\pi}{L}n\ ,\ n \in \mathcal{Z}. \tag{3.1}$$

Here we assume that the flow domain is a 'periodic box', i.e. a cube with sidelength L and periodic boundaries. This has two advantages: We avoid all mathematical subtleties re-

lated to the Fourier-representability of stationary random processes (Batchelor 1953, Orszag 1977) in infinite domains, and comparison with simulation data is straightforward. In a numerical simulation with N^3 gridpoints, the wavenumbers k_i are restricted to the range $k_i = 2\pi n/L, n = 0, \pm 1, ..., \pm(N/2-1)$. The volume average $\bar{E}$ of the kinetic energy may now be written as a sum over k-space

$$\bar{E} = \frac{1}{V}\int_V d\vec{x}\,\frac{1}{2}|\vec{v}(\vec{x})|^2 = \frac{1}{2}\sum_{\vec{k}}|\vec{v}(\vec{k})|^2 = \sum_k E(k). \tag{3.2}$$

(Note that overbars denote *spatial average* throughout, *mean* values in an ensemble of homogeneous isotropic turbulent flows are denoted by angular brackets $\langle ... \rangle$.) Here we made use of the Fourier-representation of the Kronecker-delta,

$$\delta(\vec{k}-\vec{p}) = \frac{1}{V}\int_V d\vec{x}\,\exp\{-i(\vec{k}-\vec{p})\cdot\vec{x}\}. \tag{3.3}$$

and energy spectral density $E(k)$ is the total energy in one 'k-shell', i.e.

$$E(k) = \sum_{S(k)}\frac{1}{2}|\vec{v}(\vec{k}')|^2\,, \tag{3.4}$$

where $\sum_{S(k)}$ is the summation over all modes in one k-shell, $\{\vec{k}' \mid k - 1/2\Delta k \leq |\vec{k}'| < k + 1/2\Delta k\}$. The width Δk of k-shells is customarily chosen to be unity in direct numerical simulations. For the volume average of the enstrophy we may write

$$\bar{\Omega} = \frac{1}{V}\int_V d\vec{x}\,\frac{1}{2}|\vec{\omega}(\vec{x}')|^2 = \frac{1}{2}\sum_{\vec{k}}|\vec{\omega}(\vec{k})|^2 = \sum_k k^2 E(k), \tag{3.5}$$

where $\vec{\omega}(\vec{x}) = \nabla \times \vec{v}(\vec{x})$ is the vorticity and $\vec{\omega}(\vec{k}) = i\vec{k} \times \vec{v}(\vec{k})$ its Fourier transform.

Similarly, one defines the average helicity $\bar{H}$

$$\bar{H} = \frac{1}{V}\int_V d\vec{x}\,\gamma(\vec{x}) = \sum_{S(k)}\vec{v}(\vec{k}')\cdot\vec{\omega}(-\vec{k}') = \sum_k H(k)\,, \tag{3.6}$$

where the scalar product of velocity and vorticity $\gamma(\vec{x}) = \vec{v}(\vec{x})\cdot\vec{\omega}(\vec{x})$ is known as the helicity density. Note that the helicity spectrum $H(k)$,

$$H(k) = \sum_{S(k)} H(\vec{k}') = \sum_{S(k)}\vec{v}(\vec{k}')\cdot\vec{\omega}(-\vec{k}'), \tag{3.7}$$

is *not* the Fourier transform of the helicity density correlation function $\langle\gamma(\vec{x})\gamma(\vec{x}+\vec{r})\rangle$. Rather, $H(k)$ is related to the antisymmetric part of the Fourier transform $S_{ij}(\vec{k})$ of the correlation tensor, see (3.12) below, and should properly be called the *co*-spectrum of velocity and vorticity. However, conventionally and in analogy with (3.2), $H(k)$ is simply called the 'helicity spectrum', and we shall do likewise. The helicity $H(\vec{k})$ of one mode may also be written as

$$H(\vec{k}) = 2\vec{k}\cdot[Re(\vec{v}(\vec{k}))\times Im(\vec{v}(\vec{k}))] = 2k|Re(\vec{v}(\vec{k}))|\,|Im(\vec{v}(\vec{k}))|\,\sin\phi(\vec{k}). \tag{3.8}$$

Here $Re(\vec{v}(\vec{k}))$ and $Im(\vec{v}(\vec{k}))$ denote the real and imaginary parts of the complex velocity vector $\vec{v}(\vec{k})$, $\phi(\vec{k})$ is the angle between them (Keep in mind that as a consequence of the incompressibility constraint, the cross-product of $Re(\vec{v}(\vec{k}))$ and $Im(\vec{v}(\vec{k}))$ is always aligned with $\vec{k}$). The magnitude of the helicity of one mode is limited by the energy, i.e. $|H(\vec{k})| \leq 2kE(\vec{k})$. It follows that the energy spectrum defines a 'maximal helicity' $\bar{H}_{max} = \sum_k 2kE(k)$, which corresponds to $\phi(\vec{k}) = \pi/2$ for all modes. The 'normalized average helicity' or 'Beltramization' H_N

$$H_N = \bar{H}/\bar{H}_{max}, \tag{3.9}$$

and the 'normalized helicity density' h

$$h(\vec{x}) = \frac{\vec{v}(\vec{x})\cdot\vec{\omega}(\vec{x})}{|\vec{v}(\vec{x})|\,|\vec{\omega}(\vec{x})|} = cos(\theta(\vec{x})), \tag{3.10}$$

are useful in characterizing how strongly helical a velocity field is. Here θ is the angle between the velocity and the vorticity vector. Obviously both h and H_N are normalized to lie in the interval $[-1,+1]$. One should be aware that H_N is also know as 'relative helicity' in the literature, h is sometimes referred to as 'relative helicity' or 'relative helicity density'.

We have already introduced the second order, two-point velocity correlation tensor

$$R_{ij}(\vec{r}) = \langle v_i(\vec{x})v_j(\vec{x}+\vec{r})\rangle = \langle v^2\rangle\left(\frac{b_{rr}(r)-b_{tt}(r)}{r^2}r_ir_j + b_{tt}(r)\delta_{ij} + \epsilon_{ijk}g(r)r_k\right), \tag{3.11}$$

where b_{rr} and b_{tt} are the longitudinal and transversal correlation coefficients. The Fourier transform of the correlation tensor $S_{ij}(\vec{k}) = \frac{1}{V}\int_V d\vec{x}\; R_{ij}(\vec{x})\exp\{-i\vec{k}\cdot\vec{x}\}$ is of the general form

$$S_{ij}(\vec{k}) = \frac{\langle E(k)\rangle}{N(k)}P_{ij}(\vec{k}) + \frac{i\langle H(k)\rangle}{2k^2N(k)}\epsilon_{ijk}k_k, \tag{3.12}$$

where $P_{ij}(\vec{k})$ is the projection operator $\delta_{ij} - k_i k_j/k^2$, ϵ_{ijk} the completely antisymmetric tensor and $N(k) = 4\pi\rho k^2 \Delta k$ the number of modes in one k-shell. The density of modes in k-space $\rho = (L/2\pi)^3$. One may easily show that $\langle v_i(\vec{p}) v_j(\vec{k}) \rangle = S_{ij}(\vec{k})\delta(\vec{k} + \vec{p})$. Note that we keep the averaging brackets $\langle ... \rangle$ on the r.h.s. of (3.12) to emphasize that $S_{ij}(\vec{k})$ is an essentially statistical quantity. On the other hand, the energy spectrum $E(k)$ and the helicity spectrum $H(k)$ of one realization (or one simulation) are well defined, because we restrict ourselves to a finite, periodic volume.

3.2 Initialization With Controlled Helicity

When setting up the initial flow field - a Gaussianly distributed isotropic solenoidal vector field - for a simulation of decaying turbulence, one usually employs a random number generator to obtain the components $v_i(\vec{k})$ of the velocity field in Fourier space. The desired energy spectrum $E(k)$ and the (space-) average energy $\bar{E}$ are determined by the appropriate choice of a 'shape function' $f(k)$ for the velocity amplitudes, $E(k) \sim k^2 f(k)^2$, and an overall normalization factor. Care must be taken to satisfy the constraints imposed by incompressibilty and reality in physical space. In particular, one usually ensures that the initial field is divergence-free by projecting $\vec{v}(\vec{k})$ on the plane perpendicular to the wave vector $\vec{k}$. The constraint $\vec{v}(\vec{k}) = \vec{v}^*(-\vec{k})$ imposed by the reality of the velocity field in physical space is satisfied implicitly by keeping only modes with $k_x \geq 0$ in the computation. (In practice, one simply uses a 'real to half-complex' Fourier transform routine in the x-direction, see (2.10),(2.11).) Note though that in the $k_x = 0$ - plane, the modes $\vec{v}(0, k_y, k_z), \vec{v}(0, -k_y, -k_z)$ have to be made complex conjugate to each other 'by hand'. Unless specific measures are taken, the helicity spectrum $H(k)$ and the average helicity $\bar{H}$ will vanish in the mean. Of course, in each realization, i.e. for each sequence of random numbers used to create one field, we will find deviations from the zero mean.

Let us show now how one can create a divergence-free, statistically isotropic and Gaussian velocity field such that both the energy and the helicity spectrum take on prescribed values (Polifke & Shtilman, 1989). Consider the expression for the helicity of one mode, Equation (3.8). For given amplitudes $|Re(\vec{v}(\vec{k}))|$ and $|Im(\vec{v}(\vec{k}))|$, i.e. given energy $E(\vec{k})$, the phase angle $\phi(\vec{k})$ between the real and the imaginary part of the velocity vector essentially

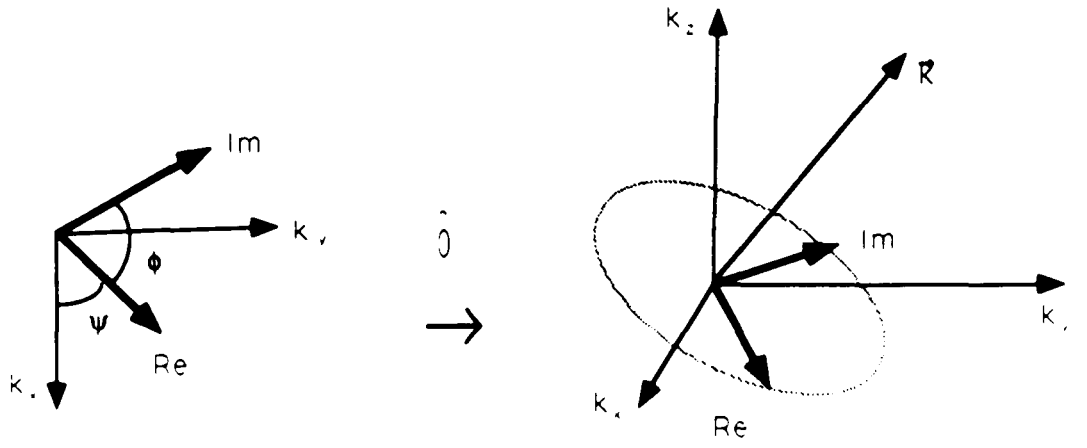

Figure 3.1: Illustration of the initialization procedure (a) setup in $k_x - k_y$ plane and (b) after the rotation into a plane perpendicular to $\vec{k}$.

determines the helicity of mode $\vec{k}$. Obviously, if the real and imaginary parts of $\vec{v}(\vec{k})$ tend to be aligned in one shell, $H(k)$ will be small, whereas preferentially perpendicular orientation (with the same handedness) will result in $H(k)$ being close to its maximum value $2kE(k)$. Thus by controlling the phase angle ϕ one can choose the initial helicity spectrum independently of the energy spectrum.

The numerical implementation of this idea proceeds in a few straightforward steps, as illustrated in Fig. 3.1. To begin, the velocity vector of each mode $\vec{k}$ is 'assembled' in the k_x - k_y - plane. We may fix the energy of mode $\vec{k}$ by simply setting $|Re(\vec{v}(\vec{k}))| = |Im(\vec{v}(\vec{k}))| = f(|\vec{k}|)$, or by multiplying the shape function $f(k)$ with a random variable that follows a second order χ^2 - distribution with two degrees of freedom (see Chapter 5 on this point). The angle ψ is chosen randomly to assure overall statistical isotropy, see Fig. 3.1 (a). As explained above, the angle ϕ determines the helicity : for the case of 'maximum helicity', $\phi = \pi/2$, for 'zero helicity' we set $\phi = 0$ or $\phi = \pi$, whereas for 'random helicity' ϕ is randomly distributed over the interval $[0, 2\pi]$. Finally, in order to satisfy the incompressibility condition, it is necessary to rotate this (complex) vector into a plane

perpendicular to $\vec{k}$ by applying an orthogonal transformation $\hat{O}(\Theta,\Phi)$, where Θ and Φ are the polar angles of $\vec{k}$, see Fig. 3.1 (b) :

$$\vec{v}(\vec{k}) \rightarrow \hat{O}(\Theta,\Phi)\vec{v}(\vec{k}) = \begin{pmatrix} (\cos^2\Phi\cos\Theta + \sin^2\Phi)v_x + \cos\Phi\sin\Phi(\cos\Theta - 1)v_y \\ \cos\Phi\sin\Phi(\cos\Theta - 1)v_x + (\sin^2\Phi\cos\Theta + \cos^2\Phi)v_y \\ -\cos\Phi\sin\Theta v_x - \sin\Phi\sin\Theta v_y \end{pmatrix}. \quad (3.13)$$

In the simulation program, this transformation is implemented as follows: We define $a = (k_x{}^2 + k_y{}^2)^{-1}, b = k_z/k, c = ak_xk_y(b-1)$ and then (3.13) is computed as

$$\hat{O}(\Theta,\Phi)\vec{v}(\vec{k}) = \begin{pmatrix} a(bk_x{}^2 + k_y{}^2)v_x + cv_y \\ cv_x + a(bk_y{}^2 + k_x{}^2)v_y \\ -bk_xv_x/k_z - bk_yv_y/k_z \end{pmatrix}. \quad (3.14)$$

In order to avoid numerical overflow at $k_z = 0$ or $k_x{}^2 + k_y{}^2 = 0$, we set the corresponding array elements equal to 10^{-40}.

Velocity fields created in this manner are - within statistical fluctuations - isotropic and Gaussian, i.e. the skewness $S = -\overline{x^3}/(\overline{x^2})^{3/2}$ of the velocity and its first derivatives is very small, the flatness $F = \overline{x^4}/(\overline{x^2})^2$ is close to 3 (here $x = v_i$ or $x = (\partial v_i/\partial x_i)$, i = 1,2,3; no summation over repeated indices). The expectation values of the energy and helicity spectra are now

$$\langle E(k)\rangle = 4\pi k^2 f(k)^2\langle\chi^2\rangle, \quad (3.15)$$

$$\langle H(k)\rangle = 8\pi k^3 f(k)^2\langle\chi^2\rangle\langle\sin\phi\rangle.$$

We have verified that we indeed obtain an average helicity equal to the maximal value $\bar{H}_{max} = \sum_k 2kE(k)$ for initialization with 'maximum helicity'. The case of random helicity corresponds to traditional initialization procedures, where different sequences of random numbers will yield different helicity spectra and total helicities. One expects, of course, that the mean of these quantities over many realizations will be zero. We have evaluated the relative helicity H_N of a series of 500 random helicity fields with an energy spectrum that peaks at wavenumber $k_0 \approx 4$; then the number of modes in the energy containing range is of order 10^3 in our simulation. The results are : $\langle H_N\rangle = 0.0015, \langle|H_N|\rangle = 0.025$. The standard deviation of H_N for the series of 500 realizations is equal to 0.03, the maximum $|H_N|$ is equal to 0.11 . One may conclude that the helicity typically obtained when initializing with random helicity is quite small. However, one must bear in mind that shifting the peak of

the energy spectrum to lower values, or decreasing the number of initially excited modes in some other way, may change the situation drastically. Finally, for zero helicity initialization the relative helicity H_N is of order 10^{-12}.

3.3 Numerical Simulations of Decaying Turbulence

In order to study the effects of mean helicity on the dynamics of homogeneous turbulent flows, we have conducted a series of direct numerical simulations of decaying turbulence. For numerical details we refer to the previous Chapter. The initial fields for these runs are identical to each other in every respect except helicity. The initial energy spectrum was chosen to be

$$E(k) \sim k^4 e^{-2(k/k_0)^2}, \tag{3.16}$$

with k_0 equal to 4 and average initial energy $\bar{E}$ equal to 2.8. Other initial parameters are : kinematic viscosity ν equal to 0.015, turnover time τ equal to .45, integral scale $L = 3\pi/4\sum_k(E(k)/k)$ equal to .64, Taylor Microscale $\lambda = \left(\overline{(\partial u_i/\partial x_i)^2}/\overline{uk_i^2}\right)^{1/2}$ equal to .44, Taylor Microscale Reynolds number $R_\lambda = v_{rms}\lambda/\nu$ equal to 45. During the early stage of the simulation, the energy, which initially is concentrated at small wavenumbers, spreads towards high wavenumbers without suffering significant dissipation. As a result, the average enstrophy $\bar{\Omega} = \sum_k k^2 E(k)$ usually increases initially. One assumes that the flow is 'most developed' once the enstrophy starts to decay and the statistical characteristics of the velocity derivatives attain values typical of turbulence at moderate Reynolds numbers, i.e. a flatness F of approximately 4 and a skewness S of approximately -0.5 (see Kerr, 1985).

Fig. 3.2 shows the energy spectra for run O_{zero}, accumulated at times $t = 0, 0.2, 0.4, ..., 2$, i.e. during more than four turnover times. (Note that all the spectra presented in this work are compensated for nonuniform mode density (Rogallo, 1988), which yields much smoother spectra at small wavenumbers.) There is only a slight upward turn of the spectra at high wavenumbers, which indicates that the simulation is reasonably well resolved. In agreement with this assessment, the maximum Kolmogorov wavenumber $k_D = (\epsilon/\nu^3)^{1/4}$ is equal to 28.9 . The initial field for this run has zero helicity in all modes. The mature stage of the simulation is reached at time $t \approx 0.35$.

In Fig. 3.3 we present the equivalent data for run O_{max}, a simulation with a maximally helical initial field, i.e. $H(k) = 2kE(k)$ for all wave numbers at $t = 0$. As one would expect, the velocity and vorticity are strongly aligned in this flow, we find that initially the spatial mean of the square of the normalized helicity density $\overline{h^2} = \overline{\cos^2\Theta} = 0.88$, where Θ is the angle between the velocity and the vorticity vector. In this simulation there is no growth of enstrophy $\bar{\Omega}$, and the developed phase is not reached until time $t \approx 1.2$; see Figs. 3.4 and 3.5 which show the time evolution of the skewness and flatness of the velocity derivatives of both runs up to time $t = 2$. From Figs. 3.2 and 3.3 we may conclude that the presence of high mean helicity does not change the qualitative features of the time-development of the energy spectrum. It is obvious though, that helicity slows down the flow of energy towards higher wavenumbers. This is seen more clearly in Figs. 3.6 and 3.7 which show the inertially weighted energy spectra $E(k)\epsilon^{-2/3}k^{5/3}$ at $t = 0.4$ and $t = 1.2$. Comparing these figures with Figs. 2 and 8 in André & Lesieur, we see that in both their EDQNM model and our direct numerical simulation of a maximally helical flow the energy of the large scales significantly exceeds the Kolmogorov inertial range value $E(k) \approx 2\,\epsilon^{2/3}k^{-5/3}$.

The time evolution of the energy spectrum is determined by

$$(\frac{d}{dt} + 2\nu k^2)E(k,t) = T(k,t), \tag{3.17}$$

where the transfer-term $T(k,t)$ is based on triple velocity correlators. Making use of the rotational form (2.8) of the NSE one may write

$$T(k,t) = \sum_{S(k)} Re[\vec{v}(\vec{k}') \cdot \vec{\lambda}(-\vec{k}')]. \tag{3.18}$$

In Figs. 3.8 and 3.9 we plot the normalized transfer term $T_N(k,t) = T(k,t)L/(\nu\bar{E}^{3/2})$ for runs O_{zero} and O_{max}. About two turnover times later, at time t = 0.4 (Fig. 3.8), shortly after the maximum of enstrophy is reached in run O_{zero}, the flow of energy out of the energy containing range is significantly reduced in the helical case. At time $t = 1.2$ (Fig. 3.9) the total normalized transfer of the two runs differ only by about 25 percent (see also Table 3.1 below). Also note the good agreement of our results for the transfer spectrum in the non-helical case with experimental data (see, e.g. Landahl & Mollo-Christensen,1986).

The reduced transfer of energy suppresses the growth of enstrophy $\bar{\Omega}$, which in homogeneous turbulence is proportional to the viscous dissipation ϵ , i.e. $\bar{\epsilon} = -2\nu\bar{\Omega}$. Thus, in the

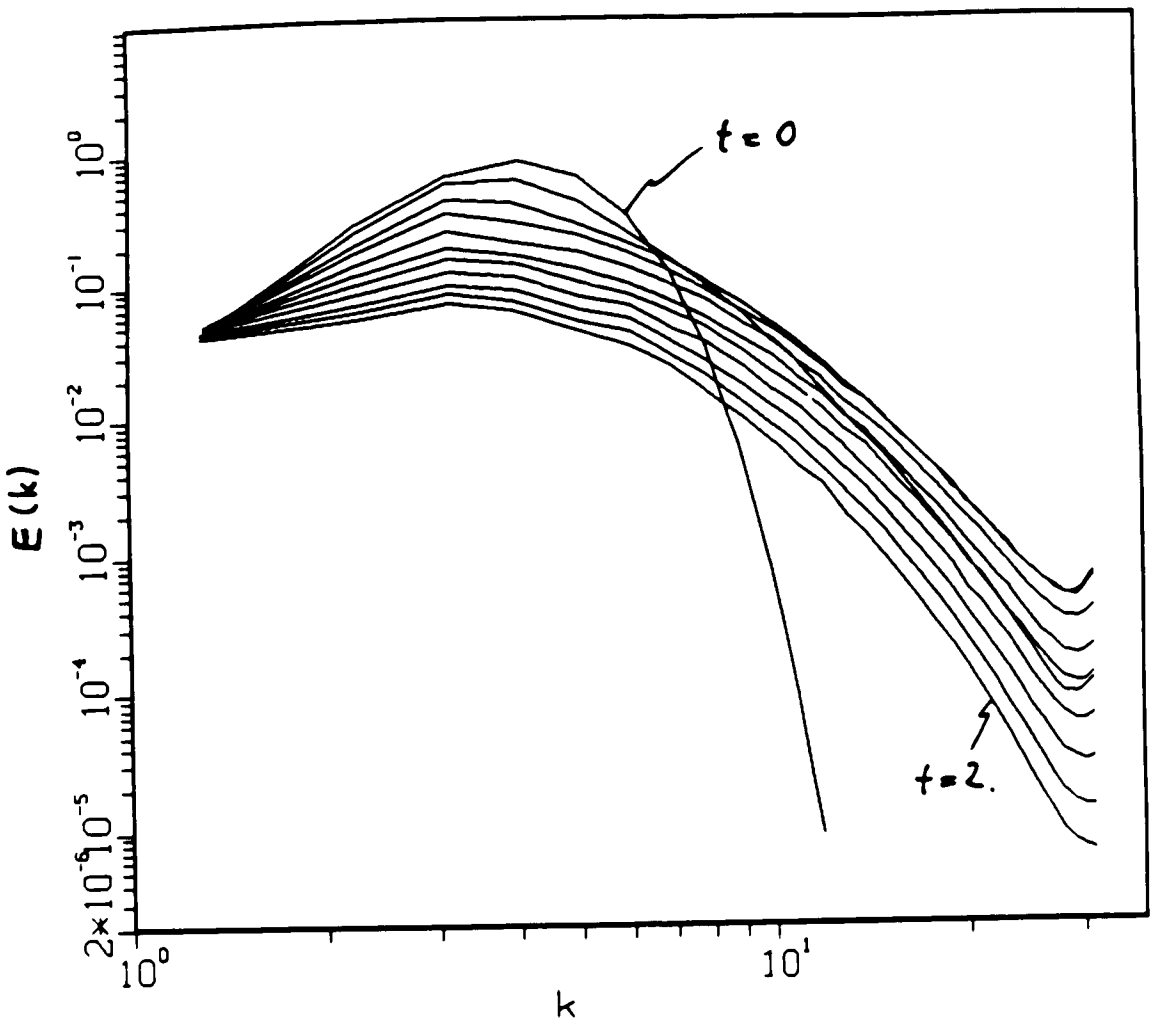

Figure 3.2: Energy spectra $E(k,t)$ of run O_{zero}, accumulated over $t = 0$ up to $t = 2$, $\Delta t = 0.2$

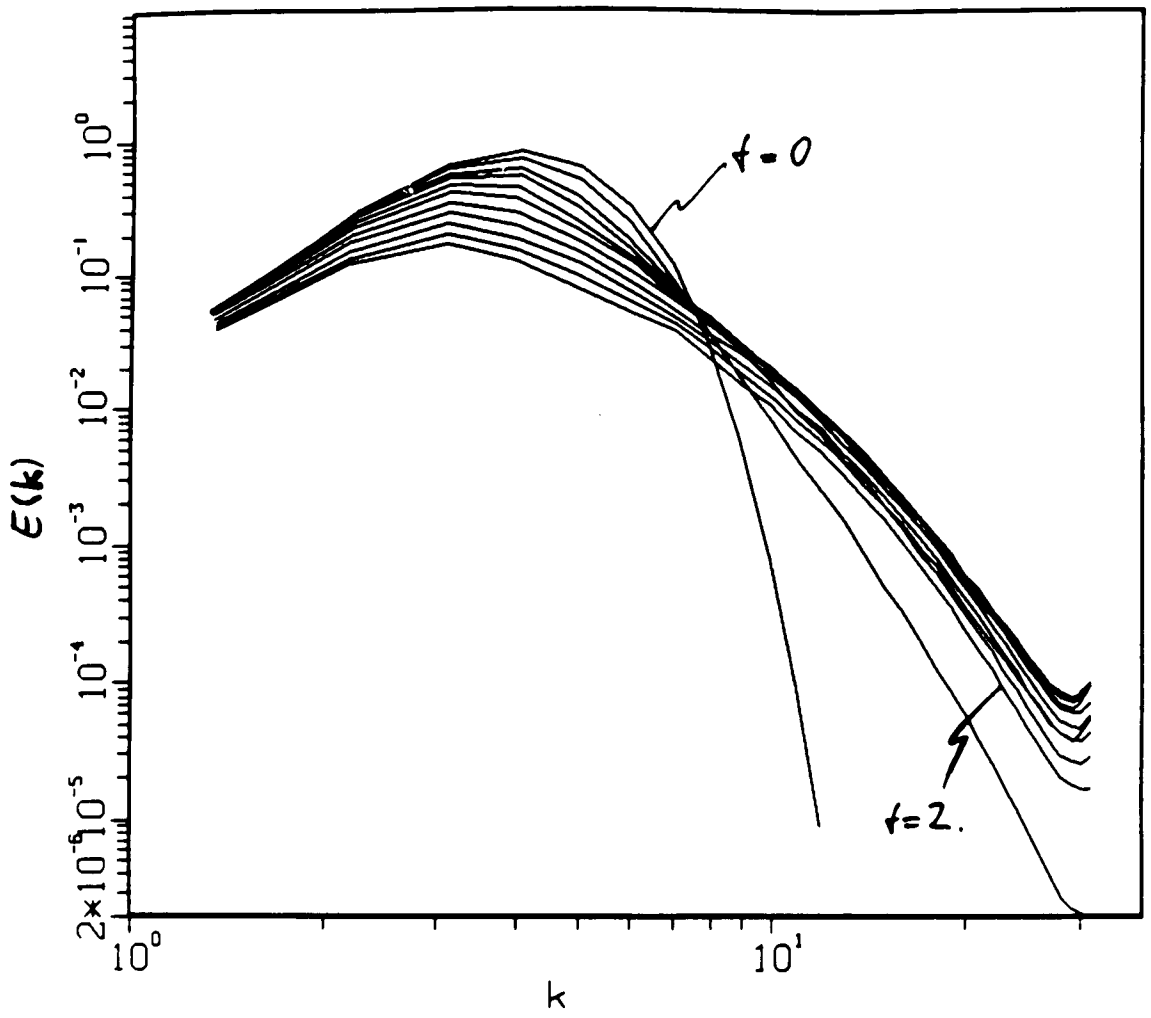

Figure 3.3: Accumulated energy spectra $E(k,t)$ of run O_{max}.

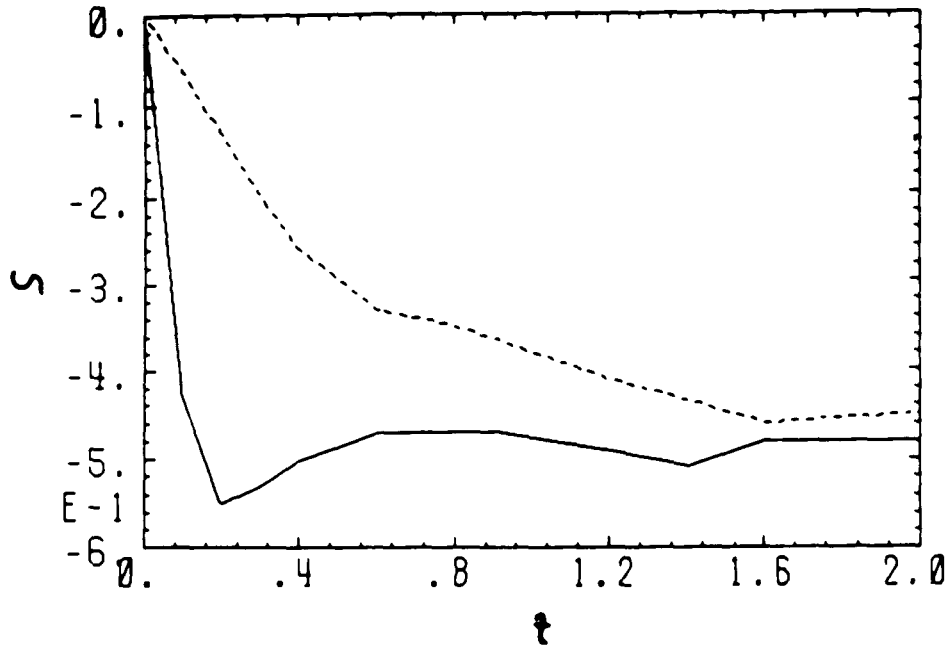

Figure 3.4: Skewness S as a function of time. O_{zero}: solid line; O_{max} :dashed line.

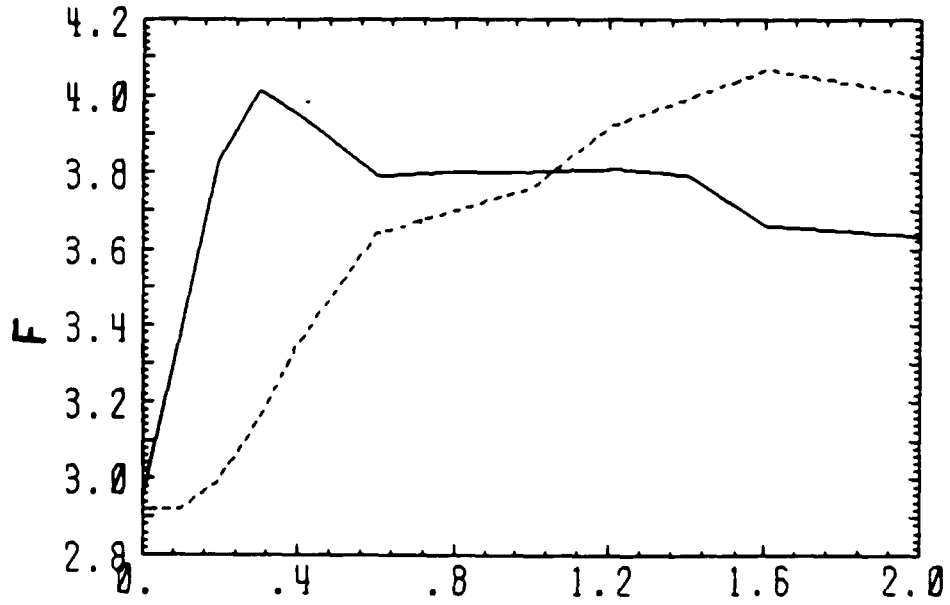

Figure 3.5: Flatness F as a function of time. O_{zero}: solid line; O_{max}: dashed line.

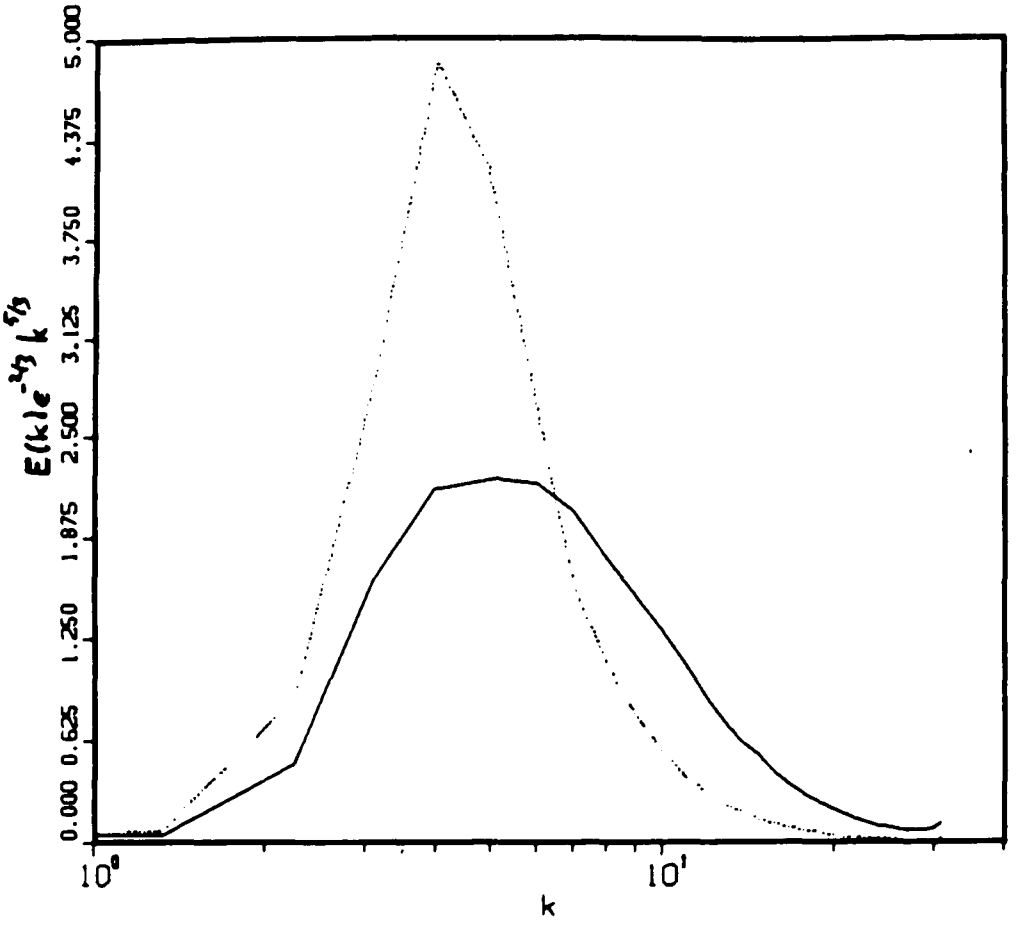

Figure 3.6: Inertially weighted energy spectra $E(k)\epsilon^{-2/3}k^{5/3}$ as a function of wave number. O_{zero}: solid line, O_{max}: dashed line. $t = 0.4$.

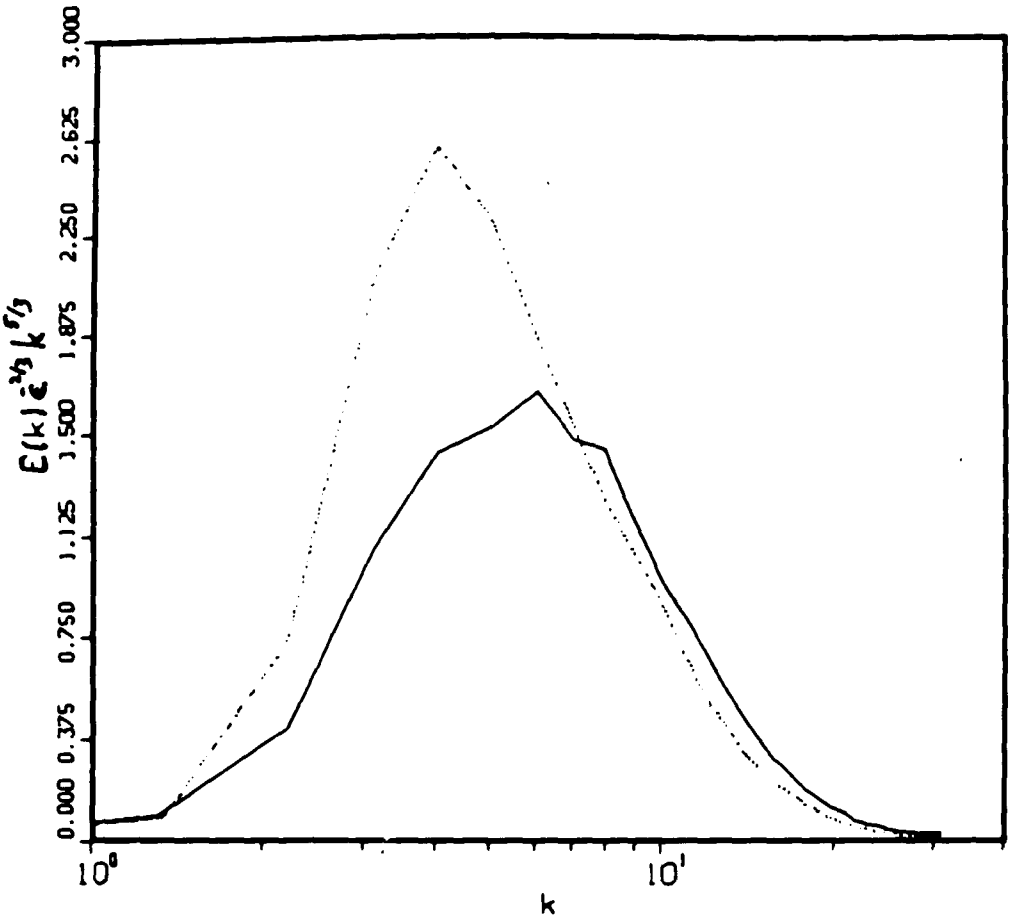

Figure 3.7: Inertially weighted energy spectra $E(k,t)\epsilon^{-2/3}k^{5/3}$ as a function of wave number. O_{zero}: solid line, O_{max}: dashed line. $t = 1.2$.

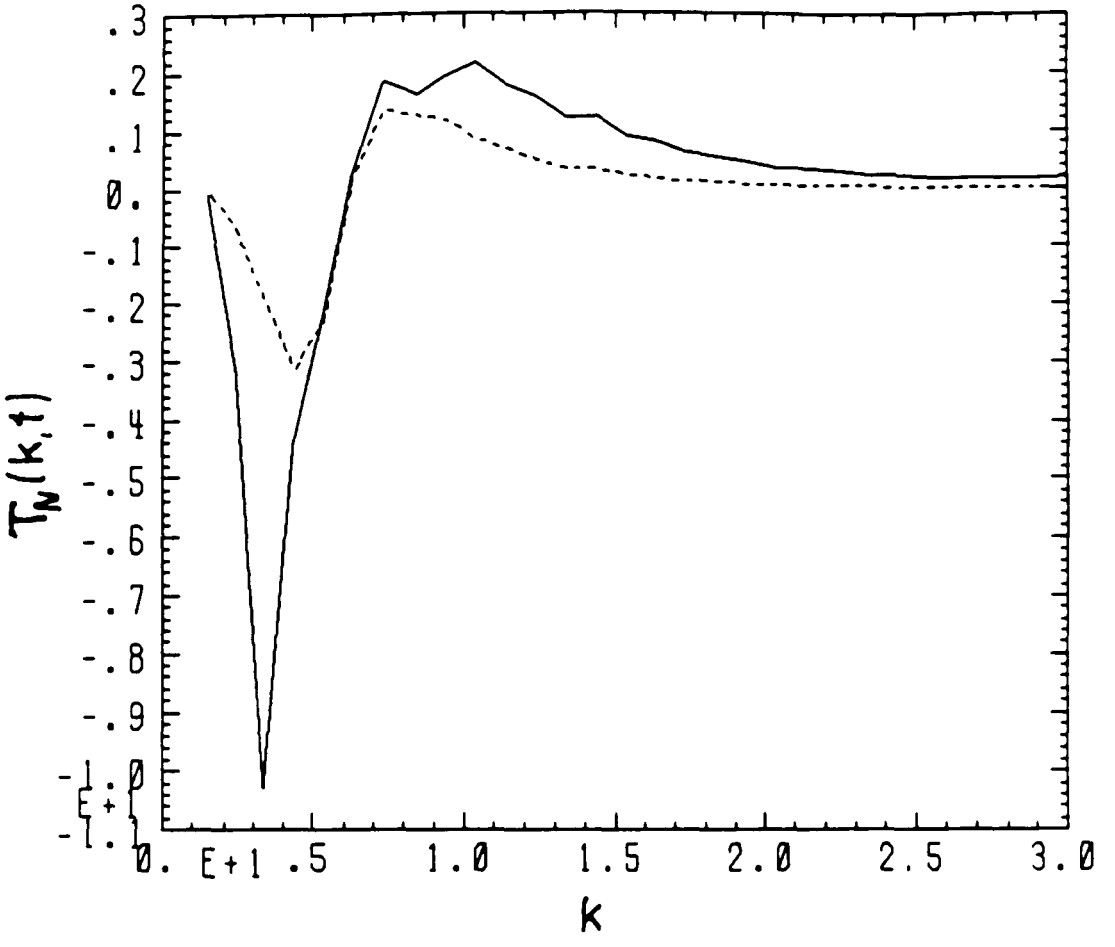

Figure 3.8: Normalized transfer term $T_N(k,t)$ as a function of wave number, $t = 0.4$. O_{zero}: solid line, O_{max}: dashed line.

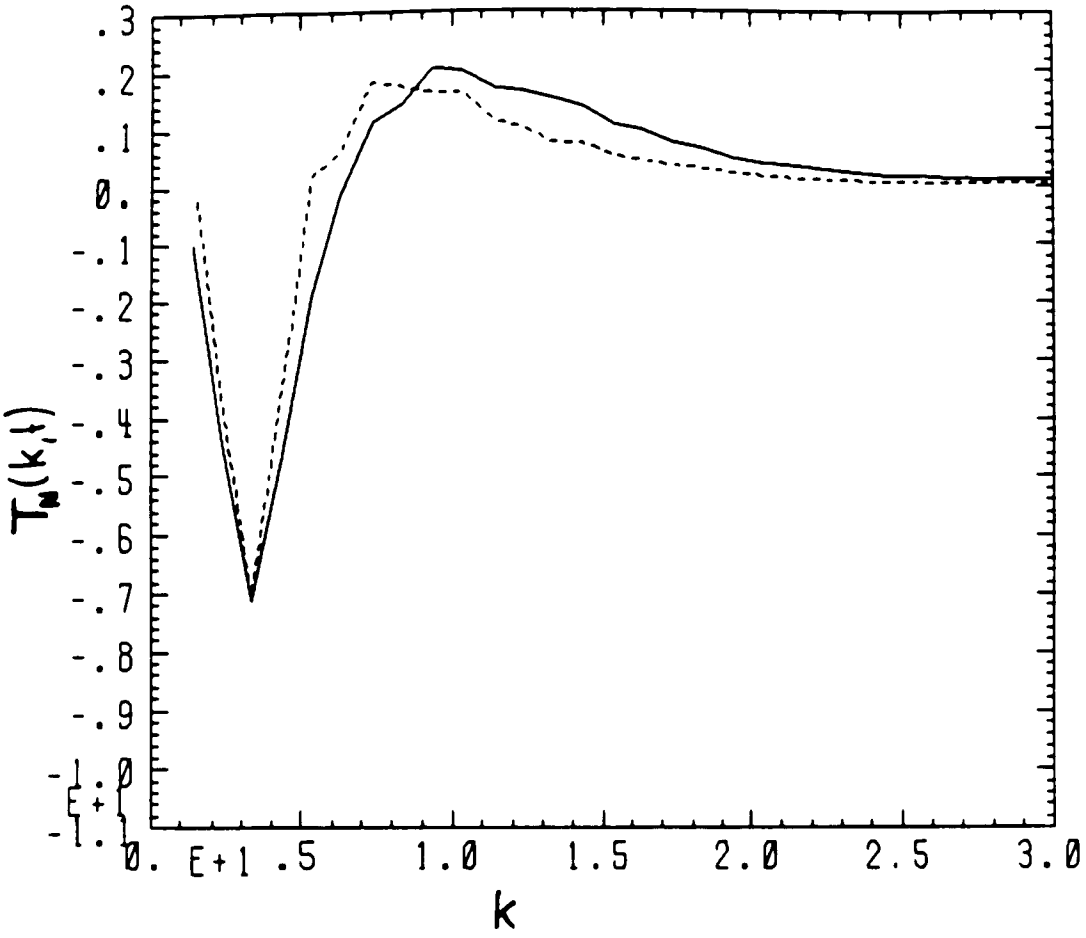

Figure 3.9: Normalized transfer term $T_N(k,t)$ as a function of wave number, $t = 1.2$. O_{zero}: solid line, O_{max}: dashed line.

earlier stage of the simulation the helical flow will decay slower than its non-helical counterpart. After about two turnover times though, the helical flow will have more enstrophy than the non-helical flow, for the very reason that it decays slower initially. Furthermore, the helical flow does not remain maximally helical (see also Kraichnan, 1973 on this point). This is illustrated for run O_{max} in Fig. 3.10, which shows that after about four turnover times the helicity has spread over the entire range of wave numbers while undergoing significant dissipation. Especially the small scales are no longer maximally helical. Indeed, Fig. 3.11 shows that both the average helicity $\bar{H}$ and the normalized helicity H_N decay rapidly with time (Note that there can be no viscous creation of helicity if the spectrum $H(k)$ is of the same sign for all modes.)

It is important to assess what value of H_N is required to significantly influence the nonlinear dynamics of the decaying flow. In Table 3.1 we present data from runs O_{zero} , O_{max} and 4 other runs O_{20}, O_{40}, O_{60} and O_{80}, which had the same initial energy spectrum as O_{zero} and O_{max} and a helicity spectrum $H(k)$ equal to 20, 40, 60 and 80 percent of the maximum value $2kE(k)$ for all wavenumbers, respectively. As remarked in the previous section, the distribution of the angle ϕ between the real and the imaginary part of $\vec{v}(\vec{k})$ determines the value of relative helicity. We have verified by numerical comparison that the details of the distribution of ϕ do not influence the evolution of the flow. In the simulations reported here the desired level of helicity was achieved by assigning maximum positive or negative helicity ($\phi = \pm\pi/2$) in appropriate proportions to the modes in Fourier space.

In the first rows of Table 3.1 we list the time t, average energy $\bar{E}(t)$, average enstrophy $\bar{\Omega}(t)$, relative helicity $H_N(t)$, the mean square of the normalized helicity density $\overline{h^2}$, and Taylor microscale Reynolds number $R_\lambda(t)$. Recall that $\bar{E} = 2.8$, $\bar{\Omega} = 56$ and $R_\lambda = 45$ at $t = 0$. Note that only for the maximally helical flow O_{max} there is no initial growth of enstrophy. In the last two rows of Table 3.1 we present quantities that seem adequate to measure the strength or effectiveness of the energy transfer in a turbulent flow: the normalized mean-square nonlinear term $Q(t)$

$$Q(t) = \overline{|\vec{v} \times \vec{\omega} - \nabla\tilde{p}|^2} / (\overline{u^2}\,\overline{\omega^2}), \tag{3.19}$$

where $\tilde{p} = p + v^2/2$ is the kinematic pressure, and the sum S_T of the normalized transfer

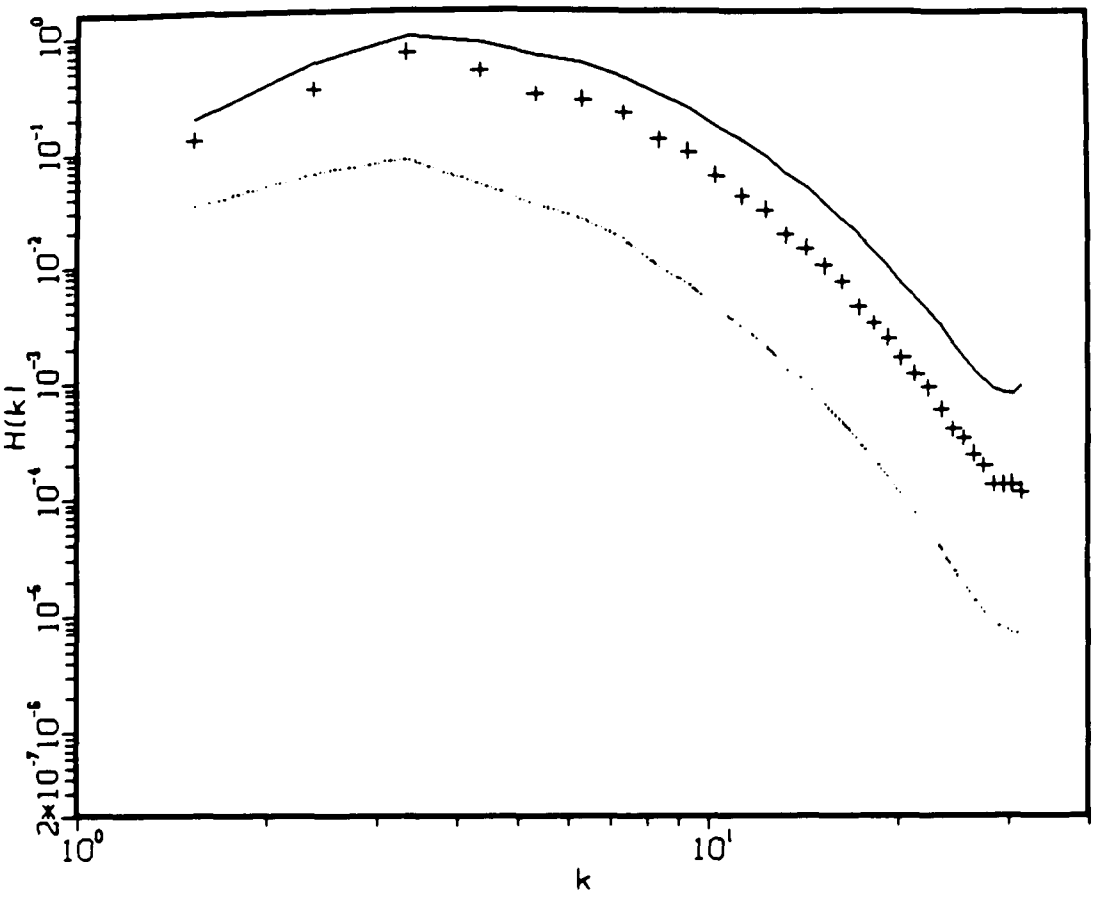

Figure 3.10: Helicity spectrum $H(k)$ (+-markers) of run O_{max} at $t = 2$, maximum helicity $H(k)_{max}$ (continuous line) and quasi-Gaussian standard deviation $\sigma_G(H(k))$ (dotted line, see the next chapter).

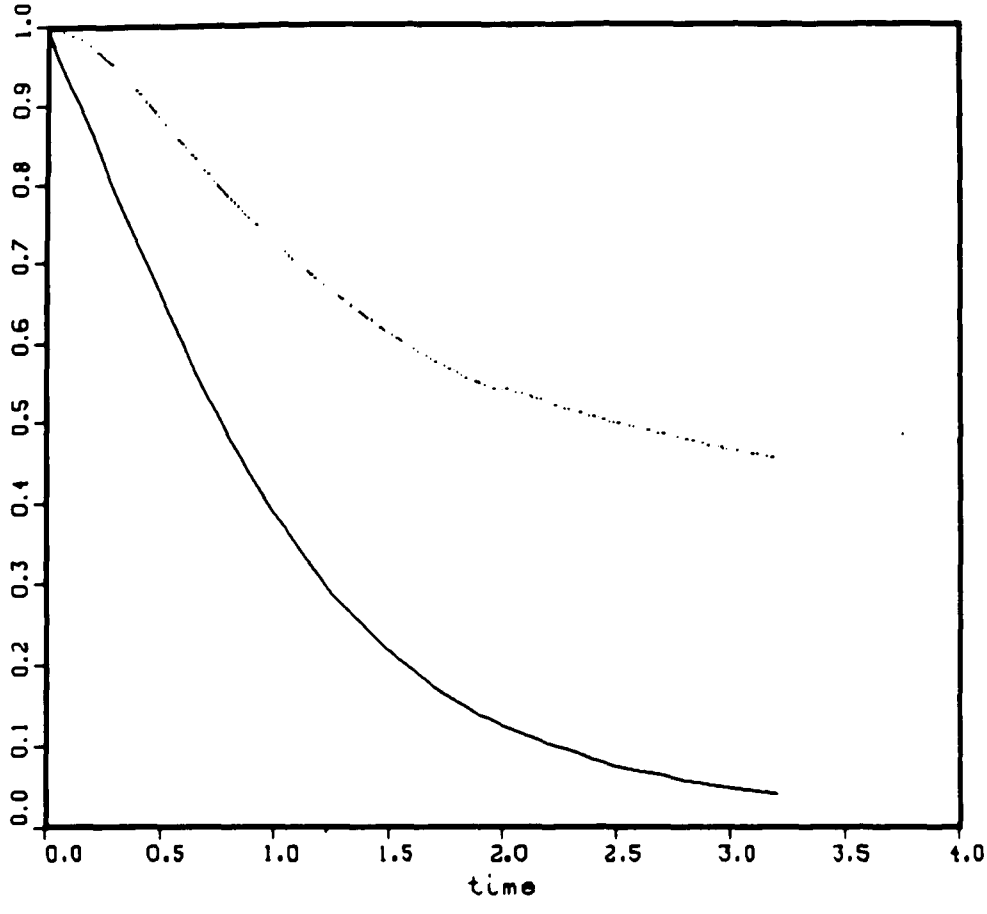

Figure 3.11: Time evolution of the average helicity $\bar{H}$, normalized by its initial value (solid line) and of the normalized helicity H_N (dotted line).

run	O_{zero}	O_{20}	O_{40}	O_{60}	O_{80}	O_{max}	O_{zero}	O_{max}	O_{zero}	O_{max}
t	0.4	0.4	0.4	0.4	0.4	0.4	1.2	1.2	2.0	2.0
$\bar{E}(t)$	2.0	2.0	2.0	2.1	2.1	2.2	.75	1.2	.35	.62
$\bar{\Omega}(t)$	78	78	74	68	59	49	28	32	9.3	16
$H_N(t)$	.00	.18	.33	.52	.72	.92	.02	.68	.04	.54
$\overline{h^2}(t)$	.36	.37	.40	.46	.56	.77	.36	.56	.35	.48
$R_\lambda(t)$	27	27	28	31	34	38	17	25	14	19
$Q(t)$	.14	.14	.134	.12	.09	.06	.14	.09	.14	.10
$S_T(t)$	21	20	12	17	14	7.9	19	14	19	17

Table 3.1: Data from DNS of decaying turbulence with different mean helicities. Note that $\bar{E}(t=0) = 2.8$ and $\bar{\Omega}(t=0) = 56$ for all runs.

$T_N(t)$ over the energy containing modes (all k such that $T(k,t) < 0$):

$$S_T(t) = -\sum_{T(k,t)\leq 0} T_N(k,t). \tag{3.20}$$

Obviously, $S_T(t)$ indicates how rapidly the energy of the energy containing modes is being transferred to the smaller scales. Similarly, $Q(t)$ relates the average magnitude of the nonlinear term of the NSE, which is responsible for the energy transfer, to the average magnitude of energy and enstrophy. (See also Kraichnan & Panda (1989) and Chapter 5 for further details on the normalized mean-square nonlinear term in turbulent flows.) The data in Table 3.1 indicate that the presence of non-zero mean helicity has significant consequences for the dynamics and nonlinearity of turbulent flows only if H_N is quite large. We remark that the maximum Kolmogorov wavenumber k_D for run O_{max} was 26.6, compared with 28.9 for O_{zero}. As a consequence, run O_{max} is slightly better resolved, consider the upward turns of the energy spectra in Figs. 3.2 and 3.3.

3.4 Simulations of Forced Turbulence

In simulations of quasi-stationary homogeneous isotropic turbulence the Navier-Stokes equation is augmented by a random force $\vec{f}$

$$\frac{\partial \vec{v}}{\partial t} = \vec{\lambda} - \nabla \tilde{p} + \nu \nabla^2 \vec{v} + \vec{f}. \tag{3.21}$$

The initialization procedure described in Section 3.2 may readily be modified to provide a (helical) isotropic Gaussian random force; $\delta-$correlated in wave number and frequency

$$\langle f_i(\underline{k}) f_j(\underline{k}') \rangle = \{P_{ij}(\vec{k}) F_0(k) + i\epsilon_{ijk} k_k G_0(k)\} \delta(\underline{k} - \underline{k}'), \tag{3.22}$$

where $\underline{k} = (\vec{k}, \omega)$. We shall compare in the following simulations with non-helical forcing and maximally helical forcing $G_0(k) = F_0(k)/k$. As in the previous Section, we are mainly concerned here with the influence of helicity on the energy transfer and the nonlinearity of a turbulent flow. Let us nevertheless discuss first some general points that are not related to helicity.

No consensus has been reached so far on the optimal choice of the wave number range and the power-law dependence of the random forcing spectrum. (The overall forcing amplitude is chosen by trial and error such that a well-resolved quasi-stationary state is reached after a transitory period of a few turnover times.) In simulations of forced turbulence similar to ours (but with non-helical forcing), Panda *et al.* (1989) chose $F_0(k) \sim k^{-3}, 0 < k < 1/2\, k_{max}$, i.e. they imposed only a high-k cutoff on the forcing at one half of the maximum wave number. Preliminary runs of this kind at lower resolution (32^3) displayed a clearly visible bend in the energy spectrum $E(k)$ at the cutoff $1/2\, k_{max}$. We therefore followed a suggestion by Rogallo (1988) and performed two simulations with $F_0(k) \sim k^{-5}, 0 < k < 1/2\, k_{max}$: run CFR with non-helical forcing and run CFM with maximally helical forcing ($k_{max} = 32$ in our runs). Time-averaged results from these simulations are presented in Table 3.2. In these two simulatons the fluctuations with time in the quasi-stationary state are quite significant, and they do not seem to diminish with time, i.e. they are not a transitory effect. To illustrate this, we present a plot of the average energy $\bar{E}(t)$ of run CFR in Fig. 3.12 over a period of 60 turnover times. Similarly, the average enstrophy $\bar{\Omega}(t)$ fluctuates wildly in the range $25 < \bar{\Omega} < 50$. Panda *et al.* (1989) also report fluctuations of average energy and enstrophy with time, although not as severe as here. We believe that the strong fluctuations occur because too much energy accumulates at the largest scales of the simulation, $k = 1 - 2$, if the range of forcing extends down to the lowest wave numbers. There are very few modes in low-k shells, and the size of the corresponding eddies is comparable to the dimension of the computational domain - a very undesireable situation. The fluctuations in run CFR and CFM are more severe than the fluctuations reported by Panda *et al.* (1989), because

run	T	$\bar{E}$	$\bar{\Omega}$	R_λ	L	λ	k_D	F	S	H_N	$\overline{h^2}$	Q	S_T
CFR	58	2.8	35	60	1.3	.65	24	4.2	.42	.02	.35	15	.16
CFM	20	3.5	36	76	1.5	.74	24	4.3	.44	.48	.44	13	.16
EFR	28	1.3	32	27	.66	.45	22	3.7	.47	.00	.36	19	.14
EFM	23	1.5	29	34	.70	.51	23	3.7	.37	.74	.59	14	.08

Table 3.2: Time averaged quantities from simulations of forced turbulence. T - number of turnover times; $\bar{E}$ - average energy; $\bar{\Omega}$ - average enstrophy; R_λ - Taylor microscale Reynolds number; L - integral length scale; λ -Taylor microscale; k_D - Kolmogorov wave number; F, S - flatness and skewness of velocity derivatives; H_N - normalized helicity; $\overline{h^2}$ - mean square normalized helicity density; Q - normalized mean square nonlinear term; S_T - total normalized transfer.

our forcing spectrum is considerably steeper, therefore an even larger portion of the total energy is fed into the largest scales.

We therefore decided to carry out simulations where the forcing is restricted to a narrow band of wave numbers, $F_0(k) \sim k^{-5}, 3 < k < 4$. The time-averages obtained from simulations EFR (non-helical forcing) and EFM (maximally helical) are also presented in Table 3.2. As anticipated, the fluctuations with time are now much weaker than those of runs CFR, CFM, and Panda's simulations, consider the time evolution of $E(t)$ from run CFR in Fig. 3.12. The average energy $\bar{E}$ and the Taylor-microscale Reynolds number R_λ of runs EFR and EFM is of course much lower than in runs where the forcing extends to the lowest wave numbers, because there is very little energy in the largest scales. On the other hand, the average enstrophy $\bar{\Omega}$, which is proportional to viscous dissipation $\epsilon = 2\nu\Omega$ and therefore essentially determined by the resolution of the simulation, is of comparable magnitude in all four runs .

The small scale properties of the E-runs are quite similar to those of the C-runs, consider the skewness S and flatness F of the velocity derivatives, the Taylor-microscale λ and the Kolmogorov wave number k_D in Table 3.2., and also the energy spectra $E(k), k > 10$ in Figs. 3.13, 3.15 and 3.14, 3.16.

As in the work by Panda *et al.* (1989), the energy spectrum $E(k)$ of run CFR, which was forced over a wide range of wave numbers, osculates a $k^{-5/3}$-Kolmogorov spectrum.

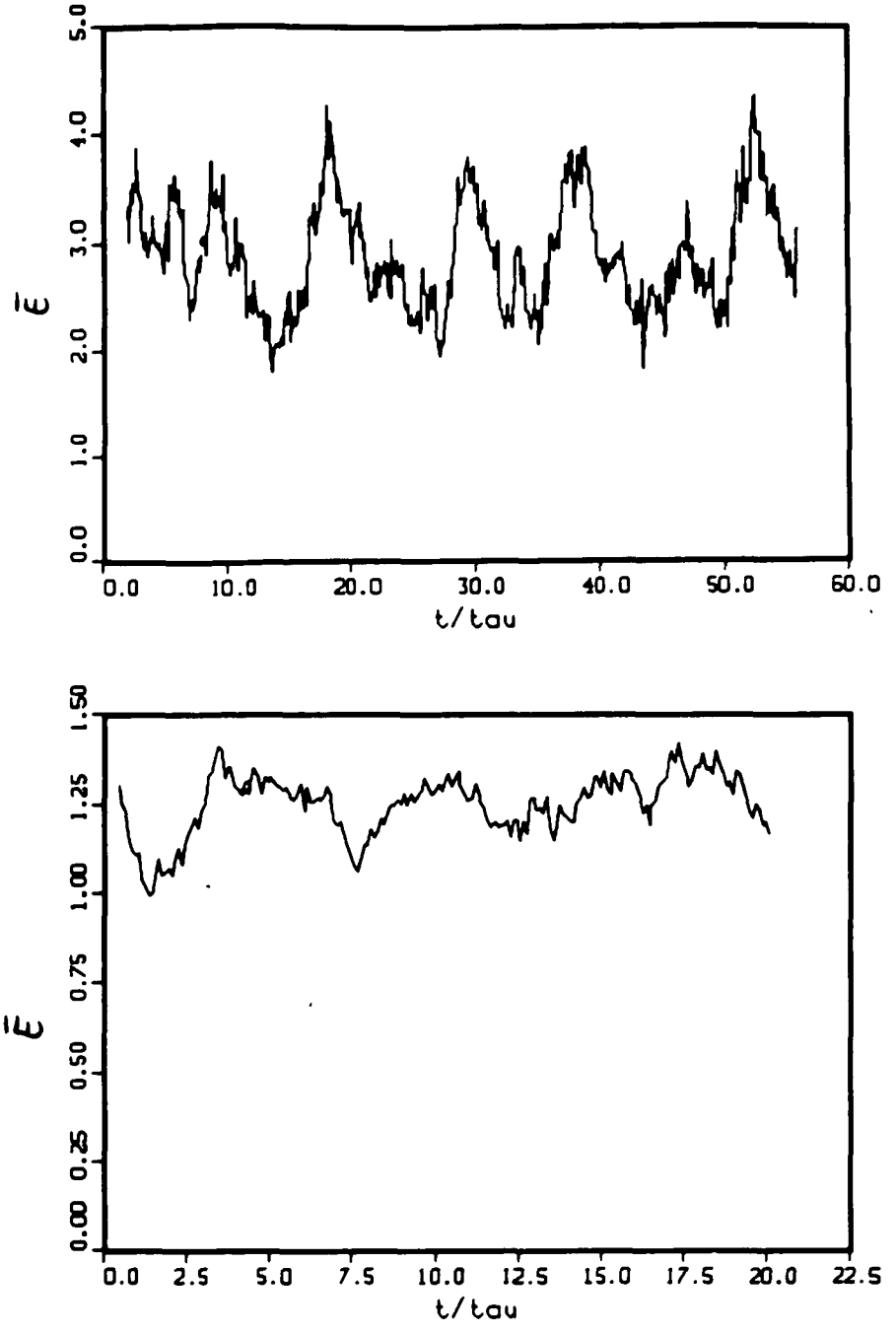

Figure 3.12: Time evolution of the average energy $\bar{E}$ of run CFR (top) and EFR (bottom).

However, a plot of the inertially weighted energy spectrum $\epsilon^{-2/3}k^{5/3}E(k)$ on a linear scale indicates that one should not speak of an 'inertial range' in such low-resolution simulations, see Fig. 3.13. This figure also indicates that the Kolmogorov constant $C_K \approx 2$ in run CFR, larger than the value $C_K \approx 1.6$ reported by Panda *et al.* (1989). We suggest that this is because the Reynolds numbers accessible to direct numerical simulations are not high enough to allow for true self-similarity. Consequently, the higher value of the molecular viscosity $\nu = 0.015$ (compared to $\nu = 0.01$ for the 64^3 simulations in Panda *et al.*) might well account for the discrepancy in C_K. The lower value of viscosity might also be the reason why the energy spectra $E(k)$ in Panda *et al.* (1989) do not display a clearly visible bend at the cutoff k_{max} of the forcing.

The forcing in a narrow band (runs EFR,EFM) leads to a rather bizarre peak in the compensated energy spectrum, see Figs. 3.15 and 3.16. Fortunately, the shape of the energy spectra for $k > 5$ indicate that the small scale properties of these runs are not severely affected by this peak. Indeed, the data concerning the small scales in Table 3.2 are entirely within the range expected for well resolved direct numerical simulations of turbulence at moderate Reynolds numbers. We conclude that it is most advantageous for simulations of quasi-stationary isotropic turbulence to force in a continuous band, $F_0(k) \sim k^n$, $k_0 < k < 1/2\,k_{max}$. The lower cutoff of the forcing should be $k_0 \approx 3 - 4$, probably higher for simulations at higher resolution, the choice of the power-law exponent n possibly depends on the value of the molecular viscosity.

Let us now turn our attention to the influence of helical forcing on the characteristics of a turbulent flow. The helicity spectra of runs CFM and EFM are plotted in Fig. 3.17. We see that there is considerable helicity on all scales, i.e. there is a cascade of helicity towards the small scales. However, only the wave numbers that are forced most strongly ($k \approx 1$ for CFM and $k \approx 3$ for EFM) are maximally helical, and it seems that the normalized helicity decreases with increasing scale. As a result, the time average of the normalized helicity H_N is considerably less than 1: $H_N = 0.48$ for CFM and $H_N = 0.74$ for EFM. Nevertheless, there is a considerable influence on the dynamics. Although the amplitude of the forcing does not differ in the helical and non-helical simulations, the helical flows have more energy, especially the wave number ranges where the forcing is strongest (see Table 3.2

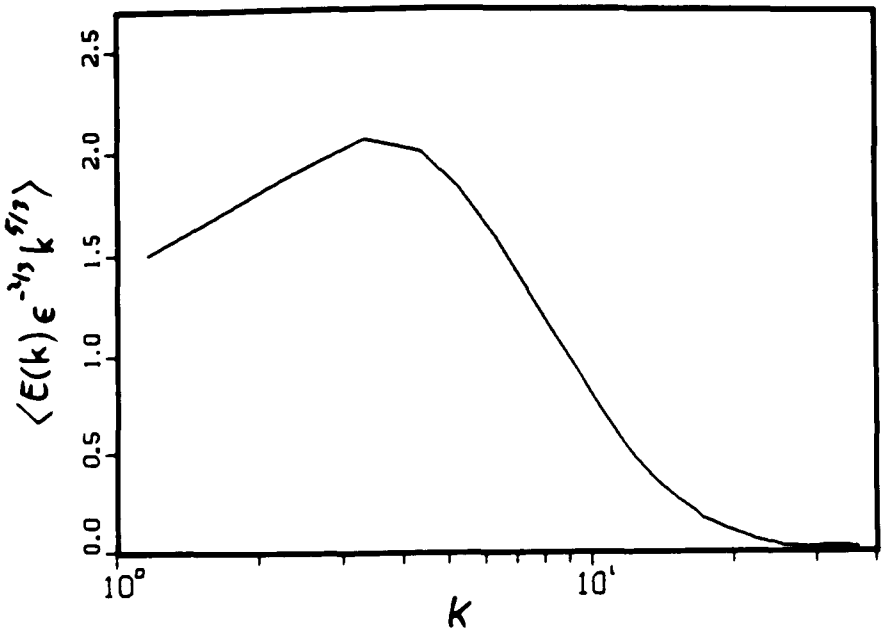

Figure 3.13: Time-averaged, inertially weighted energy spectrum $E(k)\epsilon^{-2/3}k^{5/3}$ of run CFR.

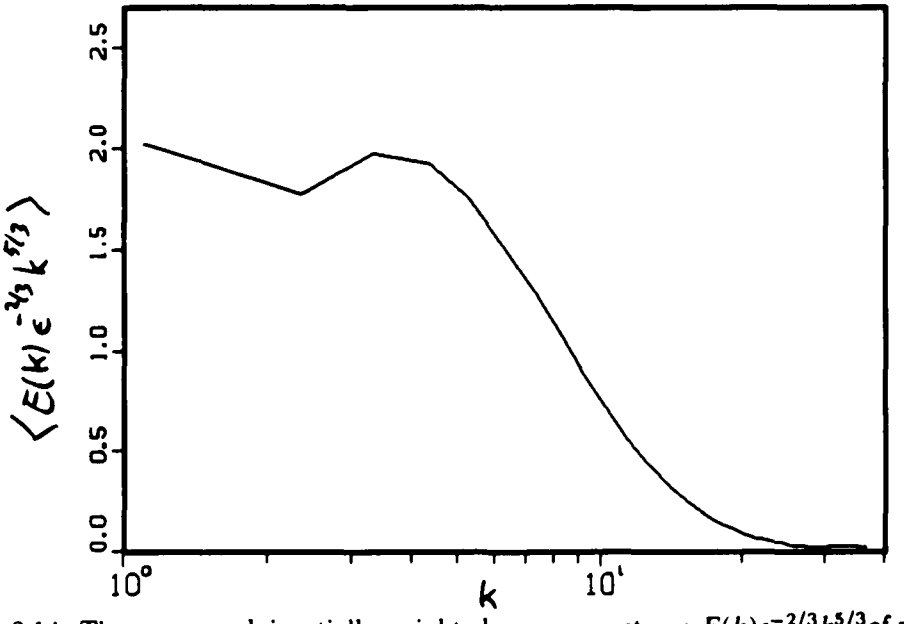

Figure 3.14: Time-averaged, inertially weighted energy spectrum $E(k)\epsilon^{-2/3}k^{5/3}$of run CFM.

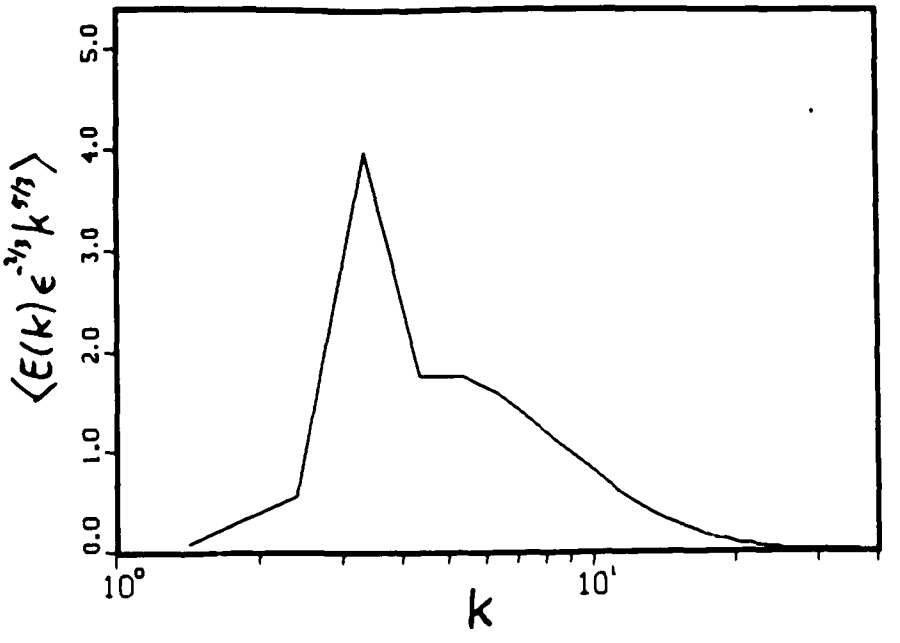

Figure 3.15: Time-averaged, inertially weighted energy spectrum $E(k)\epsilon^{-2/3}k^{5/3}$of run EFR.

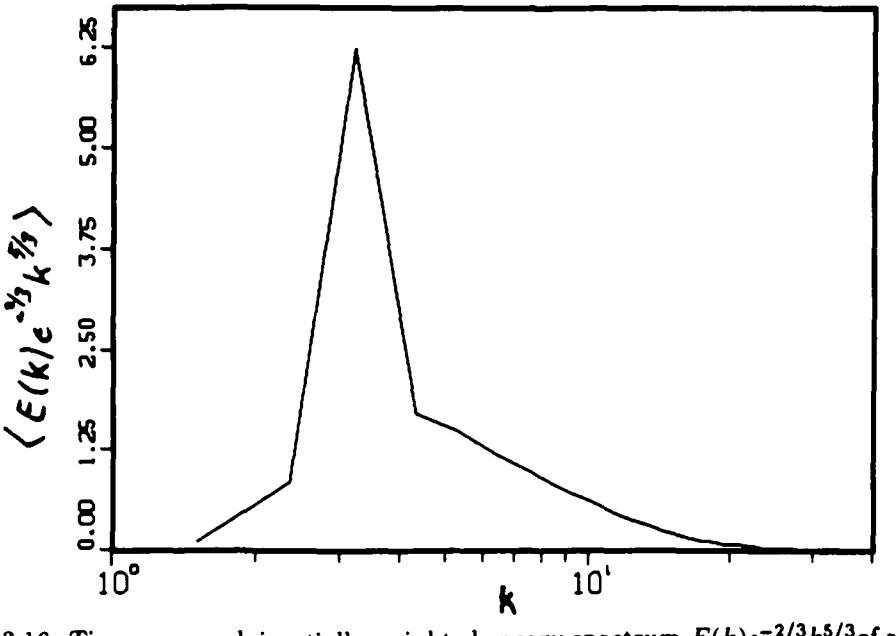

Figure 3.16: Time-averaged, inertially weighted energy spectrum $E(k)\epsilon^{-2/3}k^{5/3}$of run EFM.

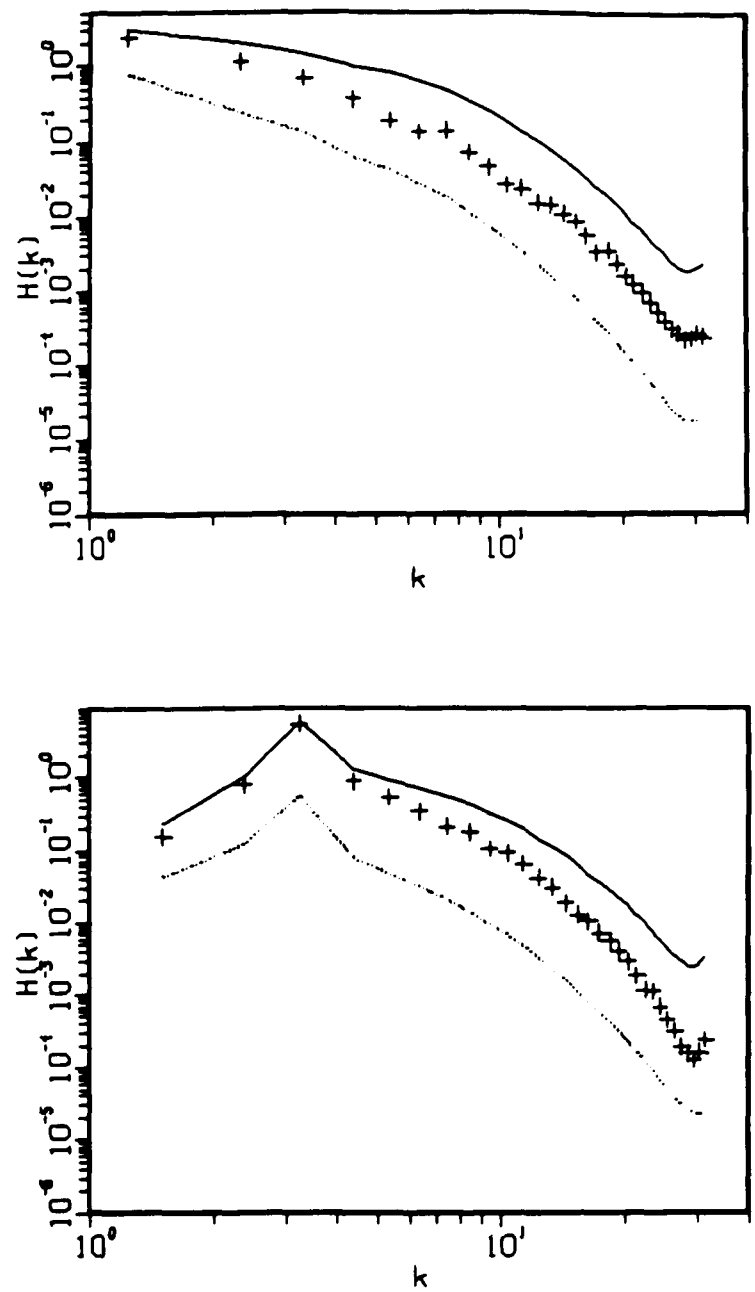

Figure 3.17: Helicity spectrum $H(k)$ (+ signs), maximum helicity $2kE(k)$ (continuous line) and standard deviation $\sigma_G(H(k))$ (dotted line) of run CFM (top) and EFM (bottom).

and Figs. 3.13 - 3.16). Note that the enstrophy $\bar{\Omega}$ does not depend strongly on the helicity of the forcing, because the enstrophy is proportional to the rate of dissipation, which in a stationary state will be equal to the rate at which energy is fed into the system. As already mentioned, the latter is determined by the available resolution and does not depend on the helicity in our simulations. Mean helicity also depresses the total normalized transfer S_T and the mean-square nonlinear term Q (see the previous section). The depression is much more pronounced for run EFM, where the normalized helicity H_N is considerably higher. Comparing Tables 3.1 and 3.2, we see that the presence of mean helicity affects decaying and forced turbulent flows in roughly the same way.

3.5 Conclusions

We have developed an algorithm for the direct numerical simulation of homogeneous turbulent flows with non-zero mean helicity. In simulations of helical decaying flows we have found that the presence of strong mean helicity $\bar{H}$, i.e. normalized helicity $H_N \approx 0.5 - 1$, results in a significant reduction of the normalized mean square nonlinear term and of the transfer of energy towards smaller scales. This is in agreement with EDQNM simulations by by André & Lesieur (1977). As a consequence of the reduced energy transfer, the buildup of enstrophy typically observed in the early stage of a DNS is inhibited, and the average viscous dissipation $\bar{\epsilon}$ is reduced. Note that the latter is not in contradiction with results by Rogers & Moin (1987), who observed that in turbulent flows with vanishing mean helicity there is no significant correlation between the helicity density γ and viscous dissipation ϵ. Furthermore, if the helicity of the initial field is large, the flatness and skewness of the velocity derivatives reach values typical of turbulent flows at moderate Reynolds numbers at later times. In a decaying helical flow the normalized helicity H_N decreases rapidly with time, it follows that after a few turnover times an initially strongly helical flow will decay much like a non-helical flow.

In a quasi-stationary flow the helicity injected by helical forcing will accumulate mostly in the forced (large) scales. Our data indicate that, again, the presence of significant mean helicity reduces the mean square nonlinear term and the energy transfer towards smaller scales, and we observe that the forced scales are significantly more energetic if the forcing

is helical. Note that the rate of dissipation in a forced, quasi-stationary simulation will be equal to the rate of energy input by the forcing and cannot be affected by the helicity of the forcing. Although there is a cascade of helicity to the smaller scales in the case of helical forcing, the normalized helicity is observed to decrease with increasing wave number, i.e. the small scales are not strongly helical. This supports Kraichnan's (1973) conclusion that the inertial range cascade in helically forced turbulence should not differ asymptotically from the non-helical case.

These findings lend support to Lilly's (1986) work, who suggested that certain types of storms owe their notable stability and longevity to the effect of helicity on the turbulent energy transfer. We must emphasize, though, that the large normalized helicity ($H_N \approx 0.8 - 1.$) of the mean velocity field in these storm systems is due to very special forcing mechanisms and boundary conditions, and most likely not a result of an intrinsic self-organizing tendency of homogenous turbulent flows.

Chapter 4

Fluctuations of Helicity

The results of direct numerical simulations presented in the previous chapter show - in agreement with earlier work by André & Lesieur (1977) - that the presence of strong mean helicity in a turbulent flow leads to a depression of the mean square nonlinear term and a reduction of the transfer of energy to the small scales. It is therefore of obvious interest to investigate whether spatial or temporal helicity fluctuations are 'dynamically significant', i.e. large enough to noticeably influence - at least locally or momentarily - the nonlinear term or the energy transfer. One might also ask if there is a mechanism that can cause the mean helicity of an initially non-helical flow to grow to a dynamically significant magnitude? Such ideas have been at the core of theoretical work on the structure of turbulence, which we have already outlined in the Introduction. Let us recall briefly the development of ideas up to the point when this work was begun. Levich & Tsinober (1983a,1983b) suggested that the large scales of a decaying turbulent flow should become strongly helical because of an inverse cascade of mean-square helicity. This concept is based on the properties of the 'I-invariant' $I = \int \gamma(\vec{x})\gamma(\vec{x}+\vec{r})d\vec{r} = \langle H^2 \rangle / V$, which is an inviscid invariant of the NSE and was used by the authors to define an intrinsic scale, $\mathcal{L} = I/\bar{E}^2$. It was argued that during the decay, $dE/dt < 0$, I can stay unchanged through a upscale transfer of helicity fluctuations towards larger scales, $d\mathcal{L}/dt > 0$. Moffatt (1985) proposed a scenario of a universal spatial structure of homogeneous turbulence, where long-lived, relatively quiescent regions of high helicity density are separated by (vortex) sheets of turbulent activity. More recently Hussain (1986) suggested that vortical coherent structures are not necessarily long-lived, and it was acknowledged that the time-scale of helicity fluctuations might correspondingly be quite

small (Levich, 1987). Levich & Shtilman (1988) argued that the inviscid conservation of the I-invariant should lead to a build-up of (universal) phase correlations $\langle H(\vec{k})H(\vec{k}')\rangle \neq 0$ for $\vec{k} \neq \vec{k}'$ at all scales, rather than an inverse cascade. The presence of wave packets of coherent helicity in a turbulent field would cause helicity correlations to grow, and thereby make possible the conservation of I in spite of the decay process. It was suggested that the phase correlations will be most pronounced at the large scales, because those scales essentially determine the value of I. In support of their arguments, the authors reported that the helicity spectrum $H(k)$ in direct numerical simulations displays large fluctuations in time, especially at low wave numbers. Also, the distribution function of the normalized helicity density h of Fourier transformed wave-packets ('filtered fields') was found to be highly skewed. Levich & Shtilman (1988) concluded tentatively that the dynamical evolution of turbulent flows should generally favor the appearance of phase coherence. In physical space, a build up of coherent helicity fluctuations could lead to an increase of the correlation length of the helicity density. In analogy with the theory of second order phase transitions, Levich & Shtilman (1988) suggested that a spontaneous breaking of (reflexional) symmetry might be associated with such an increase in correlation length, a concept that was elaborated on by Kit *et al.* (1988).

However, as one is concerned here with the *fluctuations* of helicity, one is advised to argue very carefully when relating observations made in one (or a few) simulations to theoretical scenarios. Modern theories of turbulence are usually formulated in the language of statistical mechanics, i.e. results are given as ensemble means or expectation values, whereas a numerical simulation is only one realization from the ensemble of 'infinitely many' flows. Often this does not lead to great difficulties. For example, one usually assumes that the energy spectral density $E(k)$ of one simulation is representative of the ensemble averaged energy spectrum $\langle E(k)\rangle$. One may do so, because the *relative* magnitude of fluctuations $|E(k) - \langle E(k)\rangle| \,/\langle E(k)\rangle$ is quite small in large scale numerical simulations. On the other hand, in a reflectionally symmetric ensemble of turbulent flows the ensemble means of helicity, its spectral density, etc., are generally zero. Therefore, helicity fluctuations will always be 'large' when compared to the ensemble mean, and the 'statistical variability' (Eswaran & Pope, 1988) of helicity related quantities will be very high. Indeed, initializing

simulations with different sets of random numbers (but otherwise identical parameters) typically results in quite different initial values of $\bar{H}$, $H(k)$, etc., and also in quite different temporal behavior of these quantities.

The average helicity $\bar{H} = \sum_{\vec{k}} H(\vec{k})$ and especially the helicity spectrum $H(k) = \sum_{S(k)} H(\vec{k})$ of numerical simulations will be non-zero even in the absence of 'anomalous' or 'coherent' fluctuations, because the volume of the computational domain is finite and the simulations are not capable of modelling the thermodynamic limit. (For example, the helicity of 'random helicity' Gaussian fields, where the phase angle $\phi(\vec{k})$ is distributed uniformly over $[0, 2\pi]$, is typically a few percent of the maximum helicity. The mean $\langle H \rangle$ over an ensemble of such fields vanishes.) It is clearly not feasible to make the computational domain much larger than the integral scale of the simulated turbulent flow, or to run a simulation many times with different random numbers used in the initialization. It is therefore necessary to supplement numerical data with a careful statistical analysis, which allows to assess the statistical significance of observed helicity fluctuations. We will compare the magnitude of observed fluctuations with an estimate of the standard deviation σ_G of helicity obtained from a 'random-phase' or 'quasi-Gaussian' approximation. Only fluctuations that significantly exceed their respective σ_G-value should be called 'anomalous' or 'coherent' fluctuations. (Whether fluctuations 'of order σ_G' are dynamically significant in fully developed turbulent flow may be judged by simple scaling arguments, see below.)

Let us outline the contents of this chapter: In the next section we derive the random-phase approximation for the standard deviation σ_G and demonstrate that it is essentially equivalent to a quasi-Gaussian approximation, first employed in this context by Levich & Tsinober (1983a). In Section 4.2 we show that this approximation is compatible with simple Kolmogorov scaling supplemented by elementary statistical considerations. We then argue that one should expect sweeping corrections to σ_G at large Reynolds numbers, because the helicity density γ is not Galilean invariant. We also discuss briefly the limits of validity of the quasi-Gaussian approximation, which is known to yield unphysical results when used straightforwardly in closure schemes (Orszag, 1977). Possible implications of the scaling properties of the viscous term in the helicity balance equation (1.5) for fully developed turbulence are discussed in Section 4.3 . We conclude this Chapter with numerical data

from simulations of decaying and quasi-stationary turbulence, where it is found that the fluctuations of the helicity of the large scales are in good agreement with the random-phase approximation. The small scales, however, fluctuate in a seemingly coherent fashion and therefore also with larger amplitudes than the value of σ_G would lead one to expect.

4.1 The Quasi Gaussian Approximation

Recall the alternative expression (3.8) for the helicity of one mode

$$H(\vec{k}) = 2\vec{k} \cdot [Re(\vec{v}(\vec{k})) \times Im(\vec{v}(\vec{k}))] = 2k|Re(\vec{v}(\vec{k}))|\,|Im(\vec{v}(\vec{k}))|\,\sin\phi(\vec{k}). \qquad (4.1)$$

Obviously, the helicity of a mode of given energy $E(\vec{k}) = \frac{1}{2}(R(\vec{k})^2 + I(\vec{k})^2)$ (let us denote $R(\vec{k}) = |Re(\vec{v}(\vec{k}))|$ and similarly for $I(\vec{k})$) strongly depends on the phases and in particular on the 'phase angle' $\phi(\vec{k})$ between the real and the imaginary part of the velocity $\vec{v}(\vec{k})$. Also, to assume that in reflexionally symmetric flows with vanishing mean helicity the helicity $H(\vec{k})$ of each mode is vanishing imposes a very severe constraint on the phases. Instead, one would expect that small values of helicity are obtained by mutual cancellations of uncorrelated contributions of alternating sign from different modes and scales. This suggests that a random-phase approximation should yield a first estimate of the typical magnitude of the helicity spectrum $H(k)$ or the average helicity $\bar{H}$ in one realization (one simulation) of an isotropic (non-helical) ensemble of turbulent flows. In this approximation, one assumes that the phases $\phi(\vec{k})$ of all modes fluctuate randomly and *independently* from each other. If one observes in a numerical simulation fluctuations of helicity that are significantly larger (or smaller) than the random-phase estimate, one may conclude that wave packets of coherent phase (or 'coherent helicity') are present in the flow.

By assumption, the distribution function of ϕ is uniform over the interval $[0, 2\pi]$ and R, I and ϕ are statistically independent (recall that the real and imaginary part of one mode may be regarded as *two* degrees of freedom.) The helicity spectrum is now zero in the ensemble mean:

$$\langle \sin\phi(\vec{k}) \rangle = \langle H(\vec{k}) \rangle = \langle H(k) \rangle = \langle \bar{H} \rangle = 0, \qquad (4.2)$$

and the variance of the helicity spectral density $\mathrm{Var}(H(k)) = \langle H(k)^2 \rangle - \langle H(k) \rangle^2$ is simply equal to the mean square of the helicity spectrum, for which we obtain approximately

(Polifke & Shtilman, 1989):

$$\begin{aligned}\langle H(k)^2\rangle &\approx \sum_{k-\frac{\Delta k}{2}\le\vec{k}',\vec{p}'<k+\frac{\Delta k}{2}} 4k^2\,\langle R(\vec{k}')R(\vec{p}')I(\vec{k}')I(\vec{p}')\rangle\,\langle\sin\phi(\vec{k}')\sin\phi(\vec{p}')\rangle \qquad (4.3)\\ &= \sum_{S(k)} 4k^2\langle R^2(\vec{k}')\rangle\langle I^2(\vec{k}')\rangle = N(k)\;4k^2\left\langle\frac{E(k)}{N(k)}\right\rangle^2\\ &= \frac{4k^2}{N(k)}\langle E(k)\rangle^2 = \frac{1}{\pi\rho\Delta k}\langle E(k)\rangle^2.\end{aligned}$$

Here $\langle\sin\phi(\vec{k}')\sin\phi(\vec{p}')\rangle = \langle\sin^2\phi(\vec{k})\rangle\left[\delta(\vec{k}'+\vec{p}')+\delta(\vec{k}'-\vec{p}')\right] = \delta(\vec{k}'+\vec{p}')$ because of the complex conjugate symmetry of the velocity field $\vec{v}^*(\vec{k}) = \vec{v}(-\vec{k})$. Note that $\langle\sin^2\phi\rangle = \frac{1}{2}$, because $Re(\vec{v}(\vec{k}))$ and $Im(\vec{v}(\vec{k}))$ are confined to lie in the plane perpendicular to $\vec{k}$. Also, we assumed here that the average energy per mode does not fluctuate too strongly in one k-shell, and therefore $\langle R(\vec{k})^2\rangle = \langle I(\vec{k})^2\rangle = \langle E(k)\rangle/N(k)$. The number of modes within one k-shell $N(k) = 4\pi k^2\rho\Delta k$. Note that the variance of $H(k)$ is proportional to $1/N(k)$, which is just what elementary probability theory would lead us to expect.

In similar manner one may derive an estimate for the mean square of the average helicity $\bar{H}$

$$\langle\bar{H}^2\rangle \approx \frac{1}{\pi\rho\Delta k}\sum_k\langle E(k)\rangle^2, \qquad (4.4)$$

which is - up to a normalization factor - just the finite volume equivalent of the I-invariant (Levich & Tsinober, 1983a):

$$I = \lim_{V\to\infty}\int d\vec{r}\,\langle\gamma(\vec{x})\gamma(\vec{x}+\vec{r})\rangle = \lim_{V\to\infty}\frac{1}{V}\left\langle\left[\int_V d\vec{x}\,\gamma(\vec{x})\right]^2\right\rangle = \lim_{V\to\infty}\frac{1}{V}\langle H^2\rangle. \qquad (4.5)$$

Using a 'quasi-Gaussian approximation', Levich & Tsinober (1983a) have estimated

$$I \approx A\int dk\;E(k)^2. \qquad (4.6)$$

Recall that $\bar{H} = H/V$ is the volume average of helicity and the density of modes in k-space $\rho = V/(2\pi)^3$, therefore this is equivalent to (4.4), with $A = (2\pi)^3/\pi$.

Indeed, it is well known (Heisenberg, 1948, Monin & Yaglom, 1975) that a random-phase approximation is equivalent to a quasi-Gaussian approximation, also know as 'quasi-normal

approximation'. (The 'Millionshchikov hypothesis', which assumes that all forth-order two-point correlation tensors may be decomposed into products of second order tensors, is a weaker version of the quasi-Gaussian assumption, see Monin & Yaglom, 1975.) In the quasi-Gaussian approximation ('QGA') one neglects fourth order cumulants, i.e. fourth order moments are approximated by sums of second order moments,

$$\langle abcd\rangle \approx \langle ab\rangle\langle cd\rangle + \langle ac\rangle\langle bd\rangle + \langle ad\rangle\langle bc\rangle, \tag{4.7}$$

as if the random variables were Gaussian. Moreover, in Fourier space only correlators of opposite wave number $\langle v_i(\vec{k})v_j(-\vec{k})\rangle$ will survive. However, third order correlators are not assumed to be zero (therefore *qausi*-Gaussian approximation). It is instructive to repeat the derivation (4.4) of the mean square of the helicity spectrum, this time making explicit use of the general form (3.12) of the correlation tensor $S_{ij}(\vec{k})$ and the quasi-Gaussian approximation (4.7):

$$\begin{aligned}
\langle H(k)^2\rangle &= \left\langle \left[\sum_{S(k)} H(\vec{k}')\right]^2 \right\rangle \qquad (4.8)\\
&= \left\langle \left[\sum_{S(k)} -iv_i(\vec{k}')\epsilon_{ijk}k_j v_k(-\vec{k}')\right]^2 \right\rangle \\
&= -\sum_{k-\frac{\Delta k}{2}\le \vec{k}',\vec{p}' < k+\frac{\Delta k}{2}} \epsilon_{ijk}\epsilon_{rst}k'_j p'_s \langle v_i(\vec{k}')v_k(-\vec{k}')v_r(\vec{p}')v_t(-\vec{p}')\rangle .
\end{aligned}$$

Decomposing the fourth order moments into second order moments $\langle v_i(\vec{p})v_j(\vec{k})\rangle = S_{ij}(\vec{k})\delta(\vec{k}+\vec{p})$, and exploiting the symmetry of the correlation tensor, we obtain after some algebra

$$\langle H(k)^2\rangle_G = \langle H(k)\rangle^2 + \frac{1}{\pi\rho\Delta k}\langle E(k)\rangle^2 - \frac{1}{4\pi k^2\rho\Delta k}\langle H(k)\rangle^2. \tag{4.9}$$

The subscript 'G' is to remind us that this is an estimate obtained with the help of the quasi-Gaussian assumption. The mean helicity spectrum will be zero in a reflexionally symmetric ensemble, and we see that in this case we indeed have reproduced the result (4.4) of the random phase approximation. Note, however, that the QGA yields valuable results where the random phase approximation is not applicable, i.e. in the presence of

mean helicity. Consider, e.g. a maximally helical ensemble $\langle H(k)\rangle = 2k\langle E(k)\rangle$, where $\phi = \pi/2$ for all modes. According to (4.9), the variance of $H(k)$ will be vanishing. This is an (almost) correct result: the helicity of every mode in every realization must be maximal if the ensemble average is to be maximal; statistical fluctuations of helicity are possible only inasmuch as the energy spectrum $E(k)$ itself is fluctuating. In general one may state that the presence of mean helicity will reduce the magnitude of fluctuations.

One may also derive an approximation for the mean square of the volume-averaged helicity (compare with (4.4)) and of the viscous dissipation term

$$\langle \bar{H}^2\rangle_G = \left[\sum_k \langle H(k)\rangle\right]^2 + \frac{1}{\pi\rho\Delta k}\sum_k \left[\langle E(k)\rangle^2 - \frac{1}{4k^2}\langle H(k)\rangle^2\right], \tag{4.10}$$

$$\langle [2\nu \sum_k k^2 H(k)]^2\rangle_G = \left[2\nu\sum_k k^2\langle H(k)\rangle\right]^2 + \frac{\nu^2}{\pi\rho\Delta k}\sum_k \left[4k^4\langle E(k)\rangle^2 - k^2\langle H(k)\rangle^2\right]. \tag{4.11}$$

It is essentially the scaling behavior of the viscous term (4.11) in the limit of large Reynolds numbers that has inspired the work on the importance of helicity fluctuations in turbulence. We shall turn to this point in Section 4.4.

The QGA approximates the probability distribution function of the helicity spectrum in a non-helical flow as a bell curve of width $\sigma_G(H(k)) = (\langle H(k)^2\rangle_G - \langle H(k)\rangle^2)^{-1/2}$. In other words, the typical magnitude of the helicity spectrum in a DNS with non-helical initial conditions or forcing should be of the order of the standard deviation $\sigma_G(H(k))$. In our simulations both the density ρ and the width of k-shells Δk are equal to one, and if we assume that the energy spectrum of one simulation is representative of the ensemble, $\langle E(k)\rangle \approx E(k)$, we obtain with the quasi-Gaussian or random-phase approximation (4.9):

$$\sigma_G(H(k)) \approx \sqrt{\frac{1}{\pi}}E(k), \tag{4.12}$$

which is the expression given in Polifke & Shtilman (1989). Similarly, we obtain from (4.10) for the space average helicity $\bar{H}$

$$\sigma_G(\bar{H}) \approx \sqrt{\frac{1}{\pi}\sum_k E(k)^2}. \tag{4.13}$$

Obviously, $\sigma_G(H(k))/H_{max}(k) \sim 1/k$. It follows (with Tables 3.1, 3.2) that fluctuations of helicity in fully developed turbulence will be dynamically insignificant if their magnitude is

of order σ_G, simply because then the helicity will only be a small fraction of the maximum helicity.

4.2 Kolmogorov Scaling and Sweeping Corrections

It is not difficult to show that order of magnitude estimates for the fluctuations of helicity in agreement with the QGA may be obtained by Kolmogorov-type scaling arguments, if one takes into account that helicity is not a positive definite quantity.

In fully developed homogeneous isotropic turbulence the rate of decay of kinetic energy ϵ should be determined by the properties of the largest eddies, i.e. one may estimate that

$$\bar{\epsilon} = d\bar{E}/dt \sim \frac{U^3}{L}. \tag{4.14}$$

Here U is the typical velocity of the large eddies, L their size. Kolmogorov argued that at sufficiently large Reynolds numbers $R = UL/\nu$ a so-called 'inertial range' will develop, throughout which kinetic energy is cascading towards smaller scales at a transfer rate equal to the rate of viscous dissipation ϵ without undergoing significant dissipation. Inertial range length scales are much smaller than the large scales L of the flow and much larger than the dissipative length scale η. Following the presentation given in Landau & Lifshitz (1987), one may now estimate the change $\Delta v(r)$ in turbulent velocity over a distance r, where r is an inertial-range length scale. Namely, $\Delta v(r)$ should only depend on the value of the energy transfer ϵ, and on the length r. Dimensional considerations show that

$$\Delta v(r) \sim \epsilon^{1/3} r^{1/3}. \tag{4.15}$$

This yields immediately Kolmogorov's 5/3-law for the power-law behavior of the energy spectrum $E(k)$ in the inertial range

$$E(k) \sim \epsilon^{2/3} k^{-5/3}. \tag{4.16}$$

Similarly, in the absence of mean helicity one might estimate the change $\Delta\gamma(r)$ in the helicity density over a distance r

$$\Delta\gamma(r) \sim \epsilon^{2/3} r^{-1/3}. \tag{4.17}$$

The corresponding power-law exponent for the helicity spectrum $H(k)$ is

$$H(k) \sim \epsilon^{2/3} k^{-2/3}. \tag{4.18}$$

However, the helicity spectrum $H(k) = \sum_{S(k)} H(\vec{k})$ is the sum over a (large) number $N(k)$ of positive and negative contributions $H(\vec{k})$ from the modes $\vec{k}$ in one shell. These contributions will tend to cancel each other, and the more modes, the more complete the cancellations will be. In fact, elementary probability theory tells us that we should expect fluctuations of order $1/\sqrt{(N(k)}$, where $N(k)$ is the number of modes in one k-shell. Therefore, scaling plus statistics yields for the order of magnitude of the helicity spectrum

$$|H(k)| \sim \sigma(H(k)) \sim N(k)^{-1/2} \epsilon^{2/3} k^{-2/3}. \tag{4.19}$$

(Again, we mean to say that the probability distribution function of the helicity spectrum should have the given width.) Recall that $N(k) \sim \rho k^2 \Delta k$, and we recover with (4.16) the random-phase or quasi-Gaussian prediction (4.12)

$$|H(k)| \sim E(k), \tag{4.20}$$

which illustrates that indeed the choice of the random-phase approximation is the appropriate 'zeroth-order' approximation for of helicity fluctuations.

Let us now discuss possible causes for deviations from the QGA. It is well know that the non-uniform spatial distribution of viscous dissipation ϵ leads to intermittency corrections to the power-law exponents of the original Kolmogorov theory. However, these effects are most likely quite small for low-order moments, we shall therefore not discuss them here. Instead, we turn our attention to 'sweeping corrections'. It was pointed out by Tennekes (1975) that sweeping effects, i.e. the consequences of the advection of small eddies by larger ones should lead to significant deviations from the Kolmogorov scaling law $E(\omega) \sim \epsilon \omega^{-2}$ for the frequency spectrum of the kinetic energy (here ω denotes the frequency). Tennekes argued that the advection past the observation point of inertial-range eddies of scale r by large scale eddies of velocity U should determine the kinetic energy at frequency $\omega = U/r$. This leads to an (Eulerian) frequency spectrum $E(\omega) \sim \epsilon^{2/3} U^{2/3} \omega^{-5/3}$. It is important here that the inertial range scales are statistically independent from the large scales in the sense that the large scales do not 'distort' the small scales and thereby influence the dynamics of

their decay. Such statistical independence is also implied in the Kolmogorov theory, where it is assumed that the energy containing scales influence the small scales only indirectly by determining the rate of energy transfer. However, one must also realize that the advection of the small scale eddies by larger ones must lead to small scale phase correlations, i.e. the small scale wave packets must have the correct group velocity. In a velocity field with truly Gaussian statistics these phase correlations will be absent (Kraichnan, 1989). Clearly, the random-phase approximation discards such correlations, and advection effects may only be treated in a very qualitative (but straightforward) manner:

Equation (4.17) states that the helicity density $\gamma = \vec{v} \cdot \vec{\omega}$ should scale just like the product of velocity difference $\Delta v(r) \sim \epsilon^{1/3} r^{1/3}$ and vorticity difference $\Delta\omega(r) \sim \epsilon^{1/3} r^{-2/3}$. However, the helicity density is not Galilean invariant (Speziale, 1987). In the presence of a large scale advecting flow U, $U >> \Delta v(r)$, the difference in helicity density will scale with the advecting velocity U and the fluctuations of vorticity, i.e.

$$\Delta\gamma(r) \sim U\epsilon^{1/3} r^{-2/3}. \tag{4.21}$$

This simply means that the helicity of the small scales is mainly determined by the orientation of the small scale vorticity relative to the large scale flow. The corresponding correction to the power law of the helicity spectrum $H(k)$ in the inertial range is

$$|H(k)| \sim U\epsilon^{1/3} k^{-4/3}, \tag{4.22}$$

which will dominate the QGA estimate (4.20) at sufficiently high Reynolds number. One might object that the helicity spectrum $H(k)$ is - unlike the helicity density γ - Galilean invariant (Levich, 1987). This is so because adding a constant mean flow to a turbulent velocity field only affects the $\vec{k} = 0$ mode, which of course has zero vorticity and zero helicity in any coordinate frame. However, sweeping effects are of course not real (global) Galilean transformations, and the above equations should be understood as a merely dimensionally consistent attempt to incorporate the phase correlations caused by the advection of small eddies.

How much confidence may we put into the (sweeping corrected) QGA estimates for the magnitude of helicity fluctuations? It is well know (Monin & Yaglom, 1975) that the small scales of turbulent flows are not Gaussianly distributed. Also, the existence of structures in

physical space implies the existence of phase-correlations in Fourier space. Straightforward use of the quasi-Gaussian assumption in closure models of homogeneous isotropic turbulence has led to nonphysical results, i.e. negative energy spectra (Monin & Yaglom, 1975). One may argue qualitatively that this happens because evolution equations based on QGA retain too much information about earlier times (Leslie, 1973). In Orszag's (1977) words, the quasi-Gaussian models are not capable of representing the effects of 'nonlinear scrambling'. Note, however, that modified 'eddy-damped' quasi-normal schemes (Orszag, 1977) have been quite successful in reproducing inertial range properties of homogeneous turbulent flows (André & Lesieur, 1977).

We are certainly less ambitious in our use of the quasi-Gaussian assumption. After all, we do not attempt to model the time-evolution of the helicity; we only estimate the typical magnitude of the helicity (spectrum) of a *given* turbulent velocity field. Therefore, 'memory effects' will be insignificant in our approximation scheme, and we might hope to obtain estimates that are correct within an order of magnitude. Nevertheless, we must expect to find experimental deviations from QGA predictions. As a matter of fact, the interesting physics will be represented by the deviations from rather than the agreement with the random-phase assumption.

4.3 Implications for Decaying Turbulence at large Reynolds Numbers

In this Section we shall discuss possible consequences of the scaling behavior of the viscous term (4.11) in the helicity balance equation (1.5). Specifically, we will show that in the absence of phase correlations the volume average of helicity itself is an adiabatic invariant *in (almost) every realization* of a reflexionally symmetric ensemble of fully developed decaying turbulent flows. This also implies the adiabatic conservation of the I-invariant (Levich & Tsinober, 1983a) in the absence of phase correlations.

If turbulence is 'fully developed' ($R \gg 1$), a change in the molecular kinematic viscosity ν will not affect the decay rate ϵ. Instead, the small scales will adjust to the value of viscosity, i.e. with decreasing ν the dissipative range will move to smaller and smaller scales. Indeed, dimensional considerations show that the Kolmogorov scale η, where the

inertial range terminates, must scale as

$$\eta \sim (\frac{\nu^3}{\epsilon})^{1/4}. \tag{4.23}$$

It therefore seems appropriate to describe isotropic decaying turbulence at very large Reynolds number as the limiting case

$$\begin{aligned} &\nu \to 0, \\ &\eta \sim \nu^{3/4} \to 0, \\ &dE/dt = \epsilon = const. \end{aligned} \tag{4.24}$$

In this limit, the rate of change of average helicity $\bar{H}$ due to viscosity vanishes in the absence of mean helicity and phase correlations. Let us show how this comes about: In the absence of external stirring forces, the rate of change of average helicity $d\bar{H}/dt = -2\nu \sum_k k^2 H(k)$. It follows with the QGA estimate (4.11), which in the case of vanishing mean helicity $\langle H(k) \rangle = 0$ is essentially a random phase approximation, that

$$\left\langle \left(\frac{d\bar{H}}{dt} \right)^2 \right\rangle = \left[2\nu \sum_{k=1}^{k_D} k^2 \langle H(k) \rangle \right]^2 + \frac{\nu^2}{\pi \rho \Delta k} \sum_{k=1}^{k_D} \left[4k^4 \langle E(k) \rangle^2 - k^2 \langle H(k) \rangle^2 \right]. \tag{4.25}$$

Here we have explicitly indicated that the summation extends up to the Kolmogorov wave number $k_D \sim 1/\eta$. We assume here that $\langle H(k) \rangle = 0$, therefore only the second term on the r.h.s. of (4.25) is non-zero, and we see that in the limit of very large Reynolds number the total helicity becomes 'adiabatically invariant' ,

$$\lim_{\nu \to 0} \left\langle \left(\frac{d\bar{H}}{dt} \right)^2 \right\rangle \sim \lim_{\nu \to 0} \nu^2 \sum_{k=1}^{k_D} k^4 E(k)^2 \sim \lim_{\nu \to 0} \nu^2 {k_D}^{1+4-10/3} \sim \lim_{\nu \to 0} \nu^{3/4} = 0. \tag{4.26}$$

(Note that if we take sweeping corrections into account, we will obtain a $\nu^{1/4}$ power law.) This of course implies the adiabatic invariance of the I-invariant (Levich &Tsinober, 1983a, Levich & Shtilman 1988)

$$\lim_{\nu \to 0} \frac{dI}{dt} = 0. \tag{4.27}$$

By 'adiabatic invariance' we mean to say that in fully developed turbulent flow the time scale for changes in the average helicity due to viscosity will be much larger than the turnover time of large eddies, or the time scale for viscous decay of energy. Note that

this is not a trivial consequence of the conservation of helicity in Euler flows, where $\nu = 0$ and $d\bar{E}/dt = d\bar{H}/dt = 0$. Adiabatic invariance in the framework of the random phase approximation results from the scale separation characteristic of fully developed turbulence, and from the statistically independent fluctuations of the helicity spectral density. Let us elaborate: the value of $\bar{H}$ is essentially determined by the energy containing scales, and may be quite large because of the relatively small number of modes in low-k shells. Viscous dissipation of $\bar{H}$, on the other hand, occurs at large wave numbers $k \sim k_D$, and is determined by a large number of modes ($N(k) \sim k^2$). Therefore, contributions from individual modes of opposite sign to the viscous term $\nu \sum_{k \approx k_D} k^2 H(k)$ will effectively cancel each other. Indeed, *if the phases are random*, deviations from the (zero) mean will be proportional to $1/\sqrt{N(k)} \sim 1/k$. In the limit (4.24) of fully developed turbulence, $k_D \to \infty$, the fluctuations will cancel each other completely, and viscosity can no longer dissipate helicity. These considerations also make clear that the adiabatic invariance of helicity - although formulated as an ensemble average - should hold for (almost) every realization in the ensemble of flows.

However, in a decaying turbulent flow the adiabatic invariance of I (or $\bar{H}$) is inconsistent with the decay process itself: It cannot be that both $I = const.$ and $I = 8\pi^2 \int E(k)^2 dk$, while energy is being dissipated, $E(k) \to 0$. This was already realized by Levich & Tsinober (1983a) who argued that – in analogy to two dimensional turbulence – an inverse cascade of helicity fluctuations might allow I to remain constant in spite of the decay. Levich & Shtilman (1988) pointed out that alternatively the adiabatic invariance of I (or $\bar{H}$) could necessitate a break-down of the quasi-Gaussian approximation during the course of the decay. If the random phase approximation $\langle H(\vec{k}) H(\vec{k}') \rangle = 0$ for $\vec{k} \neq \vec{k}'$ no longer holds, I can exceed the QGA estimate $I = 8\pi^2 \int E(k)^2 dk$ significantly. In other words, wave packets of coherent helicity should emerge during the decay of a turbulent flow. It was put forward by Levich & Shtilman and Kit *et al.* (1988) that especially the low-k modes, which determine the value of I and $\bar{H}$, should develop phase coherence. It was suggested that large scale fluctuations of helicity are a universal feature of decaying homogeneous turbulent flows, which may be identified with large-scale coherent structures, and possibly give rise to a spontaneous breaking of reflexional symmetry.

In our opinion, however, it was not realized that even extreme phase coherence or phase

alignment cannot maintain a constant level of helicity fluctuations for indefinite times, simply because the energy spectrum $E(k)$ imposes an upper limit on the value of helicity $\bar{H}$, i.e.

$$|\bar{H}| \leq \sum_{k=1}^{k_D} 2kE(k). \tag{4.28}$$

This implies that the growth of large-scale phase coherence cannot truly avoid the inconsistencies associated with the adiabatic invariance of I and the decay process. Even more important, it was not appreciated that – as we shall demonstrate below – a minute amount of phase coherence *at the small scales* suffices to break the adiabatic invariance of helicity fluctuations, and allows viscous dissipation of helicity fluctuations along with the energy. Instead, Levich (1987) and Levich & Shtilman (1988) argued that only extreme intermittency could lead to viscous dissipation of helicity at small scales, a scenario that was discarded as 'unlikely'.

Evidently one cannot predict the buildup of either large- or small-scale coherence within the framework of the random phase approximation, where phase correlations are discarded at the outset. Even worse, we shall show below that a precise analytical description of phase correlations in an ensemble of developed turbulent flows is a rather tricky problem. Thus our attempt to make the appearance of small scale phase correlations due to the adiabatic invariance of helicity plausible will have to be based on qualitative arguments and comparison with numerical experiments.

To begin, let us illustrate by example how phase correlations in the dissipative range may lead to significant viscous dissipation of helicity $\bar{H}$ even for fully developed turbulent flows. Imagine that $\langle H(\vec{k})H(\vec{k}')\rangle > 0$ for all $k \approx k_D$ due to the presence of positive mean helicity $\langle H(k)\rangle > 0$. For simplicity, assume

$$H(k) \approx \frac{1}{\rho\Delta k}E(k), \tag{4.29}$$

i.e. the helicity spectrum is positive and of order $\sigma_G(H(k))$ in the dissipative range. Then the first term on the r.h.s. of (4.25) will not vanish in the limit of very large Reynolds number

$$\lim_{\nu\to 0}\left[\nu\sum_{k=1}^{k_D} k^2\langle H(k)\rangle\right]^2 \sim \lim_{\nu\to 0}\left[\nu\sum_{k=1}^{k_D} k^2 E(k)\right]^2 \sim \bar{\epsilon}^2 = const. \tag{4.30}$$

Obviously, the absence of cancellations in the dissipative range, which is a result of the phase-correlations, breaks the invariance of helicity $\bar{H}$. For fully developed turbulence, the degree of phase-alignment required to achieve this will be small , consider that if (4.29) holds

$$H(k)/H_{max}(k) \approx E(k)/2kE(k) \sim 1/k, \tag{4.31}$$

certainly too small to affect the energy transfer in developed turbulence directly .

However, one notices that there is an apparent contradiction here. If the helicity $\bar{H}$ is adiabatically invariant, and the mean helicity $\langle \bar{H} \rangle$ is initially zero, one must ask what the source of the helicity is that should accompany the phase alignment suggested by (4.29).

In order to resolve this contradiction, let us consider in detail the evolution of an ensemble of decaying turbulent flows at large Reynolds number under the assumption that at the initial moment t_0 the random phase approximation is exact. Although rather tedious, the detailed discussion of the evolution of such an ensemble is well motivated: Firstly, as a 'Gedankenexperiment ', it should convince us that the source of the correlations that break the adiabatic invariance is simply the helicity $\bar{H}_0$ present at the initial moment t_0. Secondly, we want to demonstrate that it is necessary to consider the statistics of *sub*ensembles, which makes predicting the appearance of such correlations analytically very difficult.

At the initial moment $t = t_0$, the probability distribution function $P(\bar{H})$ of the (space-) averaged helicity $\bar{H}$ will follow a Gaussian distribution with zero mean and width σ_G ;

$$P(\bar{H}) = \frac{1}{\sqrt{2\pi\sigma_G^2}} exp\{-\bar{H}^2/2\sigma_G^2\}, \tag{4.32}$$

$$\sigma_G(\bar{H}) = \sqrt{\frac{1}{\pi}\sum_{k=1}^{k_D}\langle E(k)\rangle^2}. \tag{4.33}$$

Let us divide the ensemble into subensembles characterized by their initial value of helicity $\bar{H}_0 = \bar{H}(t = t_0)$, and decompose the full ensemble average $\langle ... \rangle$ into an average over a subensemble $\langle ... \rangle_{H_0}$ and an average over the set of subensembles [...], i.e. an average over the possible values of initial helicity $\bar{H}_0$.

$$\langle ... \rangle = [\langle ... \rangle_{H_0}] \tag{4.34}$$

Dividing the ensemble average into an average over initial configurations [...] and an average$\langle ... \rangle_{H_0}$ over the statistics within one subensemble, i.e. statistics compatible with a given value of initial helicity $\bar{H}_0$, is reminiscent of averaging procedures employed in the theory of spin glasses (see Binder & Young, 1986). For both turbulence and spin glasses the separate averaging over the configuration is necessitated by the fact that the system is 'quenched', i.e. the relaxation time of the initial helicity or, correspondingly, the configuration of exchange bonds between spins, exceeds all other relevant time scales.

It was assumed that the initial flow is fully developed and extends over a wide range of scales. The normalized helicity H_N of (almost) all realizations will then be very small, and the results of the previous Chapter indicate that during the first few turnover times the evolution of the subensembles will not be influenced significantly by the helicity. In other words, the constraint imposed on the flows in one subensemble by its characteristic value of initial helicity is initially very weak, and consequently the different averages yield identical results

$$\langle ... \rangle_{H_0} = \langle ... \rangle_{H_0'} = [\langle ... \rangle_{H_0}], \tag{4.35}$$

for almost any quantity of interest. Of course, this is not so for helicity itself and quantities related to it, where obviously

$$\langle \bar{H} \rangle_{H_0} = \bar{H}_0 \, , \, \langle \bar{H} \rangle_{H_0'} = \bar{H}_0', \tag{4.36}$$

and

$$[\langle \bar{H} \rangle_{H_0}] = 0. \tag{4.37}$$

However, because the value of $\bar{H}$ will be determined by the large scales and does most likely not influence the small scales, we may assume to very good approximation that

$$\langle \bar{H}(k) \rangle_{H_0} = 0 \;\; \text{for} \;\; k \approx k_d \tag{4.38}$$

It follows that the adiabatic invariance of helicity should hold in every subensemble during the first turnover times:

$$\lim_{\nu \to 0} \langle (d\bar{H}/dt)^2 \rangle_{H_0} \to 0. \tag{4.39}$$

However, as the energy decays, $E(k) \to 0$ the normalized helicity $\langle H_N \rangle_{H_0}$ will eventually increase. This may manifest itself, e.g., in a slanted distribution of the normalized helicity

density h, or an absolute value of the averaged helicity larger than its quasi-Gaussian standard deviation $[(|\bar{H}|)_{H_0}] > \sigma_G(\bar{H})$, accompanied by the appearance of phase correlations $\langle \bar{H}(\vec{k})\bar{H}(\vec{k}')\rangle \neq 0$ for $\vec{k} \neq \vec{k}'$. Most important, the anomalously large helicity will cascade to the small scales, and we may expect that

$$\langle \bar{H}(\vec{k})\rangle_{H_0} \neq 0, \tag{4.40}$$

$$\text{sign}(\langle \bar{H}(\vec{k})\rangle_{H_0}) = \text{sign}(\bar{H}_0),$$

for $k \sim k_D$. Hence the invariance of helicity will be broken because of the presence of non-zero mean (in the subensemble) helicity in the dissipative range. The 'source' of this mean helicity is the helicity present in the flow at the beginning of the decay, which becomes a more and more significant constraint during the course of the decay.

Note that the mean values $[\bar{H}]$ and $[H(k)]$ over the total ensemble are still zero, because positive and negative values of $\bar{H}_0$ occur with equal probability. This has profound consequences: attempts to detect the appearance of non-local correlations with an analytical scheme that works with the full ensemble are bound to fail! On the other hand, devising an approximation scheme that incorporates the division into subensembles (4.34) seems to be a very difficult problem. (Note, again, the conceptual analogy to spin glasses, where a naive average $\langle \ln Z\rangle$ over the partition function leads to nonphysical results.)

To conclude this Section, let us discuss briefly why we have presented the above analysis for the case of flow in a 'periodic box' rather than an 'infinite volume', which is customary in statistical theories of turbulence. The first, most practical motivation is to keep comparison with numerical data straightforward. Factors of 2π and larger tend to get lost when translating from $V \to \infty$ to $V = (2\pi)^3$. Secondly - maybe more important - the fluctuations of average helicity scale with $\rho^{-1/2} \sim V^{-1/2}$. If the length scale of the turbulent flow is finite, and if turbulence is self-averaging, then volume averages over an infinite domain will be equal to ensemble means. This makes it necessary to consider $V\langle \bar{H}^2\rangle$, $V\langle H(k)^2\rangle$, etc., in order to obtain finite, non-zero quantities that describe the statistics of helicity fluctuations. Although this is a well-defined and perfectly legitimate operation, we find it quite hard to grasp this situation intuitively. It also seems that some misunderstandings in interpreting numerical data stem from this difficulty. For example, it was incorrectly assumed in Levich

(1990), that the values of H^2/V in one simulation (one realization) donot differ greatly from the ensemble average $I = \langle H^2/V \rangle$. This can only be true if the integral length scale of the turbulent flow is much smaller than the size of the computational box, which is clearly not the case in direct numerical simulations. (See also Frenkel & Lipscombe (1989) for a discussion of some of the subtleties associated with the choice of volume.)

4.4 Numerical Results

Are the fluctuations of helicity found in numerical simulations of decaying and quasi-stationary turbulence within the range suggested by the quasi-Gaussian approximation, or do we find 'anomalous' fluctuations of helicity that indicate the presence of phase correlations?

We begin by evaluating the helicity spectrum $H(k)$ of run O_{zero}, see Section 3.3 . Recall that initially $H(k) = 0$ for all wave numbers and consequently $\bar{H}(t = 0) = 0$ in this run. Remarkably, in less than 1/5 turnover times the helicity $H(k)$ of each k-shell grows to a magnitude of order $\sigma_G(H(k))$, obviously an effect of the nonlinear terms in the helicity balance equation (1.5), which quickly exchange helicity between different modes and scales while preserving the total helicity. Also in the mature phase of the simulation the quasi-Gaussian approximation yields reasonable results, consider Fig. 4.1(a), which shows the helicity spectral density of run O_{zero} at time 0.4 . Here the solid line represents the maximal helicity for the given energy spectrum, $H(k)_{max} = 2kE(k)$. The dotted line shows $\sigma_G(H(k))$, the quasi-Gaussian expectation value for the standard deviation of the helicity spectrum. Positive values of helicity are denoted by '+' -signs, negative values by 'o' - signs. In good agreement with the QGA, the helicity spectrum is changing sign in a seemingly random fashion, while the magnitude of the fluctuations is clearly of order $\sigma_G(H(k))$. (On the plot, the values of $H(k)$ appear to group rather closely around σ_G . Consider, however, that the axes are scaled logarithmically.) Similarly the time evolution of the average helicity $\bar{H}$, depicted in Fig. 4.2 is in reasonable agreement with the random phase approximation: The growth of $\bar{H}$ is governed by viscosity and consequently much slower than the growth of $H(k)$; at the beginning of the mature phase (t = 0.4) $\bar{H}$ is only 3 % of $\sigma_G(\bar{H})$ and only 1 % of its maximum value. At later times, $\bar{H}$ grows significantly, reaches a peak value of

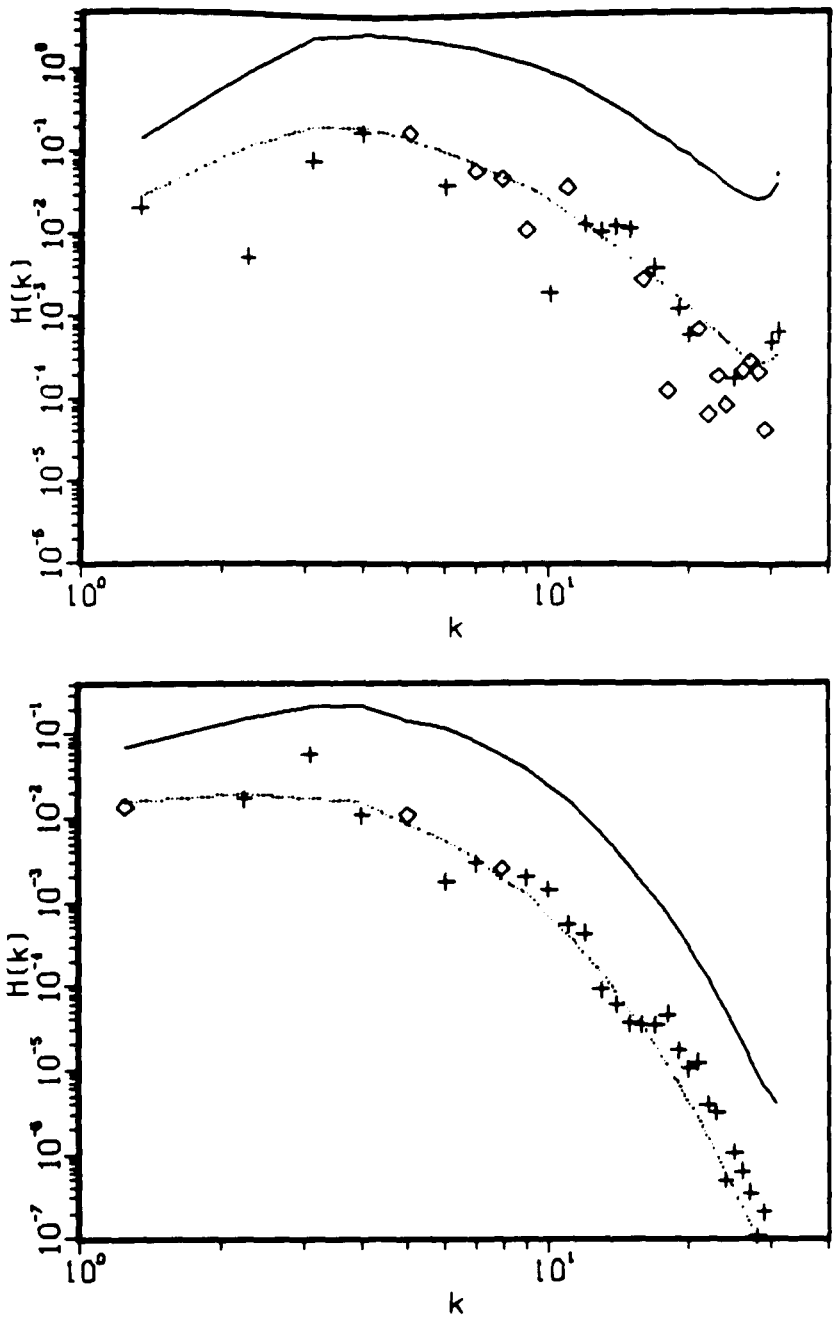

Figure 4.1: Helicity spectrum H(k) (+ for positive, ◇ for negative values) of run O_{zero} at the beginning of the developed stage, $t = 0.4$ (top) and after a few turnover times, $t = 3.2$ (bottom); Maximum helicity $H(k)_{max}$ (continuous line); quasi-Gaussian standard deviation $\sigma_G(H(k))$ (dotted line).

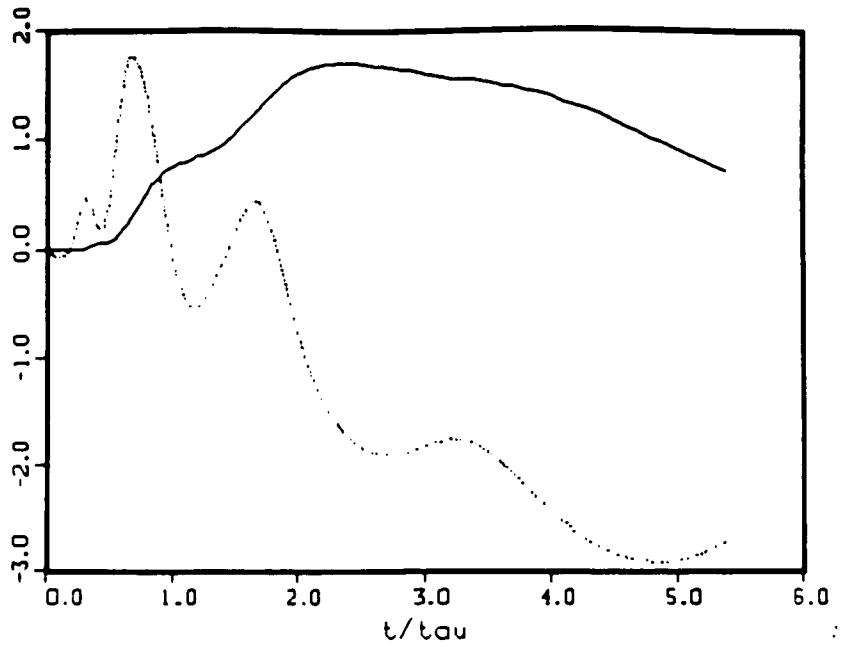

Figure 4.2: Run O_{zero}: average helicity $\bar{H}$ (continuous line) and viscous term $2\nu \sum_k k^2 H(k)$ (dotted line) as a function of time, both normalized by their respective quasi-Gaussian standard deviation. Time is scaled with the average turnover time.

1.7 times the standard deviation (about 5 % of its maximum value $\bar{H}_{max} = \sum_k 2kE(k)$) and returns to a value of $\bar{H} \approx \sigma_G(\bar{H})$ at the end of the simulation. The fluctuations are obviously not strong enough to directly influence the energy transfer (consider the data in Table 3.1), on the other hand it also seems inappropriate to claim that the growth of $\bar{H}$ is anomalously suppressed below the level suggested by the random phase approximation (Levich, 1990).

We did observe significant deviations from the QGA at the small scales: After a few turnover times it is typically found that the helicity spectrum $H(k)$ of the small scales is positive for all $k > 10$. Also, $|H(k)|$ seems to be too large. A typical example is Fig. 4.1(b), which displays the helicity spectrum at time 3.2 ($\approx$ 5 turnover times). One should keep in mind though that at such late times the Reynolds number is *very* small ($R_\lambda \approx 10$), and it is not clear whether it makes sense to relate observations made at such late times to turbulent flows.

In order to assure ourselves that such behavior is 'typical', we performed the above analysis for a number of similar decaying flows at resolution 64^3. We have also investigated

a field (HIE24, $R_\lambda \approx 80$) from a 128^3 simulation of homogeneous and isotropic decaying turbulence by Lee (1985), and from a 128^3 simulation (field C128U12 , $R_\lambda \approx 90$) of shear-driven turbulence by Rogers (1986). Remarkably, in all simulations with initially negligible helicity we did not observe fluctuations of the helicity spectrum of the large scales that seemed to be incompatible with Gaussian statistics, i.e. $|H(k)| \gg \sigma_G(H(k))$. The small scales, on the other hand, repeatedly indicate the presence of phase coherence at late times, see, e.g., Figs. 4.3 and 4.4, which show data equivalent to Figs. 4.1 and 4.2 for run BDR, a 64^3 simulation with 'random' initial helicity. The initial Taylor Microscale Reynolds number R_λ in this run was equal to 39, somewhat less than in run O_{zero} ($R_\lambda \approx 45$), correspondingly the run was somewhat better resolved. All other initial parameters of run BDR are are very similar to those of O_{zero}: kinematic viscosity ν equal to 0.015, turnover time τ equal to 0.54, integral scale L equal to 0.62, Taylor Microscale λ equal to 0.50 . (We note that during the developing stage of some of our 64^3 simulations the helicity of the small scales was found to be 2 to 3 times larger than $\sigma_G(H(k))$, resulting in a positive or negative 'tail' of the helicity spectrum similar to those displayed in Figs. 4.1(b) and 4.3(b). These simulations, however, were only marginally resolved and shall not be considered in the following.)

Although we may claim with some confidence that the above observations are typical of decaying flows, it is of obvious advantage for the study of helicity fluctuations to turn to simulations of quasi-stationary turbulence, where (assuming ergodicity) time averages may be interpreted as ensemble averages. We shall mostly present results from run CFR (see Section 3.4), which was continued for almost 60 turnover times and therefore provides a fairly large statistical sample. We emphasize though that very similar results were found for run EFR and other forced simulations that are not reported here.

Fig. 4.5 shows the time evolution of $\bar{H}$ and of the viscous term $2\nu \sum_k k^2 H(k)$, both normalized by their respective σ_G, see (4.10) , (4.11). Note that the peaks of $\bar{H}$ do not coincide with those of $\bar{E}$, see Fig. 3.12 . It seems as if the fluctuations of $\bar{H}$ around the zero mean are well described by the QGA. Indeed, one may plot the data in Fig. 4.5 as a histogram and obtain a good fit to a Gauss-curve of width 1 (Keep in mind that $\bar{H}$ is normalized by σ_G in Fig. 4.5). The viscous term, on the other hand, significantly exceeds its

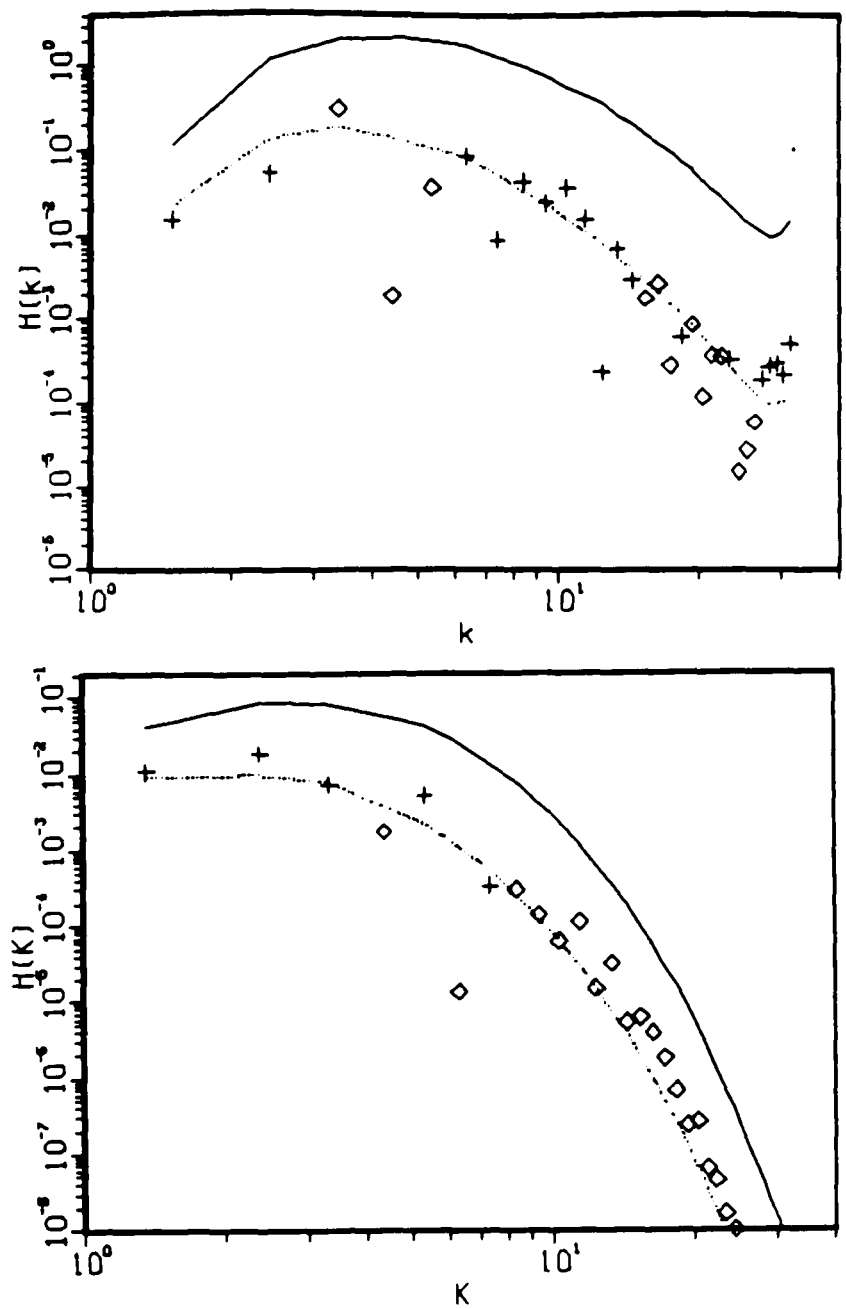

Figure 4.3: Helicity spectrum H(k) (+ for positive, ◇ for negative values) of run DBR at the beginning of the developed stage, $t = 0.4$ (top) and after a few turnover times, $t = 5.$ (bottom); Maximum helicity $H(k)_{max}$ (continuous line); quasi-Gaussian standard deviation $\sigma_G(H(k))$ (dotted line)

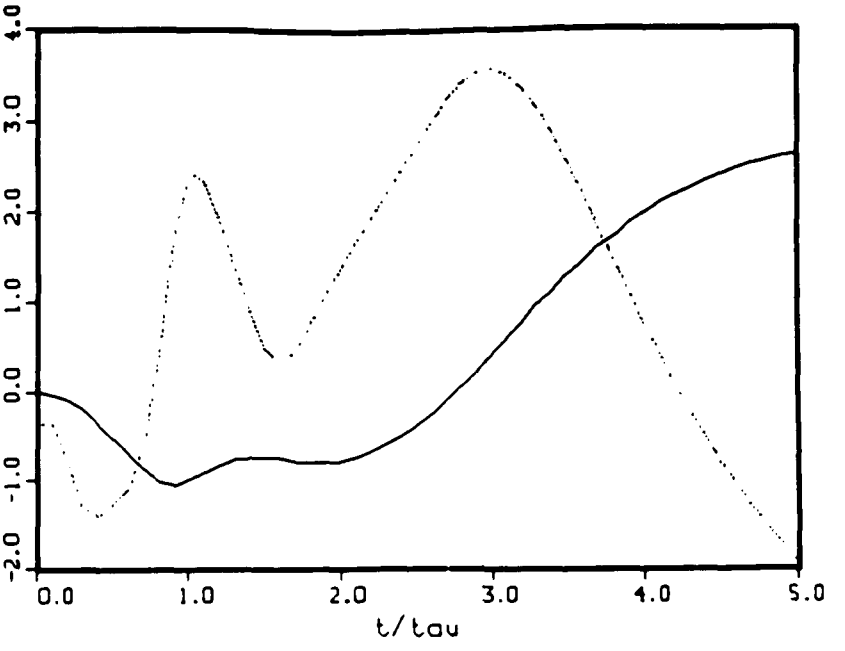

Figure 4.4: Run DBR: average helicity $\tilde{H}$ (continuous line) and viscous term $2\nu \sum_k k^2 H(k)$ (dotted line), both normalized by their respective quasi-Gaussian standard deviation, as a function of time.

σ_G value, which indicates that the fluctuations of helicity at the small scales are larger than QGA suggests. That this is indeed so is seen in Fig. 4.6, which compares the actual standard deviation $\sigma(H(k)) = \langle H(k)^2 \rangle^{1/2}$ of the helicity spectrum (□) with the QGA estimate for this quantity (continuous line). Here the spectrum $H(k)$ was sampled in intervals of about 1/10th of a turnover time during the quasi-stationary stage of run CFR, i.e. each data point in Fig. 4.5 represents more than 500 fields. The QGA estimate $\sigma_G(H(k))$ is derived with (4.12) from the average energy spectrum $\langle E(k) \rangle$.

Although multiplying σ_G with a correction factor proportional to $k^{1/3}$ (see (4.22)) yields a much better fit of the observed fluctuations to the QGA estimate, it seems unlikely that sweeping effects are the cause of the deviation of $\sigma(H(k))$ from $\sigma_G(H(k))$, because the insufficient separation of small and large scales in the simulation makes the random sweeping hypothesis inapplicable.

Instead, the 'anomalously large' values of $\sigma(H(k))$ are caused by coherent fluctuations of the helicity spectrum $H(k)$, very similar to the situation depicted in Figs. 4.1(b) and 4.3(b): If we plot the helicity spectrum at some instant of time, we frequently find that

the sign of H(k) is the same for large groups of high-k wave numbers and typically of somewhat larger magnitude than $\sigma_G(H(k))$. After maybe one turnover time, such a phase-correlated configuration decays into a short-lived disordered state, where the sign of the helicity spectrum varies in seemingly random fashion, and then again locks into a phase-correlated state.

It would seem that the above results from DNS of turbulent flows support the idea that in a decaying turbulent flow the incompatibility of the adiabatic invariance of helicity with an ongoing decay of energy must result in the appearance of small-scale phase coherence, which then breaks the invariance. Small scale phase coherence and anomalously large magnitudes of the viscous term $2\nu \sum_k k^2 H(k)$ are clearly displayed by many of the simulations discussed above. One might object that observations made in low Reynolds number DNS, where viscous growth and dissipation is significant even in the absence of phase coherence, are of questionable relevance for the high Reynolds number scenarios of 'adiabatic invariance'. Indeed, Figs. 4.2 and 4.4 display strong viscous growth and decay of average helicity $\bar{H}$ in the decaying simulations O_{zero} and DBR. Consider though that $\sigma_G(\bar{H})/\sigma_G(d\bar{H}/dt)$, the QGA estimate of the time scale for viscous changes in the average helicity, is typically 30 % larger than the time scale $\bar{E}/\bar{\epsilon}$ for changes in the average energy. This implies that even in our low Reynolds number DNS a complete absence of phase correlations and the ensuing 'normal' rate of viscous dissipation of helicity would result in anomalously large values of $\bar{H}$ in the late stage of the decay. One therefore might conclude that the phase correlations displayed in Fig. 4.1(b), where $H(k) > 0$ for all $k > 8$ and $\bar{H} \approx 1.6\, \sigma_G(\bar{H})$, have developed as a consequence of the need for enhanced dissipation of helicity. However, Fig. 4.3(b) from run DBR at time $t = 5.$, $\bar{H} \approx 2.5\, \sigma_G(\bar{H})$, is in blatant contradiction with this conclusion: here the helicity spectrum of the small scales is *negative*, which would lead to further viscous growth of *positive* mean helicity $\bar{H}$.

Also, the phase coherence displayed by the forced simulations CFR and EFR does *not* support the idea that constraints imposed by helicity are responsible for the observed coherence. If a quasi-stationary turbulent flow is maintained by a (non-helical) Gaussian random force, the evolution in time of the average helicity $\bar{H}$ will be determined by the viscous dissipation (or creation) of helicity and the injection (or extraction) of helicity by

the forcing. Because the latter was assumed to be a Gaussian process, we can calculate the amount $\Delta\bar{H}$ by which the helicity will increase or decrease during a short time interval Δt

$$\langle \Delta \bar{H}^2 \rangle = \frac{2}{\pi \rho \Delta k} \sum_k F(k) E(k), \tag{4.41}$$

where $F(k) = 4\pi k^2 F_0(k)$ is the power spectrum of the forcing (see Section 3.4). Of course, because the Gaussian random forcing is completely uncorrelated with the velocity field, it cannot lead to a nonuniform distribution of the phase angle $\phi(\vec{k})$. Therefore, in the mean the forcing will not change the helicity, $\langle \Delta \bar{H} \rangle = 0$, and the mean square of helicity may stay at its QGA level $\langle \bar{H}^2 \rangle \approx 1/(\rho \pi \Delta k) \sum_k E(k)^2$. This implies that the absence of viscous dissipation of helicity in a fully developed forced turbulent flow is not incompatible with a quasi-stationary state. No internal inconsistencies whatsoever arise from the assumption that the helicity of all scales of a forced turbulent flow is fluctuating normally. The fact that nevertheless phase coherence is clearly displayed by our forced simulations indicates that some other mechanism is responsible for the appearance of the correlations.

We do of course not claim that turbulent flows follow Gaussian statistics, or that phase correlations are absent, Figs. 4.1(b), 4.3(b) and 4.6 clearly show the opposite to be true. We merely state that so far no valid arguments have been developed that would justify the claim that the invariance properties of helicity are the *cause* of the fluctuations observed in our simulations.

To conclude this section, we present time-averaged histograms of the distribution of the normalized helicity density h of runs CFR and EFR in Fig. 4.7 . As repeatedly observed in decaying homogeneous isotropic flows (Shtilman *et al.* , 1986, Pelz *et al.* , 1986, Rogers & Moin, 1987), the plots display a slight tendency of the velocity and vorticity vector to be aligned ('horns of $\cos\Theta$'). We do not see the asymmetries found in forced simulations by Kerr (1987), this indicates that our forcing scheme does not inject mean helicity.

In our opinion, the cause of the effect is still unclear, although there is now ample numerical support from a variety of homogeneous flow simulations. It has become clear that the observed alignment cannot be related to fluctuations of helicity in a straightforward way (Levich, 1987, Speziale, 1987). Chen & Kraichnan (1989) have speculated that sweeping effects might be related to the alignment. Note, however, that the effect survives even in forced simulations, contrary to the expectations of Chen & Kraichnan (1989), who suggested

that a random forcing might easily destroy the delicate correlations between velocity and velocity gradients that must accompany the alignment.

The distributions of the normalized helicity density h of the decaying runs O_{zero} and DBR at very late times are presented in Fig. 4.8 . Remarkably, the plots are not reflexionally symmetric, indicating the presence of significant mean helicity. Indeed, for run O_{zero} at time $t = 3.2$ we have $H_N = 0.05$, $\bar{h^2} = .34, \bar{H} = 1.6\ \sigma_G(\bar{H})$, and for run DBR at time $t = 5$ we find $H_N = 0.11, \bar{h^2} = .37$, and $\bar{H} = 2.5\ \sigma_G(\bar{H})$; slightly 'anomalous' levels of helicity. Similar lack of reflexional symmetry at late times was found in wind tunnel experiments by Kit *et al.* and Dracos *et al.* (1990). Keep in mind though, that the Reynolds numbers are very low ($R_\lambda \approx 10$) in this late stage of the decay, and it is not clear whether these observations are related in any way to developed turbulence (See also the discussion of the late stage of decay of a turbulent flow in Batchelor, 1953).

4.5 Conclusions

We have investigated the statistics of helicity fluctuations in homogeneous isotropic turbulent flows. A random-phase or quasi-Gaussian approximation (QGA), first employed in this context by Levich & Tsinober (1983a), was used to obtain estimates σ_G of the standard deviation of fluctuations of the helicity spectrum $H(k)$, the average helicity $\bar{H}$, and the viscous term $2\nu \sum_k k^2 H(k)$. Quite remarkably, in this approximation the average helicity $\bar{H}$ becomes 'adiabatically invariant' in the limit of very large Reynolds number, i.e. viscosity cannot dissipate helicity in the limit $\nu \to 0$, $k_D \sim (\epsilon/\nu^3)^{1/4}$ (k_D is the Kolmogorov wave number). It was shown that the QGA estimates for the magnitude of the helicity spectrum $H(k)$ in a Kolmogorov-type inertial range is compatible with classical scaling arguments supplemented by elementary probability theory. Quite simply, $|H(k)|$ should scale with $N(k)^{-1/2}$, where $N(k)$ is the number of modes in one k-shell, because the helicity $H(\vec{k})$ is not positive definite. $N(k)$ carries no dimension, therefore one unambiguously recovers the QGA result $|H(k)| \sim N(k)^{-1/2} \epsilon^{2/3} k^{-2/3}$. We have pointed out that fluctuations of this magnitude will be 'dynamically insignificant', i.e. too small to directly influence the energy transfer and the nonlinear term. We have argued further that in fully developed turbulence with a wide range of statistically independent scales so-called 'sweeping effects' may lead to

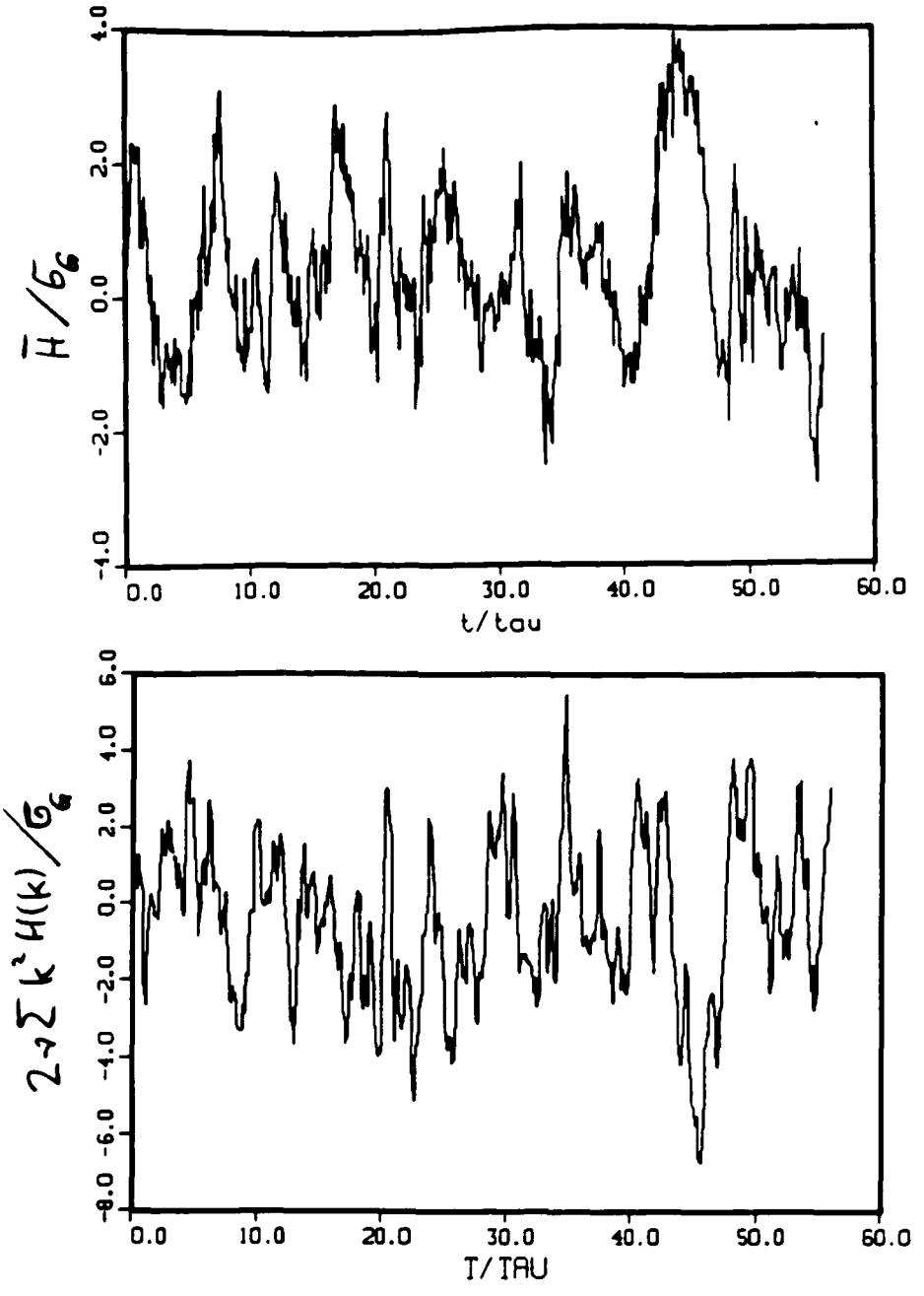

Figure 4.5: Time evolution of the average helicity $\bar{H}$ (top) and the viscous term $2\nu\sum_k k^2 H(k)$ (bottom) of run CFR. Both quantities are normalized by their respective σ_G.

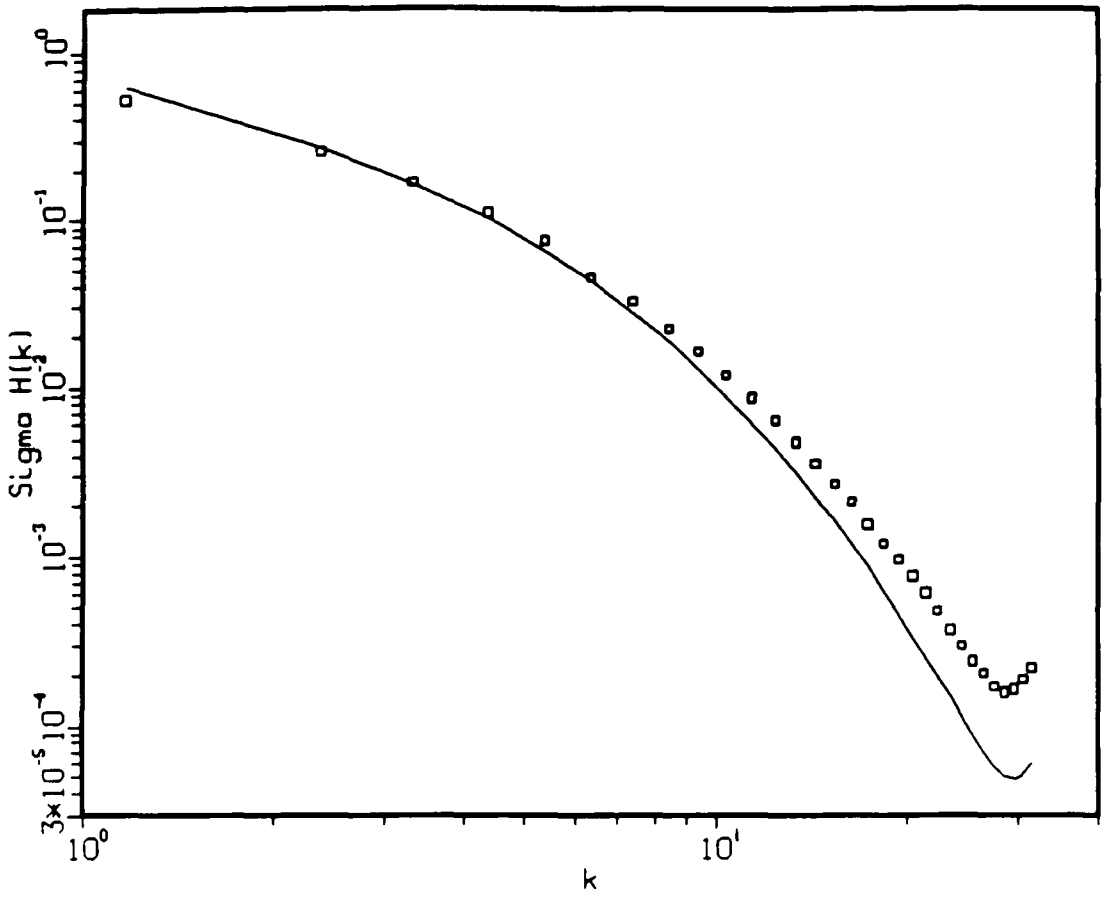

Figure 4.6: Standard deviation of H(k) (□) and its quasi-Gaussian estimate $\sigma_G(H(k))$ (line) evaluated form more than 500 velocity fields over a period of about 50 turnover times.

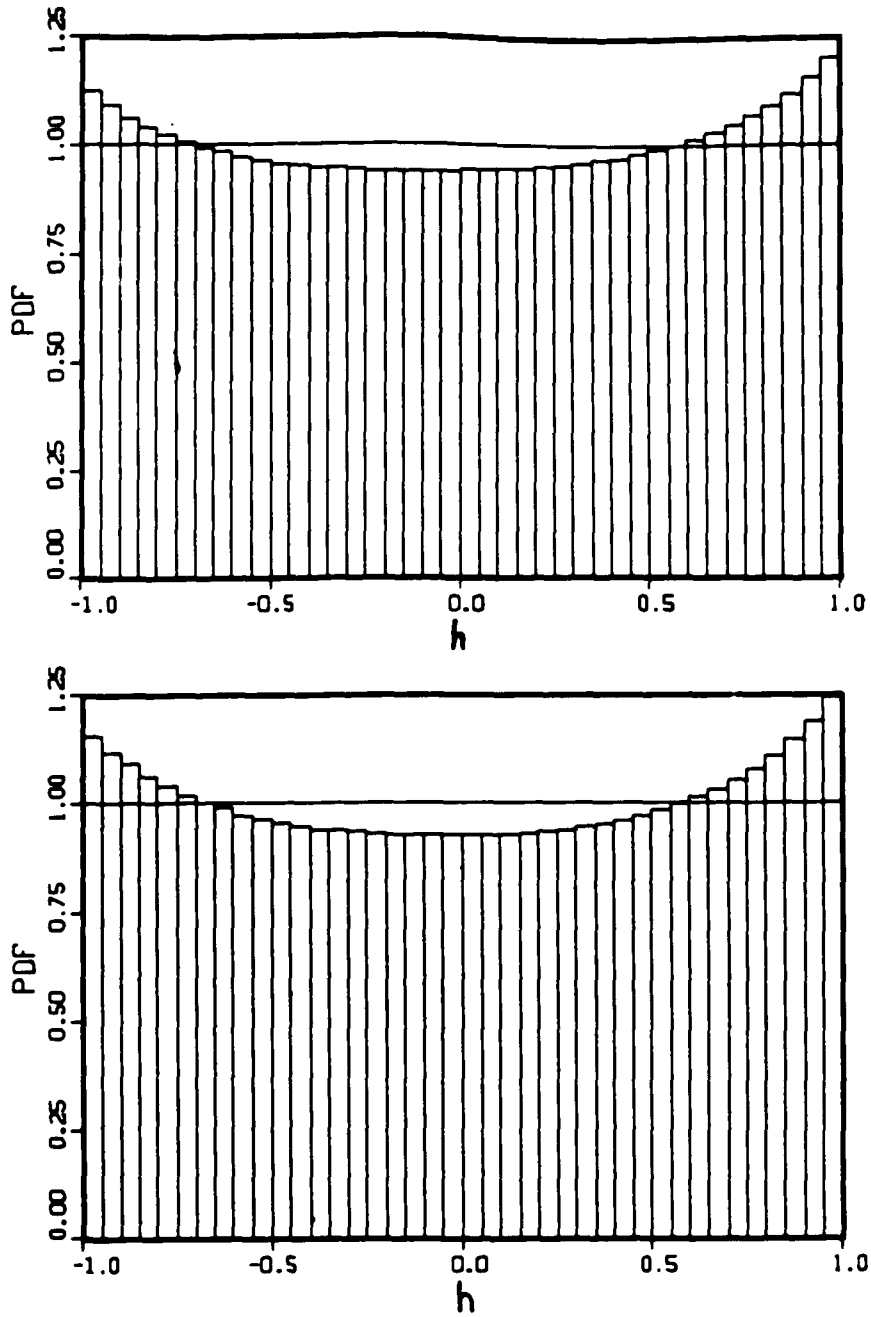

Figure 4.7: Time-averaged histograms of the distribution of the normalized helicity density h for run CFR (top) and EFR (bottom).

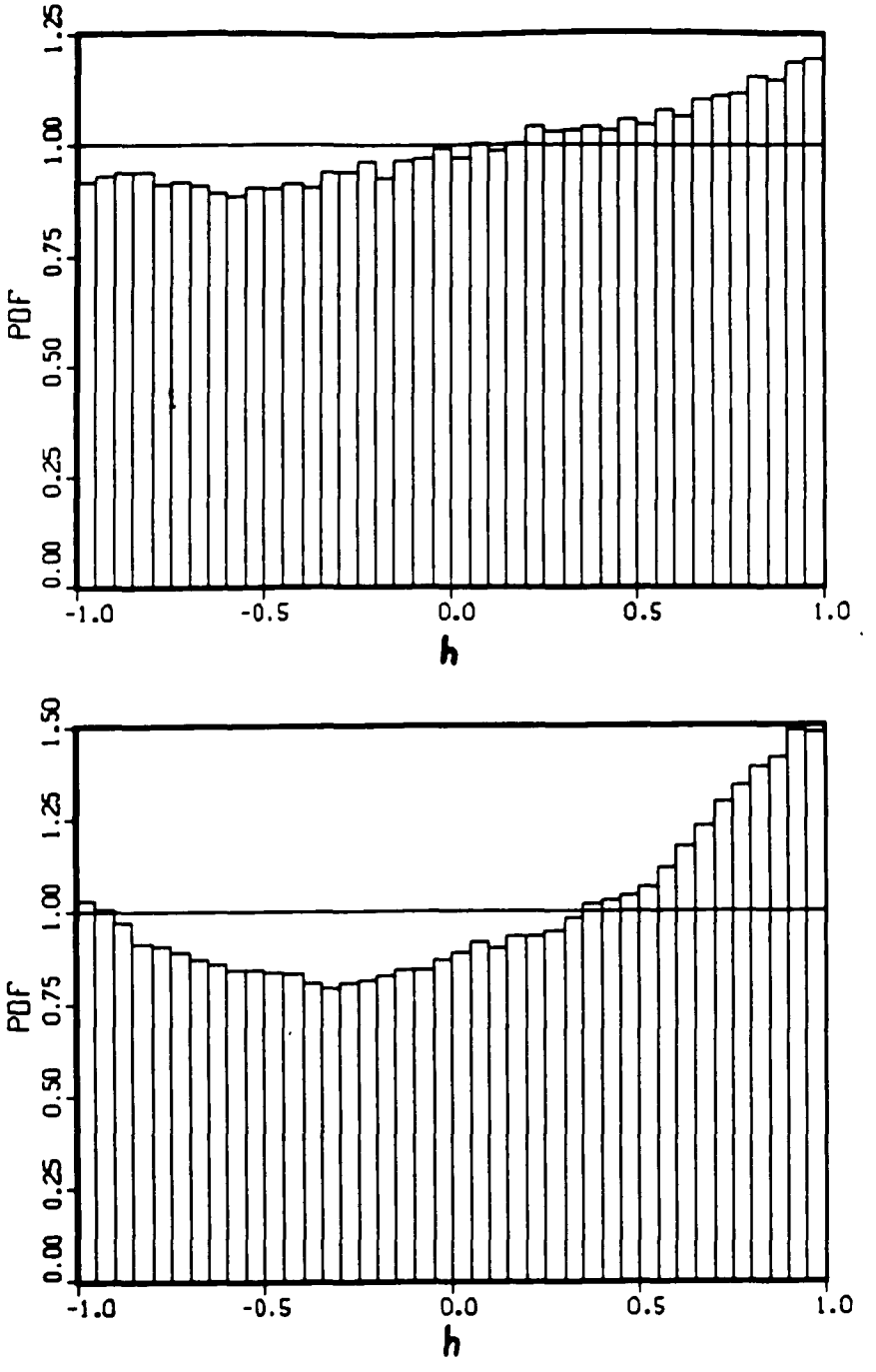

Figure 4.8: Histograms of the distribution of the normalized helicity density h for run $O_{zero}, t = 3.2$ (top) and BDR, $t = 5.$ (bottom).

corrections to the QGA estimate, because the helicity density γ is not Galilean invariant. Consequently, the difference $\Delta\gamma(r)$ in the helicity density of two points a distance r apart, will scale like $U\Delta\omega(r)$ instead of $\Delta v(r)\Delta\omega(r)$, where $\Delta v(r)(\Delta\omega(r))$ is the difference in velocity (vorticity) of the two points, U the magnitude of the large scale advecting velocity.

As already Levich & Tsinober (1983a) have pointed out, in the case of a decaying turbulent flow the QGA (or random phase approximation) leads to a contradiction: It cannot be that $\langle\bar{H}^2\rangle = (\pi\rho\Delta k)^{-1}\sum_k\langle E(k)\rangle^2$ (the QGA estimate) and also $\langle\bar{H}^2\rangle = const$ while energy is being dissipated, $E(k) \to 0$. It follows that in a decaying turbulent flow the quasi-Gaussian approximation must break down. In other words, wave packets of coherent helicity should be a 'probably universal' feature of developed turbulence (Levich & Shtilman, 1988). A build-up of phase correlations at low wave numbers (Levich, 1987, Levich & Shtilman, 1988, Kit *et al.* , 1988) could lead to anomalously large (i.e. larger than quasi-Gaussian) values of helicity fluctuations $\langle\bar{H}^2\rangle$ and possibly result in the appearance of large scale helical coherent structures. On the other hand, one may easily show that a minute amount of phase coherence at large wave numbers, i.e. non-Gaussian behavior *at the small scales*, can break the adiabatic invariance of helicity even at very high Reynolds numbers – a scenario that has hitherto been discarded as 'unlikely' (Levich, 1987, Levich & Shtilman, 1988). Viscosity can then dissipate helicity along with the energy, and it is not clear whether in this situation helicity fluctuations can play an important role in the organization or characterization of the structure of turbulence. Note that small scale coherence will not lead to an increase in the correlation length of the helicity density fluctuations. It is to be seen whether concepts of 'spontaneous symmetry breaking' (Levich & Shtilman,1988, Kit *et al.* , 1988), borrowed from the theory of critical phenomena, can be fruitfully applied to turbulence. We also have argued that predicting the appearance of small scale phase coherence analytically will be exceedingly difficult, because it would necessitate to work with sub-ensembles of decaying turbulent flows.

The QGA estimates for the standard deviation of helicity fluctuations have been used as a gauge for the fluctuations of helicity observed in direct numerical simulations of decaying and quasi-stationary turbulent flows at moderate Reynolds numbers. Complete agreement with the QGA would imply that no phase coherence exists in the simulations, and that

helicity fluctuations are dynamically insignificant in the sense that they are too small to directly influence the energy transfer. It was observed that fluctuations of the helicity spectrum $H(k)$ of the large scales and therefore also of the average helicity $\bar{H}$ are well approximated by the QGA. There is no indication of the existence of an inverse cascade of helicity fluctuations; claims to the contrary made by Levich & Shtilman (1988) are in our opinion not justified, because no meaningful statistical analysis was performed in this work. In particular, the observed fluctuations of the helicity spectrum $H(k)$, for wave numbers $k = 1,...,5$ were not compared with the maximum helicity $2kE(k)$ or the QGA estimate for the standard deviation, $\sigma_G(H(k))$. Similarly, the 'filtered fields' that displayed strongly non-uniform distributions of h are composed of very few modes ($\mathcal{O}(10)$), and it seems necessary to conduct a more detailed analysis in order to ensure that the observed anisotropies are not just statistical noise.

The small scales of our simulations are found to display a substantial amount of phase coherence, i.e. frequently the helicity spectrum $H(k)$ is of equal sign for a range of high-k wave numbers and of considerably larger magnitude than the quasi-Gaussian assumption would suggest. Remarkably, the phase coherence seems strong enough to break the adiabatic invariance of helicity, i.e. allow for sufficient viscous dissipation of helicity even in the limit of fully developed decaying turbulence (if we assume that the simulation results may be extrapolated to higher Reynolds numbers). This would resolve the dilemma caused by the adiabatic invariance of average helicity (or I) in a decaying flow. However, the sign of the helicity spectrum of the small scales is at times found to be the opposite of the sign of the average helicity. This is obviously incompatible with the assumption that the coherence has developed in order to provide a mechanism for 'anomalous' viscous dissipation of mean helicity in a decaying flow. Furthermore, small-scale phase coherence was also observed in forced flows, where there is no discernible need for enhanced dissipation of helicity (the flow is quasi-stationary, and a non-helical Gaussian random forcing cannot increase the fluctuations of helicity above the quasi-Gaussian level). We therefore argue that the adiabatic invariance of helicity is not the cause of the observed phase coherence.

We may hope to increase our understanding of the observed phase correlations by investigating in detail the dynamics and interactions of certain 'archetypes' of turbulent struc-

tures. For example, there is numerical evidence (She *et al.* , 1990) that tubelike vortex structures are formed in homogeneous turbulent flows. The nonuniform distribution of the normalized helicity density h might be related to the alignment of stretching velocity with stretched vorticity in such tubes. Note also the remark by Chen & Kraichnan (1989), who suggested that sweeping effects might be responsible for the alignment of vorticity and velocity. Furthermore, one might want to examine the fluctuations in the helicity spectrum during reconnections of vortex rings and tubes. In recent numerical studies of such processes (Kida *et al.* , 1989, Melander & Hussain, 1990) it was found that several strongly helical regions of various sizes are formed during the reconnection process.

Unfortunately, we must admit that such investigations would in a sense run contrary to the principal motivation for the study of helicity in turbulent flows. After all, helicity is besides the kinetic energy the only known inviscid integral invariant of the incompressible NSE, and it was hoped that important insights of a fundamental and general nature into the structure of turbulence might be gained from a study of this invariant. In the light of these considerations, an investigation of the helicity of particular structures would seem to be a rather pointless endeavor.

There is a special department of Hell for students of probability. ...
There is another place of torment for physicists.

Bertrand Russell, The Metaphysician's Nightmare (1954)

Chapter 5

The Suppression of Nonlinearity in Isotropic Turbulence

Kraichnan & Panda (1988) have compared velocity fields obtained from DNS of decaying turbulence with isotropic Gaussian solenoidal vector fields that have the same instantaneous energy spectrum as the turbulent fields ('corresponding Gaussian field' in the following). It was observed that, as the turbulence develops, the normalized mean-square nonlinear term Q (see Section 3.3) is reduced to about 60% of the corresponding Gaussian value. That a reduction of nonlinearity should occur in developed turbulence was suggested by Levich & Tsinober (1983a, 1983b), Moffatt (1985), and Levich (1987); for details we refer to the Introduction. It was proposed that to some extent the reduction of nonlinearity should be accompanied by large fluctuations of helicity. Indeed, Kraichnan & Panda observed that in a turbulent field the appropriately normalized mean square of the helicity density is about 120% of the value for the corresponding Gaussian field. This is in qualitative agreement with results obtained by Pelz *et al.* (1985,1986) and Rogers & Moin (1987), who observed that in DNS of homogeneous turbulent flows there is a slight tendency for the velocity and vorticity to align. However, it seems that the observed reduction of the nonlinear term is much too strong to be accounted for by the alignment of $\vec{v}$ and $\vec{\omega}$ alone. Furthermore, Kraichnan & Panda found a comparable suppression of Q in dynamical models with a quadratic nonlinearity and random coupling coefficients, and therefore conjectured that the suppression of nonlinear interactions may be a feature intrinsic to a broad class of nonlinear dynamical systems.

We concentrated on elucidating the mechanism of the reduction in isotropic turbulence, and on clarifying the role of helicity in the effect. In Fig. 5.1 we present the time evolution of the normalized mean-square nonlinear term Q of direct numerical simulations of decaying turbulence and of corresponding Gaussian fields. Circles correspond to run SDR, a 64^3 simulation of decaying turbulence in a periodic box with side length 2π with initial conditions similar to those of Kraichnan & Panda (1988) . The initial parameters were: an average energy $\bar{E} \approx 1.1$, average enstrophy $\bar{\Omega} \approx 9.0$, average helicity $\bar{H} \approx -1.9$ ($H_N \approx -.11$), Reynolds number $R_\lambda \approx 47$, eddy turnover time $\tau \approx 1.1$ (computational time). Note that the maximum of enstrophy was reached at time $t \approx 0.9$ (then $R_\lambda \approx 30$), which implies that the data in Fig. 5.1 represent mainly the developing phase of the simulation. The triangles denote Q of non-helical Gaussian fields, constructed with the initialization routine described in Section 3.2 such that they have instantaneously the same energy spectrum as the simulation field. Our results agree qualitatively with those of Kraichnan & Panda (1988): the normalized mean-square nonlinear term Q of the developed turbulent field ($t = 1.0$) is only 52 % of the corresponding Gaussian value. The crosses in Fig. 5.1 represent Q of maximally helical corresponding Gaussian (MHG) fields, i.e. $H(k) = 2kE(k)$ for all k. A comparison of Q-values of non-helical ($\triangle$) and maximally helical ($+$) Gaussian fields shows that the strong alignment of velocity and vorticity due to the presence of mean helicity in these fields does lead to a significant depression of nonlinearity. (We note that typically the mean square of the cosine of the angle between velocity and vorticity $\overline{h^2} = \overline{\cos^2\theta} \approx 0.8 - 0.9$ in maximally helical fields, compared to $\overline{\cos^2\theta} = 1/3$ for the angle between uncorrelated vector fields.) Remarkably though, Fig. 5.1 shows clearly that the depression of nonlinearity in the (non-helical) turbulent flow SDR ($\circ$) is of almost equal magnitude. This confirms - as Kraichnan & Panda (1988) suggested - that the slight alignment of velocity and vorticity generally favored by the turbulent dynamics ($\overline{h^2} = 0.36$ from run SDR at time $t = 1$, see also Figs. 4.7 and 4.8) cannot be the source of the depression. However, helicity can enhance the depression significantly: the mean-square nonlinear term of a simulation of a decaying turbulent flow that started from a maximally helical field (run SDM, $\square$ in Fig. 5.1) shows a depression to only 24 % of the value of a corresponding non-helical Gaussian field.

Note that the numbers given above differ somewhat from the results presented in Shtil-

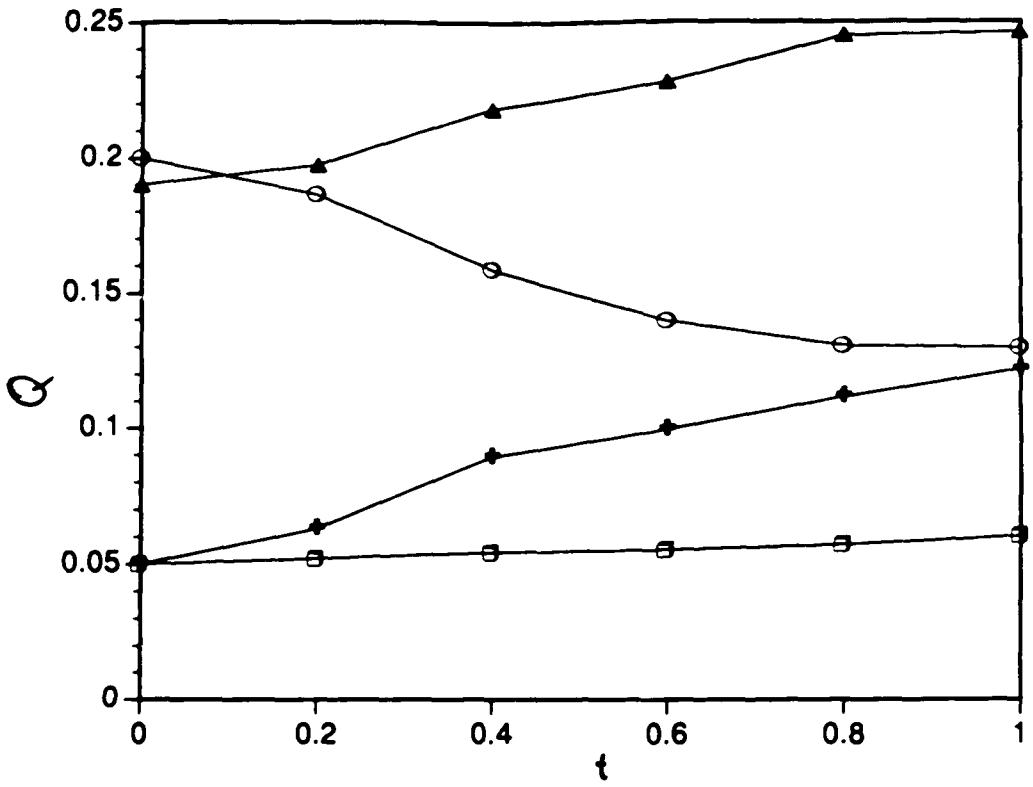

Figure 5.1: Time evolution of the normalized mean square nonlinear term Q. Run SDR (o), Gaussian field with random helicity (Δ), Gaussian field with maximum helicity (+), run SDM ($\square$).

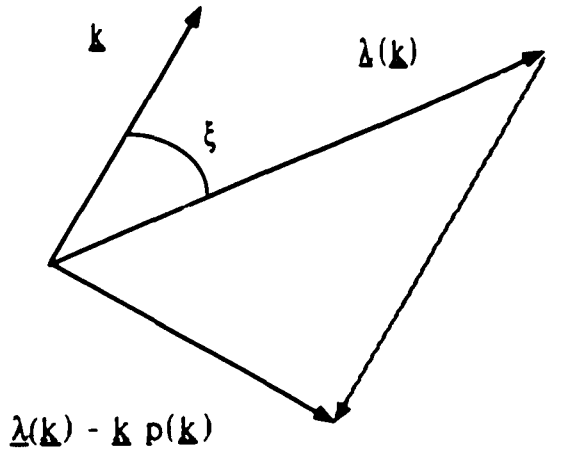

Figure 5.2: Sketch of the structure of the nonlinear term in Fourier space.

man & Polifke (1989,1990). This is due to an error in an early version of our initialization scheme: The 'maximally helical' Gaussian fields in Shtilman & Polifke (1989) actually possess only about 80 % of the maximal helicity. In particular, the real and imaginary part of the velocity vector were initialized *independently* from each other according to a χ^2 distribution. In this case the average helicity will be equal to $\langle H(k)\rangle = 8\pi k^3 f(k)^2 \langle\chi\rangle^2$ rather than $\langle H(k)\rangle = 8\pi k^3 f(k)^2 \langle\chi^2\rangle$. The ratio $\langle\chi\rangle^2/\langle\chi^2\rangle = \pi/2 \approx 0.78$, which results in a less than maximally helical field even if $\phi(\vec{k}) = \pi/2$ for all modes. Fortunately, our basic conclusions are not affected by this mistake.

As the increase in mean-square normalized helicity cannot account for the observed magnitude of the depression of nonlinearity, we must ask what the mechanism of the reduction could be? Consider Fig. 5.2. The Fourier transform $\vec{\lambda}(\vec{k})$ of the Lamb vector is determined by a convolution sum, see (2.7), and is therefore not constrained to lie in the plane perpendicular to the wave vector $\vec{k}$. Incompressibility ($\vec{k} \cdot \vec{v}(\vec{k}) = 0$) demands, however, that the total nonlinear term $\vec{\lambda}(\vec{k}) - i\vec{k}\tilde{p}(\vec{k})$ be perpendicular to the wavevector $\vec{k}$, which is assured by the contribution of the kinematic pressure $\tilde{p}(\vec{k}) = -i\vec{k} \cdot \vec{\lambda}(\vec{k})/k^2$ (note that $\tilde{p} = p + \frac{1}{2}v^2$

in physical space) to the total nonlinear term. Fig. 5.2 suggests that the total nonlinear term is small if $\vec{\lambda}(\vec{k})$ is preferentially aligned with $\vec{k}$.

There is also a more formal way of arriving at this conclusion. Let us consider the following equation :

$$\langle|\nabla\tilde{p}|^2\rangle = \langle\vec{\lambda}\cdot\nabla\tilde{p}\rangle. \tag{5.1}$$

The angular brackets denote here either spatial averaging or integration over Fourier space. Equation (5.1) can be verified by considering the expression for the kinematic pressure of a homogeneous incompressible flow field in k-space. With the help of Parseval's Theorem the identity may then be established in physical space. As an immediate consequence we can express the mean-square of the nonlinear term of the NSE as

$$\langle|\vec{\lambda} - \nabla\tilde{p}|^2\rangle = \langle|\vec{\lambda}|^2\rangle - \langle|\nabla\tilde{p}|^2\rangle. \tag{5.2}$$

The second term on the right hand side can be rewritten as

$$\langle|\nabla\tilde{p}|^2\rangle = \langle|\frac{\vec{k}}{k^2}(\vec{k}\cdot\vec{\lambda})|^2\rangle = \langle Re(\vec{\lambda}(\vec{k}))^2\cos^2\xi_R\rangle + \langle Im(\vec{\lambda}(\vec{k}))^2\cos^2\xi_I\rangle. \tag{5.3}$$

Here ξ_R denotes the the angle between $\vec{k}$ and $Re(\vec{\lambda}(\vec{k}))$, i.e. the real part of the Lamb vector, and similarly for the imaginary part. Let us assume for the moment that the absolute value of the Lamb vector is statistically independent of its orientation in Fourier space. Let us further assume that the probability distribution functions (pdf) of ξ_R and ξ_I are identical and therefore

$$\langle\cos^2\xi_R\rangle = \langle\cos^2\xi_I\rangle = \langle\cos^2\xi\rangle. \tag{5.4}$$

Then (5.2) can be rewritten as

$$\langle|\vec{\lambda} - \nabla\tilde{p}|^2\rangle \approx \langle|\vec{\lambda}|^2\rangle - \langle|\vec{\lambda}|^2\rangle\langle\cos^2\xi\rangle = \langle\lambda^2\rangle - \langle\sin^2\xi\rangle. \tag{5.5}$$

(We will comment below upon the validity of the assumptions made.) Thus we again arrive at the conclusion that an alignment of the Lamb vector $\vec{\lambda}(\vec{k})$ with the wave vector $\vec{k}$ may lead to a reduction of nonlinearity in turbulent flows.

Numerical data from run SDR indicate that this is indeed the mechanism of the reduction of nonlinearity. In Fig. 5.3 we present the pdf of the cosine of the angle between the real part of $\vec{\lambda}(\vec{k})$ and $\vec{k}$ at times $t = 0$ and $t = 0.9$. Note that the cosine of the angle between

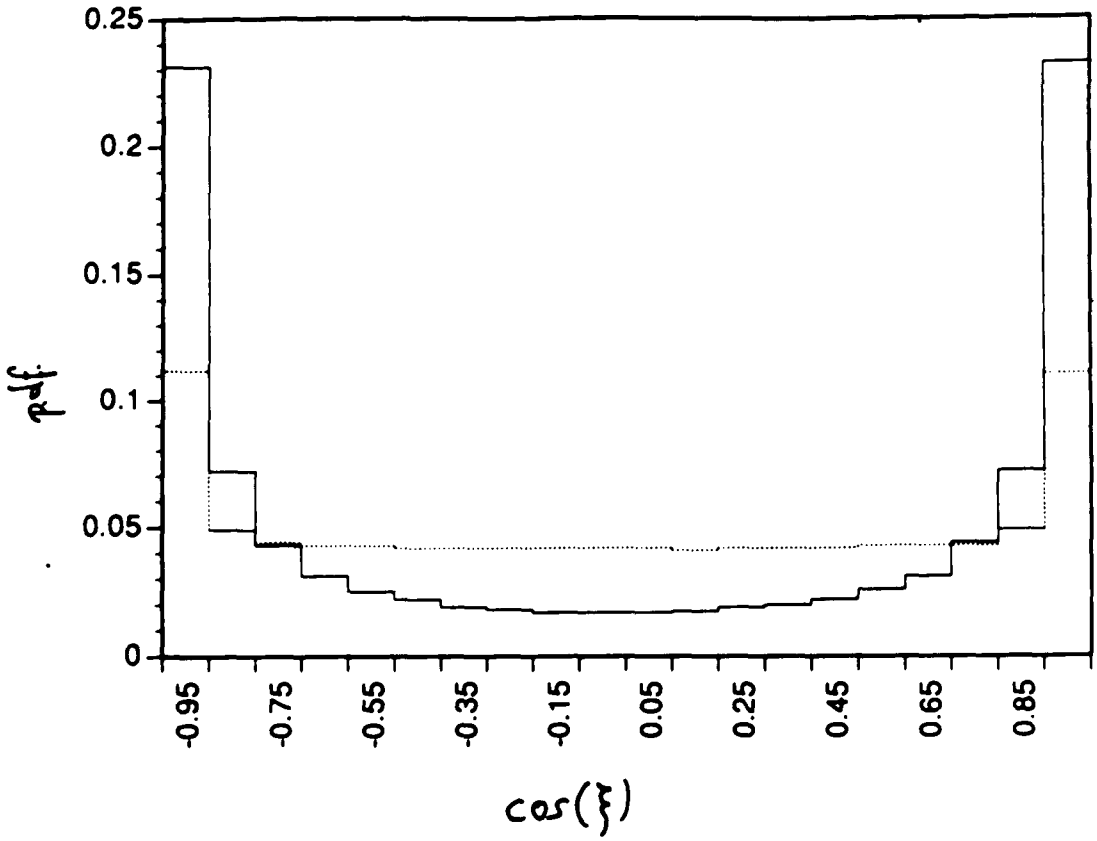

Figure 5.3: Run SDR: distribution of $\cos\xi_R$ at $t = 0$ (dotted line) and $t = 1$ (solid line).

two uncorrelated vector fields in three dimensions would be distributed uniformly. The non-uniform distribution found at $t = 0$ is a consequence of kinematical constraints on homogeneous isotropic Gaussian vector fields (Shtilman & Polifke, 1989, Tsinober, 1989). The enhanced alignment between the Lamb vector and the wave vector at time $t = 1$ is, however, a truly dynamical effect and seems to be the main contributor to the reduction of nonlinearity in a developed turbulent flow.

In physical space this implies that in a developed turbulent flow the mean square $\overline{|\nabla\alpha|^2}$ of the potential part of the Helmholtz decomposition $\vec{\lambda} = \nabla\alpha + \nabla \times \vec{\beta}$ is larger than the mean square of the solenoidal part $\overline{|\nabla \times \vec{\beta}|^2}$ (Tsinober, 1989). In other words (Frisch & Orszag, 1990), a significant part of the nonlinear term is absorbed into the pressure gradient. Recent experimental observations in a wind tunnel by Dracos *et al.* (1990) indicate that the Lamb vector indeed has a significant potential part. Furthermore, the Lamb vector of vortical structures detected by She *et al.* (1990) via numerical flow visualization is strongly divergent. See also work by Speziale (1989), who has shown that only the solenoidal part of the Lamb vector contributes to the energy cascade in turbulence. Further analysis of our simulation fields shows that the strongly non-uniform distribution of $\cos\xi$ develops in remarkably short time. This is illustrated in Fig. 5.3, where the continuous line represents the time evolution of $\langle\cos^2\xi\rangle$ of run SDR. The maximum is reached at $t \approx 0.05$, long before the simulation reaches the developed stage ($t \approx 0.9$) and long before Q experiences a significant drop.

The influence of mean helicity on the distribution of ξ_R (or ξ_I) is somewhat puzzling: initially, $\langle\cos^2\xi_R\rangle = 0.28$ for run *SDM* - less than 1/3! This means that in a maximally helical Gaussian field there is an enhanced probability for the Lamb vector $\vec{\lambda}(\vec{k})$ to be perpendicular to the wave vector $\vec{k}$, in contradiction with the assumption that a depression of nonlinearity should always be accompanied by an alignment of $\vec{\lambda}(\vec{k})$ and $\vec{k}$. During the developing phase of run SDM (dotted line in Fig. 5.3), the Lamb vector again develops the orientation already found in the non-helical case, at time $t = 1$, $\langle\cos^2\xi_R\rangle \approx 0.65$ for both SDR and SDM. We also observed that in flows where the helicity is only slightly less than maximal, the time evolution of relative orientation of $\vec{\lambda}$ is not influenced significantly by the helicity. This is illustrated by the dashed line in Fig. 5.3, which represents $\langle\cos^2\xi_R\rangle$ of

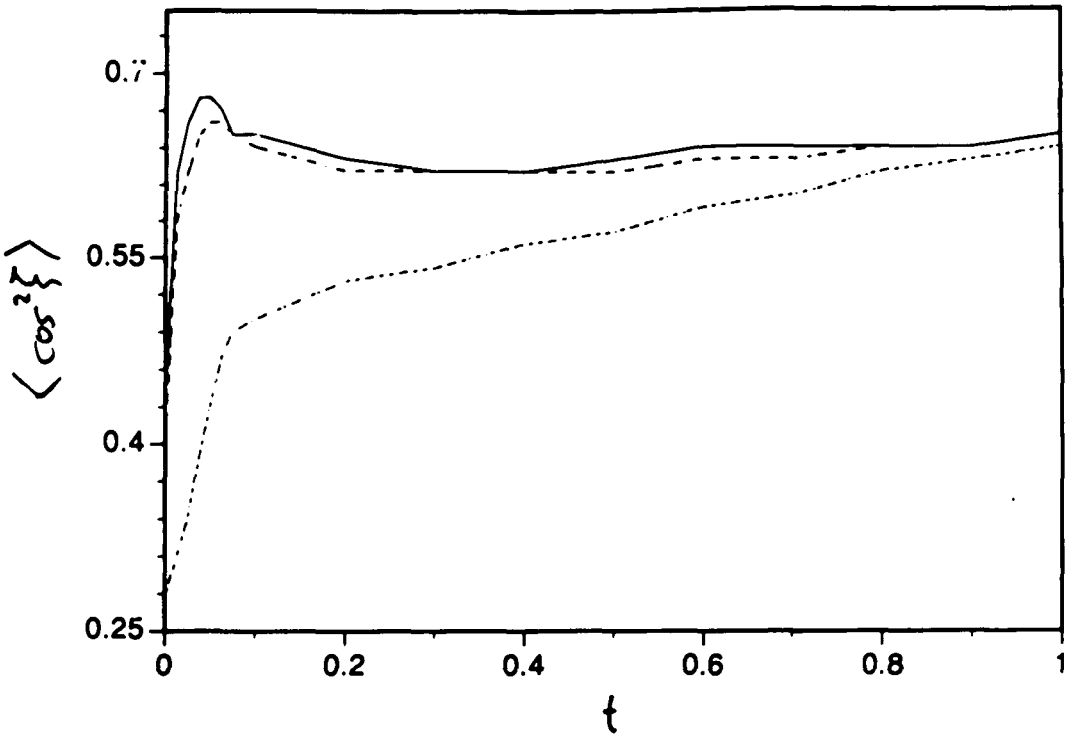

Figure 5.4: Time evolution of $\langle \cos^2 \xi_R \rangle$ in simulations of decaying turbulence that were initialized with random helicity (SDR, solid line), maximal helicity (SDM, dotted line), 80% of maximal helicity (dashed line).

a run with $H_N = 0.78$ at time $t = 0$(other initial parameters are identical to those of SDR and SDM). Note also that at These results indicate that the correlator $\langle Re(\vec{\lambda}(\vec{k}))^2 \cos^2 \xi_R \rangle$ cannot always be approximated by $\langle Re(\vec{\lambda}(\vec{k}))^2 \rangle \langle \cos^2 \xi_R \rangle$. A detailed investigation of the influence of mean helicity, energy spectra, etc., on the orientations of $\vec{\lambda}$ was not carried out and shall be the subject of future work.

In the remainder of this chapter we will present some rather qualitative speculations concerning the possible causes of the reduction of nonlinearity.

We made an observation that suggests that the reduction of nonlinearity is connected with the the build-up of an organized energy cascade from slow and energetic large scales to fast and dissipative small scales. Consider the balance equation for the energy spectrum, (3.17). In a developed turbulent flow the transfer spectrum has a strong negative peak at small wave numbers and is positive at larger k's, see Figs. 3.8 and 3.9. Quite differently, at time $t = 0, T(k,t)$ is fluctuating randomly at all scales; there is obviously no 'organized' transfer of energy between various regions in Fourier space. This is simply a consequence of the statistics of the initial field: third order moments of a Gaussian random variable vanish in the mean. In a numerical simulation that starts from a Gaussian field, the energy transfer quickly becomes ordered, i.e. the energy containing modes ($k < 4$) lose energy ($T(k,t) < 0$), whereas the small scales receive energy. It is remarkable that in run SDR the transfer is already fully developed at time $t = 0.2$ (see Fig. 5.5 and compare with Figs. 3.8 and 3.9). This is also when the distribution of ξ_R seems to attain a stationary state (Fig. 5.4). The developed phase of the simulation (maximum enstrophy Ω and values of the skewness and flatness of velocity derivatives typical of turbulence) are reached much later at time $t = 0.8$.

An observation made by Kraichnan & Panda (1989) lends further support to this hypothesis : In a numerical simulation of a quadratically nonlinear random coupling model ('modified Betchov model', see Leslie, 1973) with zero viscosity and asymmetrical coupling, it was observed that initially the mean square of the nonlinear fluctuations drops to 60% of its corresponding Gaussian value. At this stage of the systems evolution, energy is being transferred from slow, energetic modes to the fast modes, which were not excited initially. Due to the absence of dissipation, a stationary equilibrium state develops at later times,

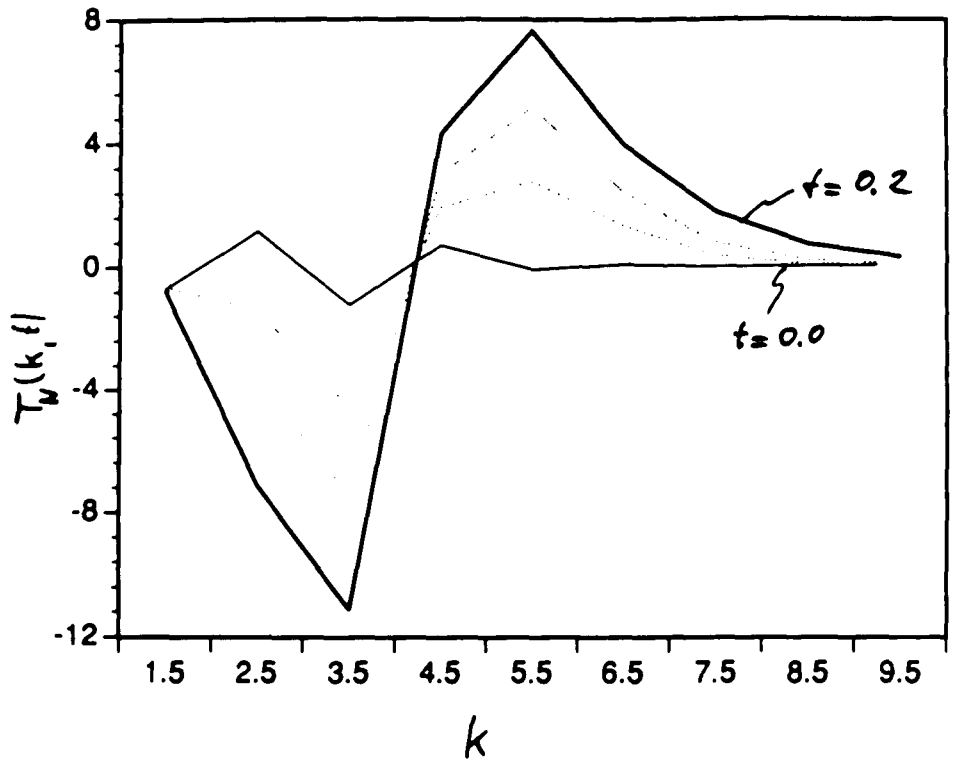

Figure 5.5: Time evolution of the normalized transfer term $T_N(k,t)$ for $k < 10$ in run SDR.

where on the average there is no significant or 'organized' transfer of energy between different modes. At that time, the nonlinear fluctuations return to their Gaussian level.

These speculations imply that turbulence does possess intrinsic 'structure' at inertial-range scales, namely it organizes itself in such a way as to favor a cascade of energy towards the dissipating scales. It is not yet known what the structures are that are formed in the process, it is likely they may not be identified with 'coherent structures' known from experimental flow visualization in inhomogeneous flows. Possible candidates for turbulent structures are self-similar hierarchies of stretching and folding vortex lines or unstable vortex sheets, which have been considered by several authors (see, e.g., Moffatt (1987) and references therein). As already remarked above, flow visualizations from direct numerical simulations of decaying isotropic turbulence have shown that highly intermittent vortical fine-scale structures do exist in homogeneous turbulence (She *et al.* , 1990), and one may argue that such structures favor an alignment of velocity and vorticity, and a Lamb vector with a predominantly potential part. We admit though that these ideas are at present merely speculations based on intuition rather than careful analysis, and in much need of further study.

Two senses are emerging for nonlinear*:*
the first is the classic hit-the-ceiling meaning;
the second a deliberate rejection of reasonableness.

William Safire, New York Times Magazin (1990)

Chapter 6

Entangledness of Vortex Lines in Turbulent Flows

The structure or 'topology' of the vorticity field of turbulent flows has attracted considerable interest in recent years ; see for example Hussain (1986), Kida (1989), Levich (1983,1987), Moffatt (1985), Sagdeev *et al.* (1986) and the proceedings of the recent IUTAM Symposium on 'Topological Fluid Mechanics' (Moffatt & Tsinober, 1990). In this study we will discuss the properties and possible usefulness of an analytical measure of the local 'entangledness' - rather than the global 'knottedness' - of vortex lines. Moreau (1961), Moffatt (1969), Arnol'd (1974) and Berger & Field (1984) have shown that the total helicity $H = \int_D \vec{v}\cdot\vec{\omega}dV$ of a localized vorticity distribution ($\vec{\omega}\cdot\hat{n}|_{\partial D} = 0$, where $\hat{n}$ is the unit normal to the surface of the domain D) is associated with the topological structure of the vorticity field $\vec{\omega} = \nabla \times \vec{v}$, i.e., the knots, twists and kinks of vortex lines and vortex tubes. The invariance of total helicity H for Euler flows can be understood as a manifestation of the fact that in inviscid flows the vortex lines move with the fluid and consequently their linkage properties are conserved.

Although a continuous flow field may be identified in a very natural manner with a topological transformation (Moffatt, 1990), one must realize that the global topology of velocity or vorticity fields is not necessarily of interest to turbulence researchers. If one pictures a turbulent flow as a tangle of interwoven vortex lines, one would like to know, e.g., whether turbulent activity is concentrated at locations where the vortex lines are closely entwined or 'entangled'. Unfortunately, it is not trivial to relate intuitive notions

of 'entangledness' with topology. Imagine, e.g., that the sketches in Figs. 6.1 represent snapshots of vortex lines in turbulent flow. The vortex lines in these Figures have the same topology, i.e. they are not linked, nevertheless we would certainly expect to find very different flow dynamics. Similarly, the linkage properties of open field structures $\vec{\omega}\cdot\hat{n}|_{\partial D} \neq 0$ depend on the field configurations outside of the volume of consideration, they are not invariant under topological transformations, see Fig. 6.2., and they cannot be probed by the integral of helicity. This is reflected by the broken gauge-invariance of the helicity H of open domains: adding the gradient of a scalar field χ to the velocity, $\vec{v} \rightarrow \vec{v} + \nabla\chi$, changes the total helicity by an amount δH

$$\delta H = \int_D \nabla\chi \cdot \vec{\omega} dV = \int_{\partial D} \chi\vec{\omega} \cdot \hat{n}\, dA \tag{6.1}$$

In general, δH will not vanish if vortex lines cross the surface ∂D of the domain D. The vorticity field $\vec{\omega}$ and the linkage properties of the vortex lines, however, are obviously invariant under such gauge-transformations. Note that Galilean transformations and advection-effects by large scale eddies may be regarded as two important examples of gauge-transformations. Clearly, helicity H cannot be a meaningful measure of the local entangledness of vortex lines.

6.1 Analytical Measures of Entangledness

Drawing on ideas originally developed in biology for the study of DNA structure (Fuller, 1978), Berger & Field (1984) have argued that although there exists no absolute measure of knottedness for open field structures, it should be possible to define a topologically meaningful and gauge-invariant relative measure of topological complexity. We shall briefly recall the work of Berger & Field.

Let space V (periodic or unbounded) be divided into two simply connected regions D and $\bar{D}$ (the complement of D). For the case of unbounded volume we assume that all surface integrals 'at infinity' vanish. Consider two vorticity fields $\vec{\omega}^{(i)}, i = 1,2$, and the corresponding velocity fields $\vec{v}^{(i)}, \vec{\omega}^{(i)} = \nabla \times \vec{v}^{(i)}$. Outside of D the two vorticity fields are identical. We assume that the velocity fields $\vec{v}^{(i)}$ are solenoidal and continuous (C^0), the normal components of both velocity and vorticity across the boundary ∂D shall be

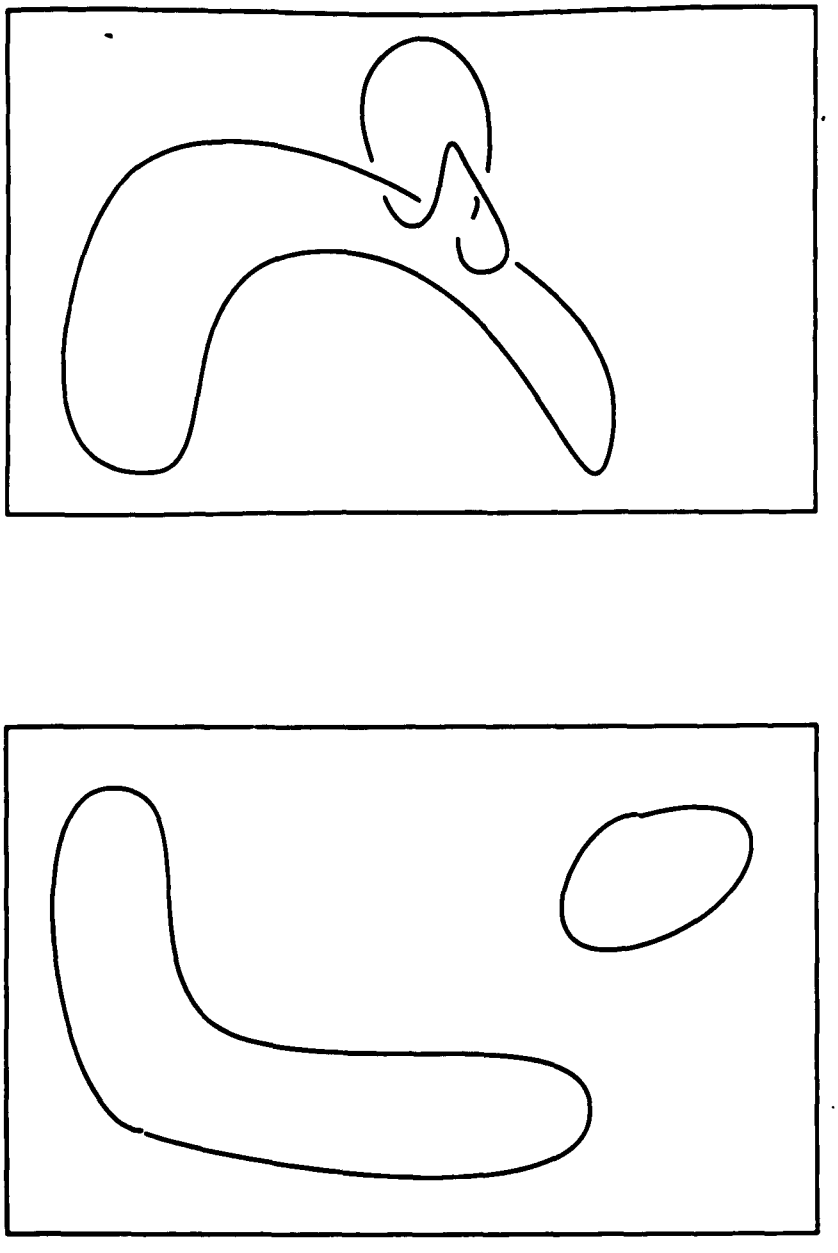

Figure 6.1: 'Vortex lines' with identical topology and different entangledness.

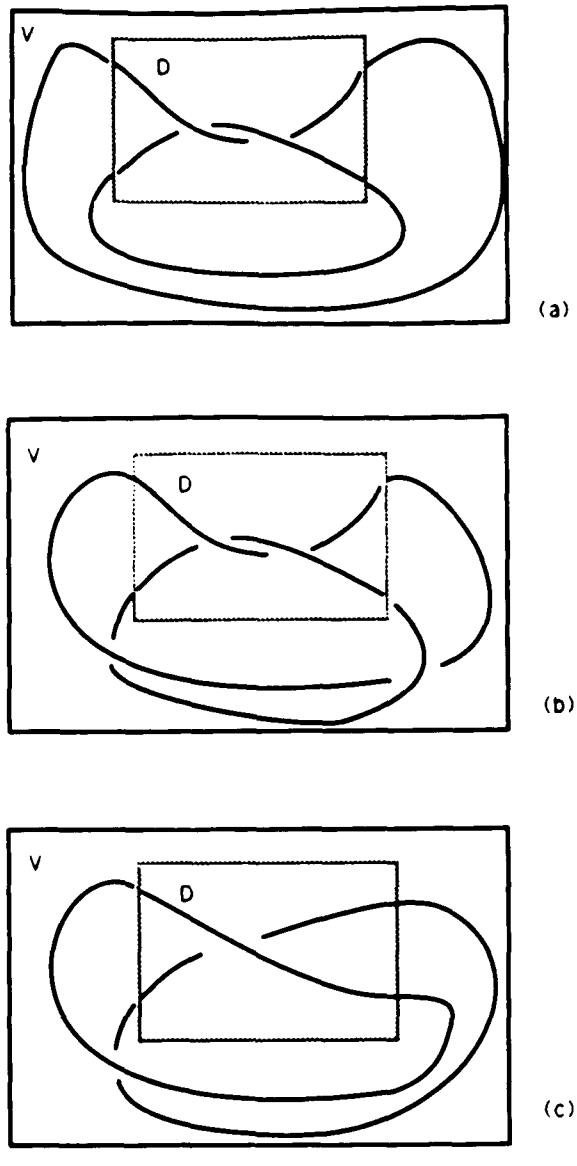

Figure 6.2: Vortex lines that are equally entangled in an open domain may have different topologies (see (a) and (b)); a topological transformation may change the entangledness of open domains (see (b) and (c)).

continuous . Berger & Field have shown that the difference $\Delta H = H^{(1)} - H^{(2)}$ of total helicities $H^{(i)} = \int_V \vec{\omega}^{(i)} \cdot \vec{v}^{(i)} dV$ depends only on the vorticity fields inside D. Rewrite

$$\Delta H = \int_V (\vec{v}^{(1)} - \vec{v}^{(2)}) \cdot (\vec{\omega}^{(1)} + \vec{\omega}^{(2)}) dV + \int_V (\vec{v}^{(2)} \cdot \vec{\omega}^{(1)} - \vec{v}^{(1)} \cdot \vec{\omega}^{(2)}) dV. \qquad (6.2)$$

The second integral vanishes after an integration by parts. Note that $\nabla \times \vec{v}^{(1)} = \nabla \times \vec{v}^{(2)}$ in $\bar{D}$, therefore outside D $\vec{v}^{(1)} - \vec{v}^{(2)} = \nabla \zeta$ for some scalar ζ . Let us separate the first integral into contributions from D and $\bar{D}$:

$$\Delta H = \int_D (\vec{v}^{(1)} - \vec{v}^{(2)}) \cdot (\vec{\omega}^{(1)} + \vec{\omega}^{(2)}) dV + \int_{\bar{D}} \nabla \zeta \cdot (\vec{\omega}^{(1)} + \vec{\omega}^{(2)}) dV \qquad (6.3)$$

$$= \int_D (\vec{v}^{(1)} - \vec{v}^{(2)}) \cdot (\vec{\omega}^{(1)} + \vec{\omega}^{(2)}) dV - \int_{\partial D} \zeta (\vec{\omega}^{(1)} + \vec{\omega}^{(2)}) \cdot \hat{n} \, dA \qquad (6.4)$$

Expressing the velocities as a functional of the vorticities with the help of the Green's function ,

$$\vec{v}^{(1)} - \vec{v}^{(2)} = \nabla \times \frac{1}{4\pi} \int_D \frac{\vec{\omega}^{(1)} - \vec{\omega}^{(2)}}{r} d\vec{r} \qquad (6.5)$$

we see that $\vec{v}^{(1)} - \vec{v}^{(2)}$ and ζ and therefore also the difference ΔH in total helicities depend only on the vorticity fields inside D. Berger & Field also show that ΔH is gauge-invariant and thus argue that ΔH can be a meaningful measure of the topological complexity of the vorticity field $\vec{\omega}$ relative to an appropriate reference field $\vec{\omega}'$. The most suitable reference field is a potential field $\vec{\omega}' = \nabla \phi$ inside D, where ϕ is the harmonic function $\nabla^2 \phi = 0$, uniquely determined by the Neumann boundary conditions $\nabla \phi \cdot \hat{n}|_{\partial D} = \vec{\omega} \cdot \hat{n}|_{\partial D}$. Note that the boundary conditions imply that ϕ is a pseudo-scalar. The potential field is the minimum enstrophy field for given boundary conditions and it is natural to assume that it is in some sense topologically simplest. Constructing $\vec{\omega}'$ with a standard Poisson solver is a straightforward numerical task. Note, however, that the evaluation of the vectorpotential $\vec{v}'$ poses a formidable computational problem.

An alternative method of investigating the topological structure of open vortex tangles with the help of a potential reference field $\vec{\omega}' = \nabla \phi$ was developed by Kuz'min & Patashinsky (1985). Here a test field $\tilde{\vec{\omega}} = \vec{\omega} - \vec{\omega}'$ is set up in a spherical subdomain D, $\vec{\omega}'$ being again the gradient of a (pseudo-) scalar ϕ , which is the solution of the appropriate Neumann problem. It is pointed out that $\vec{\omega}'$ does not contain any information about the structure of the vorticity field inside D, as it is completely determined by the vorticity field at the

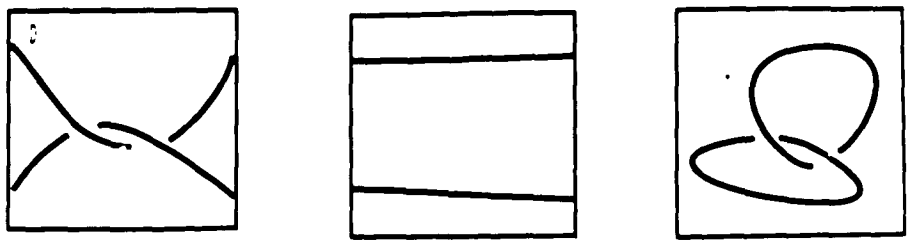

Figure 6.3:Vorticity Field $\vec{\omega}$ Reference Field $\vec{\omega}'$ Test field $\tilde{\vec{\omega}}$

boundary ∂D. Kuz'min & Patashinsky then proceed to discuss the set of moments of $\tilde{\vec{\omega}}$, defined as

$$M^{(n)}_{i_1 \ldots i_n}(\vec{x}) = \int_D r_{i_1} r_{i_2} \ldots r_{i_{(n-1)}} \tilde{\omega}_{i_n}(\vec{x} + \vec{r}) d\vec{r} \tag{6.6}$$

and suggest that a comparison of field configurations by their moments will provide a classification scheme for coherent structures. Note that the test field $\tilde{\vec{\omega}}$ forms a localized vortex tangle, as the field lines of $\tilde{\vec{\omega}}$ do not cross the boundary of D. The entangledness of the vorticity field $\vec{\omega}$ will be reflected in the linkage of the field lines of the test field $\tilde{\vec{\omega}}$, see Fig. 6.3 for a schematic illustration. Therefore, the helicity $\tilde{H} = \int_D \tilde{\vec{v}} \cdot \tilde{\vec{\omega}} dV$ of the test field should provide an alternative measure of entangledness. The boundary conditions for $\vec{\omega}'$ ensure that $\tilde{H}$ is invariant under a gauge-transformation $\vec{v} \rightarrow \vec{v} + \nabla\chi$:

$$\delta\tilde{H} = \int_D \nabla\chi \cdot \tilde{\vec{\omega}} dV = \int_{\partial D} \chi(\vec{\omega} - \vec{\omega}') \cdot \hat{n}\, dA = 0 \tag{6.7}$$

The helicity of the test field $\tilde{H}$ - like the difference of total helicities ΔH - reduces to the usual integral of helicity for closed vortex structures, the potential reference field of which is identically zero. However, $\tilde{H}$ is in general not equal to ΔH (see below).

It was then proposed by Levich (1987), that a relative helicity H_R

$$H_R = \int_D \vec{v} \cdot \tilde{\vec{\omega}} dV \tag{6.8}$$

would as well serve as a measure of relative entangledness. The test field $\tilde{\vec{\omega}}$ is defined as above, which ensures gauge invariance. For computational purposes it is most advantageous that the evaluation of the relative helicity H_R does not require the knowledge of the

vectorpotential $\vec{v}'$ of the reference field $\vec{\omega}'$. However, it is not clear what the topological significance of H_R really is. Obviously, $\tilde{H} = H_R - \delta$, where $\delta = \int_D \vec{v}' \cdot \tilde{\vec{\omega}} dV$. Similarly, by dividing the domain of integration and regrouping the integrands we rewrite the difference ΔH of total helicities as

$$\Delta H = \int_V (\vec{v}^{(1)} \cdot \vec{\omega}^{(1)} - \vec{v}^{(2)} \cdot \vec{\omega}^{(2)}) dV = \tag{6.9}$$

$$= \int_D \vec{v}^{(1)} \cdot (\vec{\omega}^{(1)} - \vec{\omega}^{(2)}) dV + \int_D (\vec{v}^{(1)} - \vec{v}^{(2)}) \cdot \vec{\omega}^{(2)} dV + \int_D (\vec{v}^{(1)} - \vec{v}^{(2)}) \cdot \vec{\omega} dV.$$

Recall that $\vec{\omega}^{(1)} = \vec{\omega}$ in V , $\vec{\omega}^{(2)} = \begin{cases} \vec{\omega} & \text{in } \bar{D} \\ \vec{\omega}' & \text{in } D \end{cases}$. After an integration by parts we obtain

$$\Delta H = H_R + \int_D \vec{v}' \cdot \tilde{\vec{\omega}} dV \tag{6.10}$$

We see that $\tilde{H} + \delta = H_R = \Delta H - \delta$. Unfortunately, the difference term $\delta = \int_D \vec{v}' \cdot \tilde{\vec{\omega}} dV$ will in general not vanish (see the Appendix).

We argue, however, that because both $\tilde{H}$ and ΔH are reasonable measures of relative entangledness, and $\nabla^2 \vec{v}' = 0$ inside D, δ should be insignificant for most field configurations. This in turn implies that H_R may also serve as a measure of the local entangledness of vortex lines.

It seems that 'relative measures of entangledness' can be defined in a rather arbitrary fashion, given that they are gauge invariant and reduce to the integral of helicity for closed field structures. But of course, 'entangledness' as such is an intuitive notion and not mathematically well defined. Unlike the linkage properties of closed vortex lines, local 'entangledness' is not topologically invariant, and it will not be conserved for Euler flows. It is therefore perfectly acceptable that several measures of (relative) entangledness can be constructed. We hope that such measures will provide at least qualitative information about the local structure of the vorticity field. One must realize, however, that vortex line configurations may exist that are considerably entangled but have little or no (relative) helicity (Incidentally, we do not expect the inverse to be possible). Moffatt (1981) , for example, has pointed out that a Boromean ring configuration of vortex lines, although certainly 'entangled', has zero helicity. Yet simpler, cancellations due to left- and righthanded tangles cohabitant in one domain can also result in small values of helicity in regions where the

vorticity field is considerably entangled. This does not render (relative) helicity useless as a measure of topological structure, remember that topological invariants provide in general only partial information about topological characteristics.

6.2 Numerical Results

We have investigated whether relative helicity H_R does correspond to the local entangledness of vortex lines in an analysis of turbulent velocity fields obtained from direct numerical simulations. We will present mostly results from two velocity fields : field HIE24 from a simulation of decaying homogeneous isotropic turbulence by Lee (1985) , and field C128U12 from a simulation of shear driven turbulence by Rogers (1986). Both simulations were performed on a 128^3 computational grid, the Taylor microscale Reynolds number R_λ was approximately equal to 80. The vorticity field $\vec{\omega}$ is computed from the velocity fields in Fourier space. When transforming back to physical space, the fields are (Fourier-) interpolated to a 256^3 computational grid. This is done to allow the computation of the potential reference field $\vec{\omega}' = \nabla\phi$ with satisfactory numerical accuracy. Note that in the shear flow case the mean vorticity due to the homogeneous shear is subtracted from the vorticity field. A standard Helmholtz solver is used to solve the Neumann problem for ϕ in cubical subdomains of varying sizes N_D. The potential vorticity $\vec{\omega}'$ is computed from ϕ with a second order finite difference scheme. This approach yields satisfactory precision in the calculation of the relative helicity H_R for domain sizes N_D of about 10^3 and greater. Furthermore, the fields of turbulent dissipation $\epsilon = 2e_{ij}e_{ij}$, vortex stretching $\sigma = e_{ij}e_{jk}e_{ki}$ and enstrophy production $\rho = \omega_i e_{ij}\omega_j$ are evaluated. Einstein summation is implied here, and $e_{ij} = \frac{1}{2}(\partial_j v_i + \partial_i v_j)$ is the stress tensor.

As the turbulent fields under study are homogeneous, it is initially not known where regions of high relative helicity are to be found. In order to locate such regions, we position a large number N_S (typically several thousand) of test-domains of a given size N_D inside the flow domain. For each domain, the total and relative helicities H and H_R and the volume integrals over the domain $E_D, \Omega_D, \epsilon_D, \sigma_D, \rho_D$ of turbulent energy, enstrophy, dissipation, vortex stretching and enstrophy production are evaluated.

We then attempt to visualize the structure of the vorticity field by 3-D plots of vortex

lines in domains where we expect to find very high (or low) topological complexity, as indicated by the 'topological charge' $T_C = H_R/\sqrt{E_D \Omega_D}$ (Levich, 1987), i.e. the appropriately normalized value of H_R. A second order Runge-Kutta scheme is employed to integrate the vortex lines. The starting points for the integration of vortex lines were chosen to be the maxima of enstrophy in planes parallel to the y- and z-axis at various x-positions (and cyclic permutations of the axes). Then the integration advances in forward and reverse direction from the starting point until the vortex line reaches the domain boundary. Vortex lines are only plotted if the maximum of enstrophy does not lie on the boundary and if the average line strength is equal to or greater than the average vorticity inside D. It is found that although the vorticity field of these homogeneous flows is everywhere quite complicated, the vorticity field indeed tends to be more entangled in regions of high topological charge. For example, Figs. ?? and ?? show 3-D perspective plots of two domains with $N_D = 24^3$ which had the maximum topological charge T_C in a sample of 4096 domains taken from field HIE24. The two domains with lowest T_C from that sample are shown in Figs. ?? and ?? . However, beginning the vortex line integration at a fixed set of starting points, rather than at the extrema of vorticity, yields plots that appear to be equally entangled no matter what the relative helicity is. Discarding vortex lines of lesser strength brings little improvement. Clearly, a more detailed and sophisticated graphical representation of the vorticity field is called for. It might also be instructive to look at the structure of the reference field $\vec{\omega}'$ and the test field $\tilde{\vec{\omega}}$.

Another important question is whether high topological complexity T_C is mostly to be found in the active or inactive regions of turbulent flows. The relatively large number of domains sampled from each flow makes it possible to conduct a coarse statistical analysis. We have evaluated the linear correlation coefficient r(X,Y), defined as

$$r(X,Y) = \frac{\langle X - \langle X \rangle \rangle \langle Y - \langle Y \rangle \rangle}{\sqrt{\langle (X - \langle X \rangle)^2 \rangle \langle (Y - \langle Y \rangle)^2 \rangle}} \tag{6.11}$$

for various pairs of domain parameters. Angular brackets (...) denote averaging over the sample of domains. The correlation coefficient is normalized to lie in the interval $[-1, +1]$, where the extrema correspond to complete positive or negative correlation. The results presented in Table 6.1 show that relative helicity H_R correlates slightly - but statistically significantly - with ϵ , σ and ρ , i.e., with the active regions of the flow.

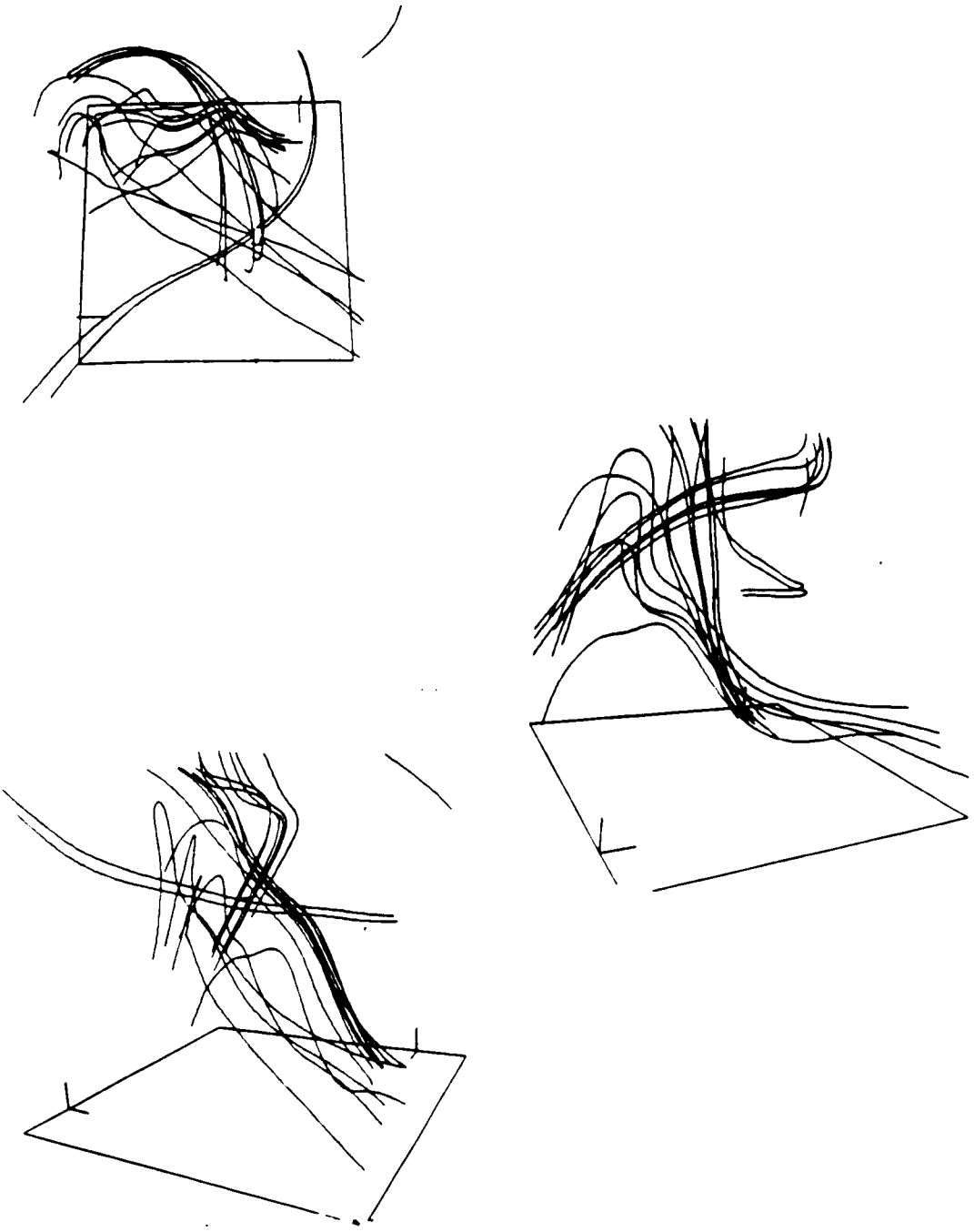

Figure 6.4: 3-D plot of region with high T_C

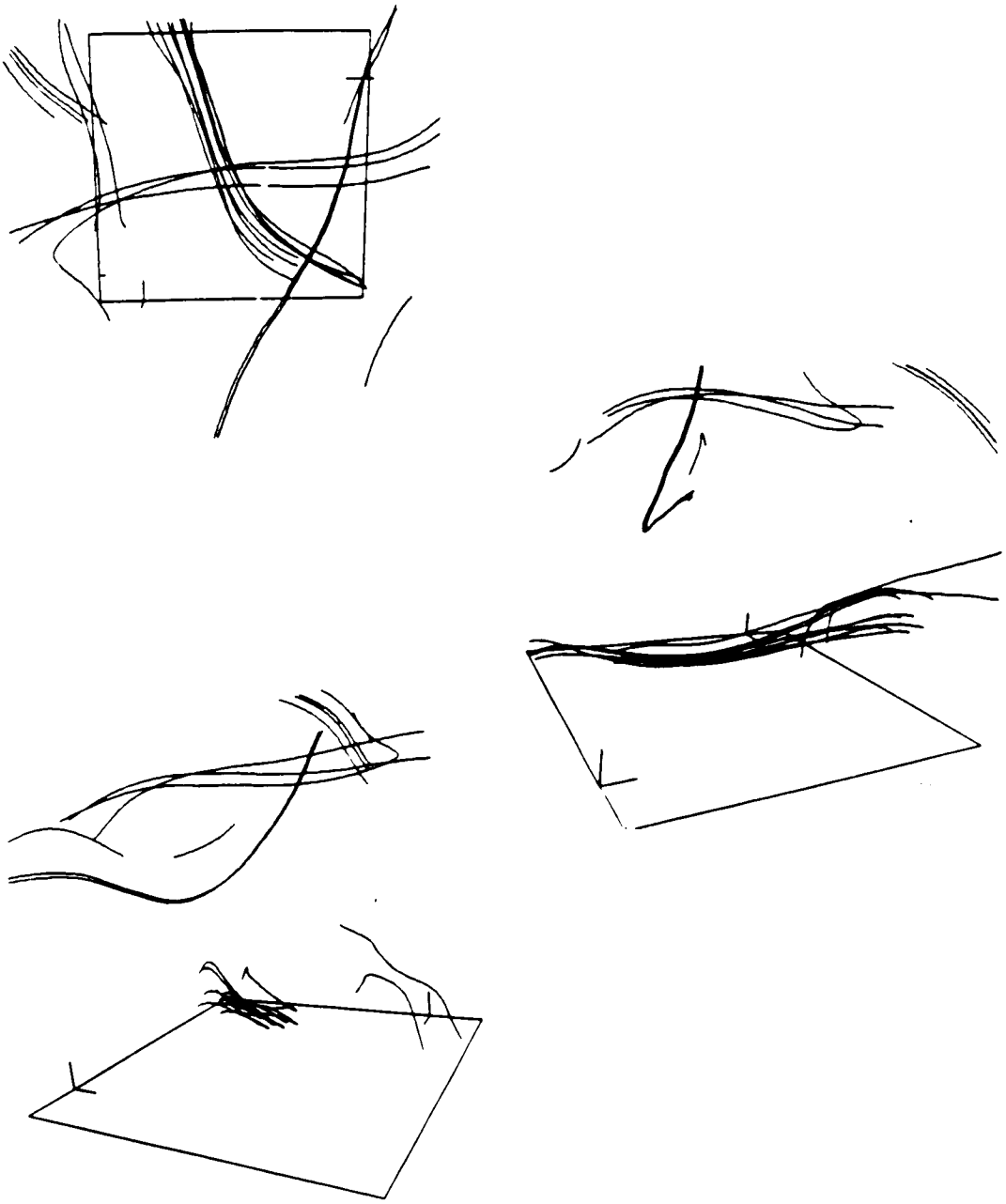

Figure 6.5: 3-D plot of region with high T_C

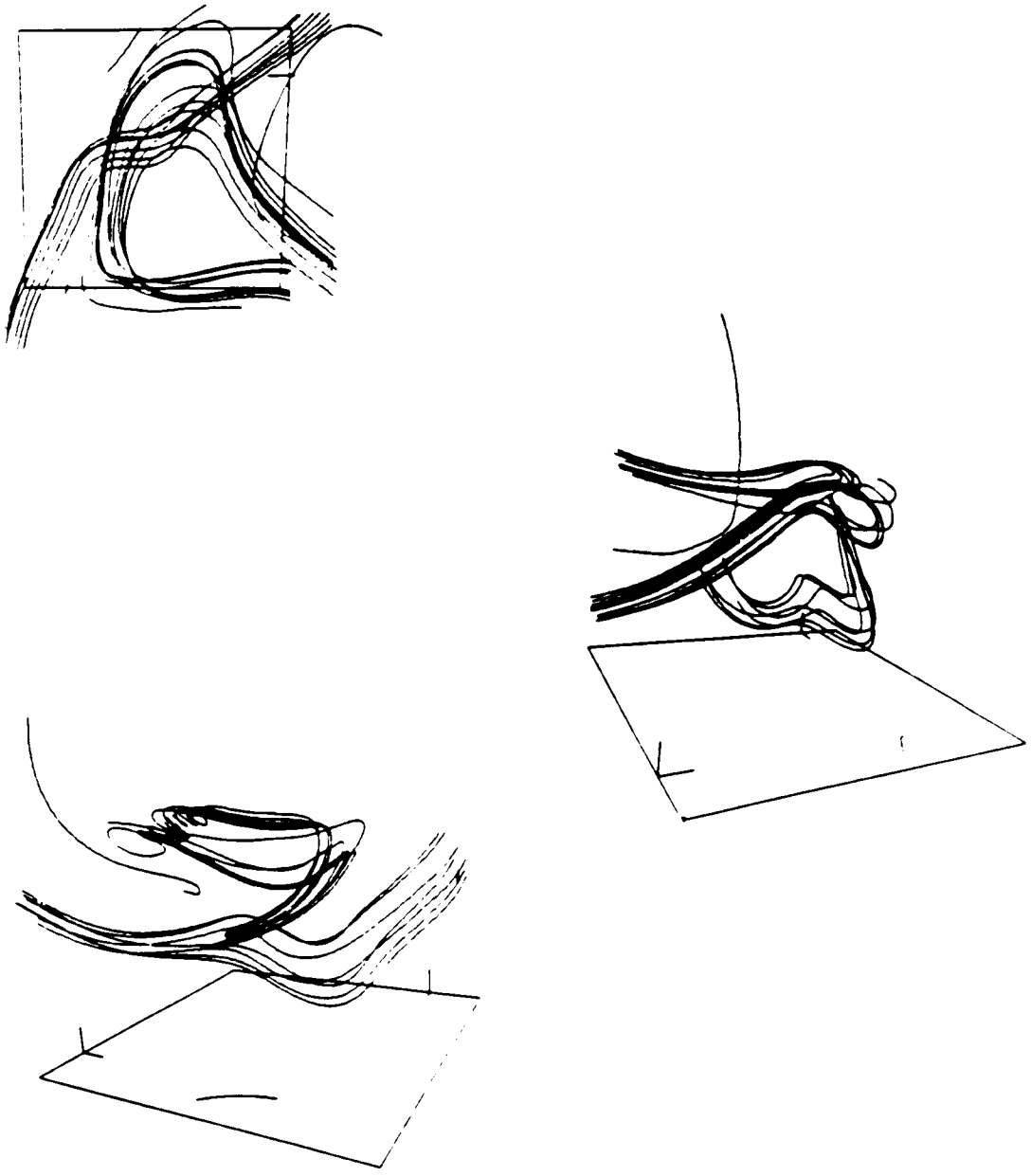

Figure 6.6: 3-D plot of region with low T_C

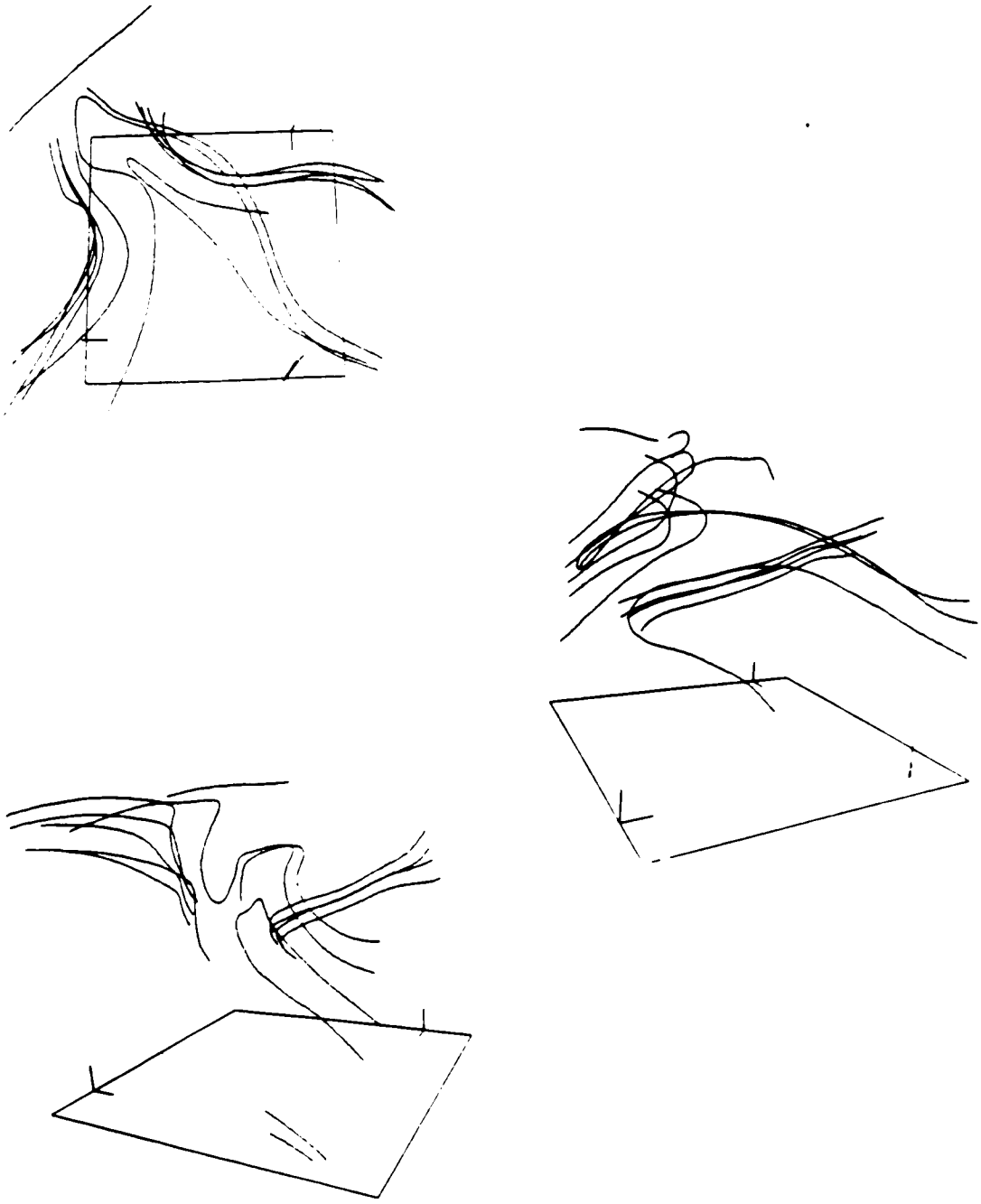

Figure 6.7: 3-D plot of region with low T_C

Field	N_S	N_D	$r\langle T^2{}_C, \epsilon\rangle$	$r\langle T^2{}_C, \rho\rangle$	$r\langle T^2{}_C, \sigma\rangle$
HIE24	8000	12^3	0.20	0.17	-0.13
	4096	24^3	0.14	0.09	-0.09
C128U12	6859	12^3	0.16	0.13	-0.13
	1728	20^3	0.19	0.16	-0.17

Table 6.1: Statistical correlations between entangledness and turbulent activity

It is appropriate to use the square of T_C , for otherwise symmetry between left- and righthanded tangles would obscure all correlations with quantities that are expected to be insensitive to handedness. For domain sizes larger than $N_D = 24$, the correlations weaken and become insignificant for N_D approximately equal to 60. This presumably indicates that taking the volume integrals over larger domains that contain both active and inactive regions amounts to a pre-averaging that destroys all statistical correlations. We have also gathered statistics from the initial field of the shear flow simulation and from a field from a simulation at lower Reynoldsnumber (C12 in Lee (1985), $R_\lambda \approx 20$). In both cases, no correlations were found. This was expected for the initial field, which is merely an amplitude field of uncorrelated modes without any structure. The absence of correlations between T_C and the active regions in the low Reynolds number case suggests that here viscous diffusion of vorticity is too strong to permit the existence of sufficiently well- defined and localized vortex tubes. It will be worthwhile to analyze turbulent flows at yet higher Reynolds number, once these come into reach of direct numerical simulation. No statistically significant correlations between the usual helicity and dissipation and vortex stretching or enstrophy production have been found. This is in agreement with results obtained by Rogers & Moin (1987). To further illustrate this point, we present in Figs. ?? and ?? contour plots of the normalized joint probability distribution function P_{NJ} = pdf(T_C, ϵ) / (pdf(T_C) pdf(ϵ)) obtained from a sample of 8000 domains with $N_D = 12^3$ from field HIE24. The normalization was chosen such that for uncorrelated quantities P_{NJ} is unity, the difference between contour lines equals 0.2. Statistical fluctuations are very strong, because the number of sample domains is too small to adequately represent the long tails in the probability distribution function of dissipation. Nevertheless, in Fig. ?? one can discern a region of $P_{NJ} > 1.2$ for low dissipation (note that the peak of the pdf of dissipation lies at $\epsilon \sim 5$) and low topological

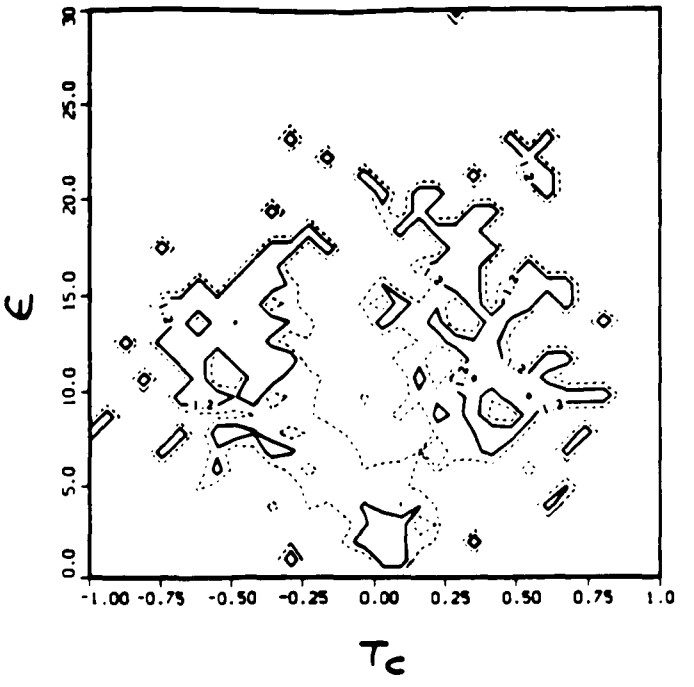

Figure 6.8: Normalized joint pdf of T_C vs. ϵ

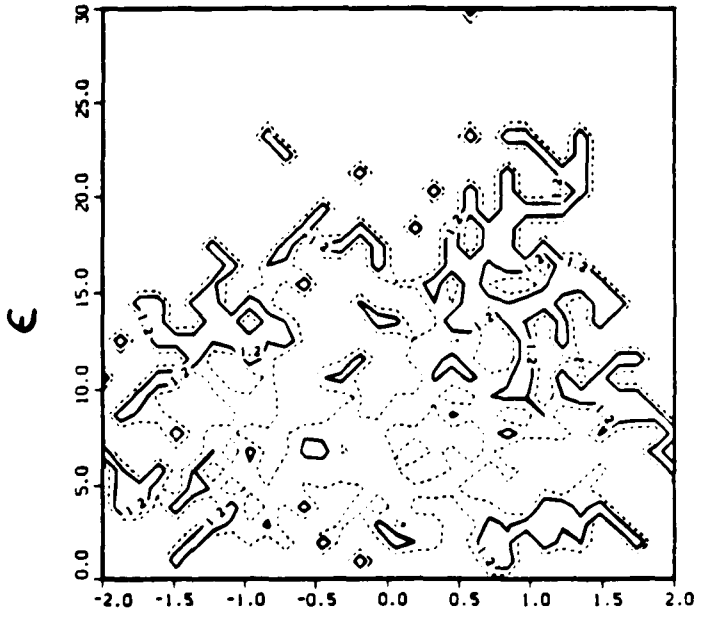

Figure 6.9: Normalized joint pdf of $H_D(E_D\Omega_D)^{-1/2}$ vs. ϵ.

charge. Correspondingly, there is a slight preference for T_C to be large where dissipation is high. The contour plot with the usual helicity, Fig. ??, apparently shows only statistical noise.

6.3 Conclusions

We have argued that relative helicity $H_R = \int_D \vec{v} \cdot (\vec{\omega} - \vec{\omega}')dV$ may serve as a measure of the 'local entangledness' of the vorticity $\vec{\omega}$ in a domain D relative to a potential reference field $\vec{\omega}'$. The gauge-invariance of H_R and the fact that the reference field is completely determined by the vorticity at the boundary of the domainimplies that the value of H_R depends only on the vorticity inside D. Analyzing vorticity fields obtained from direct numerical simulations of homogeneous turbulent flows, we have found that the vortex lines indeed appear to be more entangled in regions of high relative helicity. However, more sophisticated flow visualization techniques than the ones accessible to us are required to make this claim more convincing.

Slight (but statistically significant!) correlations between H_R and turbulent dissipation, vortex stretching and enstrophy production have been observed. We have argued that correlations with entangledness as such might be stronger, because we may assume that there are regions with small relative helicity but considerable entangledness. It is remarkable that high entangledness seems to be found preferentially in regions where turbulent dissipation is high. We emphasize that this is not in contradiction with the results presented in Chapter 3, where it was reported that viscous dissipation is reduced in decaying turbulent flows with strong mean helicity. The primary effect of mean helicity is a reduction of the energy transfer towards the smaller (dissipative) scales, which then leads – as a secondary effect – to reduced dissipation. This does not imply that there should be a (local) correlation between the helicity density γ and viscous dissipation. Similarly for the relative helicity H_R, which should be thought of as a 'probe' testing the entangledness of vortex lines in small regions. Because of the contribution of the reference field $\vec{\omega}'$, the relative helicity of small test-domains cannot be related in a direct way to the nonlinear terms of the Navier Stokes equation, and therefore has no a priori dynamical significance. However, it is intuitively plausible that dissipation and turbulent activity should in general be found in regions where

the vortex lines are entangled, because we imagine that strong gradients of velocity exist in those regions.

It has been suggested that localized vortex tangles with long life times ('topological solitons') may exist in turbulence and give rise to coherent structures (Levich, 1983, Sagdeev *et al.* , 1986). This concept is clearly not supported by our observations, which indicate that vortex tangles are not long-lived. Instead, our work is in agreement with Hussain (1986) and Levich (1987), who argued that vortical coherent structures should have comparatively short live times. Admittedly though, at present the numerical evidence is weak and not unambiguous. It is hoped that simulations at higher Reynolds number, where the vortex lines and -tubes are more localized, will allow to clarify the situation.

Her knots disorder'd and her wholesome herbs
swarming with caterpillars.

William Shakespeare, King Richard II. (1594)

6.4 Appendix

Here we shall present the proof given by Frenkel (1989) that the difference term $\delta = \int_D \vec{v}' \cdot \vec{\omega} dV$ is in general to zero.

We begin by assuming that $\delta = 0$. Then for any vorticity field $\vec{\omega}^{(1)}$ we may construct the appropriate reference field $\vec{\omega}'$ and its vectorpotential $\vec{v}'$, *uniquely determined by the normal component of vorticity at the boundary.* We may define for any scalar χ a vector field $\vec{\eta} = \vec{v}' - \nabla\chi$. By assumption

$$\int_D \vec{\eta} \cdot (\vec{\omega}^{(1)} - \vec{\omega}')dV = \delta^{(1)} + \int_{\partial D} \chi(\vec{\omega}^{(1)} - \vec{\omega}') \cdot \hat{n} dV = 0 \tag{6.12}$$

In particular, we may choose χ such that $\nabla\chi \cdot \hat{n}|_{\partial D} = \vec{v}' \cdot \hat{n}|_{\partial D}$. Once again, this is a well-defined Neumann problem with a unique solution. Now let us construct a 'vorticity field' $\vec{\omega}^{(2)} = \begin{cases} \vec{\omega}^{(1)} + \vec{\eta} & \text{in } \bar{D} \\ \vec{\omega}^{(1)} & \text{in } D \end{cases}$. (Strictly speaking, invariance properties require that $\vec{\eta}$ be multiplied with a pseudoscalar of an absolute value of 1, e.g. $\hat{x} \cdot (\hat{y} \times \hat{z})$. We omit this term for simplicity of notation.) Because $\vec{\eta} \cdot \hat{n}|_{\partial D} = 0$, the reference field for $\vec{\omega}^{(2)}$ is the same as the one for $\vec{\omega}^{(1)}$. By assumption,

$$\delta^{(2)} = \int_D \vec{v}' \cdot (\vec{\omega}^{(2)} - \vec{\omega}')\, dV = 0 \tag{6.13}$$

and also

$$\int_D \vec{\eta} \cdot (\vec{\omega}^{(2)} - \vec{\omega}')\, dV = 0 \tag{6.14}$$

This implies that

$$\int_D \vec{\eta} \cdot (\vec{\omega}^{(1)} + \vec{\eta} - \vec{\omega}')\, dV = \int_D |\vec{\eta}|^2\, dV = 0 \tag{6.15}$$

which requires that $\vec{\eta} \equiv 0$. However, $\nabla \times \vec{\eta} = \nabla \times (\vec{v}' - \nabla\chi) = \vec{\omega}' \neq 0$, therefore our assumption that $\delta = 0$ cannot be true in general .

q.e.d

References

[1] ADRAIN, R.J., Linking correlation and structure: stochastic estimation and conditional avearging. *Zoran P. Zarić Memorial International Seminar on Near-Wall Turbulence*, Dubrovnik, Yugoslavia, (1988)

[2] ANDRÉ, J.C. & LESIEUR, M., Influence of helicity on the evolution of isotropic turbulence at high Reynolds number. *J. Fluid Mech.* **81**, 187 (1977)

[3] AREF, H., The numerical experiment in fluid mechanics.
J. Fluid Mech. **173**, 15 (1986)

[4] ARNOL'D, V.I., The asymptotic Hopf invariant and its applications. *Proc. Summer School in Differential Equations*, Erewan, Armenian SSR Acad. Sci.
English translation in *Sel. Math. Sov.* **5**, 327 (1886)

[5] BATCHELOR, G.K., *The Theory of Homogeneous turbulence.*
Cambridge University Press (Cambridge, 1953)

[6] BERGER, M.A. & FIELD, G.B., The topological properties of magnetic helicity.
J. Fluid Mech. **147**, 133 (1984)

[7] BETCHOV, R., Semi-isotropic turbulence and helicoidal flows.
Phys. Fluids **4**, 925 (1961)

[8] BINDER, K. & YOUNG, A.P, Spin glasses: experimental facts, theoretical concepts, and open questions. *Rev. Mod. Phys.* **58(4)**, 801 (1986)

[9] BRISSAUD, A., FRISCH, U., LEORAT, J., LESIEUR, M. & MAZURE, A., Helicity cascades in fully developed isotropic turbulence. *Phys. Fluids* **16**, 1366 (1973)

[10] BUNEMAN, O., Vector FFT for the CRAY-2.
Buffer, publ. by NMFECC, **13(7)**, 7 (1989)

[11] CANTWELL, B.J., Organized motion in turbulent flows.
Ann. Rev. Fluid Mech. **13**, 457 (1981)

[12] CANUTO, C., HUSSAINI, M.Y., QUARTERONI, A., ZANG, T.A., *Spectral methods in fluid dynamics*, Springer Verlag (New York, 1988)

[13] CHEN, S. & KRAICHNAN, R.H., Sweeping decorrelation in isotropic turbulence. *Phys. Fluids A* **1**, 2019 (1989)

[14] DOMARADZKI, J.A., Analysis of energy transfer in direct numerical simulations of isotropic turbulence. *Phys. Fluids* **31**, 2747 (1988)

[15] DRACOS, T., KHOLMYANSKY, M., KIT, E., & TSINOBER, A., Some experimental results on velocity-vorticity measurements in turbulent grid flows.
Topological Fluid Mechanics. eds. H.K. Moffatt & A. Tsinober, Cambridge University Press (Cambridge, 1990)

[16] ESWARAN, V. & POPE, S. B., Direct numerical simulation of the turbulent mixing of a passive scalar. *Phys. Fluids* **31**, 506 (1988)

[17] FRISCH, U., POUQUET, A., LEORAT, J. & MAZURE, A., Possibility of an inverse cascade of magnetic helicity in magnetohydrodynamic turbulence.
J. Fluid Mech. **68**, 769 (1975)

[18] FRENKEL, A., private communication, (1989)

[19] FRENKEL,A., & LIPSCOMBE, T.C., New statistical invariants for homogeneous turbulence. *Phys. Lett. A* **137**, 51 (1989)

[20] FRISCH, U, & ORSZAG, S.A., *Physics Today* (January,1990)

[21] FRISCH, U., SULEM, P. L., Numerical simulation of the inverse cascade in two-dimensional turbulence. *Phys. Fluids* **27**, 1921 (1984)

[22] FRISCH, U., SHE, Z.S., & THUAL, O., Viscoelastic behaviour of cellular solutions to the Kuramoto-Sivashinsky model. *J. Fluid Mech.* **168**, 221 (1986)

[23] FULLER, F.B., Decomposition of the linking number of a closed ribbon: a problem from molecular biology. *Proc. Natl. Acad. Sci.* **75**,3557 (1987)

[24] HEISENBERG, W., Zur statistischen Theorie der Turbulenz. *Z. Phys.* **124**, 628 (1948)

[25] HUSSAIN, F., Coherent structures and turbulence. *J. Fluid Mech.* **173**, 303 (1986)

[26] KERR, R.M., Higher order derivative correlations and the alignment of small-scale structures in isotropic numerical turbulence. *J. Fluid Mech.* **153**, 31 (1985)

[27] KERR, R.M., Histograms of helicity and strain in numerical turbulence. *Phys. Rev. Lett.* **59**, 783 (1987)

[28] KERR, R.M., Simulations with helical initial conditions. Preprint, unpublished (1987)

[29] KIT, E., TSINOBER, A., BALINT, J.L., WALLACE, J.M. & LEVICH, E., An experimental study of helicity related properties of a turbulent flow past a grid. *Phys. Fluids* **30**, 3323 (1987)

[30] KIT, E., LEVICH, E., SHTILMAN, L. & TSINOBER, A., Coherence and symmetry breaking in turbulence: theory and experiment. *PCH* **10**, (615)1988

[31] KIDA, S., TAKAOKA, M. & HUSSAIN, F., Reconnection of two vortex rings. *Phys. Fluids A* **1**, 630 (1989)

[32] KRAICHNAN, R.H., The structure of isotropic turbulence at very high Reynolds numbers. *J. Fluid Mech.* **5**, 497 (1959)

[33] KRAICHNAN, R.H., Inertial ranges in two-dimensional turbulence. *Phys. Fluids* **10**, 1417 (1967)

[34] KRAICHNAN, R.H., Helical turbulence and absolute equilibrium. *J. Fluid Mech.* **59**, 745 (1973)

[35] KRAICHNAN, R.H., Eulerian and Lagrangian renormalization in turbulence theory. *J. Fluid Mech.* **83**, 349 (1977)

[36] KRAICHNAN, R.H. & PANDA, R., Depression of nonlinearity in decaying isotropic turbulence. *Phys. Fluids* **31**, 2395 (1988)

[37] KRAICHNAN, R.H., private communication, (1989)

[38] KUZ'MIN, G.A. & PATASHINSKY, A.Z., Order parameters of turbulent flows. *Phys. Lett. A* **113**, 266 (1985)

[39] LANDAHL, M.T. & MOLLO-CHRISTENSEN, E., *Turbulence and random processes in fluid mechanics* Cambridge University Press (Cambridge, 1986)

[40] LANDAU, L. D. & LIFSHITZ, E. M., *Fluid Mechanics.* 2nd Edition, Pergamon Press (Oxford, 1986)

[41] LAMB, H., *Hydrodynamics.* Dover (New York, 1945)

[42] LAUTENSCHLAGER, M., EPPEL, D.P. & THACKER, W.C., Subgrid-parameterization in helical flows *Beitr. Phys. Atmosph.* **61**, 87 (1988)

[43] LEE, M.J., Ph. D. dissertation, Stanford University,(1985)

[44] LESLIE, D.C., *Developments in the theory of turbulence.* Clarendon Press (Oxford, 1973)

[45] LEVICH, E., The soliton structures in three-dimensional turbulent flows. *Ann.New York Acad. Sci.* **404**, 73 (1983)

[46] LEVICH, E., Certain problems in the theory of developed hydrodynamical turbulence *Phys. Rep.* **151**, 120 (1987)

[47] LEVICH, E. & TSINOBER, A. On the role of helical structures in three- dimensional turbulent flow. *Phys. Lett. A* **93**, 293 (1983)

[48] LEVICH, E. & TSINOBER, A. Helical structures, fractal dimensions and renormalization-group approaches in homogeneous turbulence. *Phys. Lett. A* **96**, 292 (1983)

[49] LEVICH, E. & TSVETKOV, E. Helical inverse cascade in three-dimensional turbulence as a fundamental dominant mechanism in mesoscale atmospheric phenomena. *Phys. Rep.* **128**, 1 (1985)

[50] LEVICH, E. & SHTILMAN, L. Coherence and large fluctuations of helicity in homogeneous turbulence. *Phys. Lett. A* **126**, 243 (1988)

[51] LEVICH, E. Anomalous helicity fluctuations and coherence in turbulence: Theory and experiment. *Topological Fluid Mechanics.* eds. H.K. Moffatt & A. Tsinober, Cambridge University Press (Cambridge, 1990)

[52] LILLY, D.K., The structure, energetics and propagation of rotating convective storms. *J. Atmos. Sci.* **43**, 113 (1986)

[53] MENEVEAU, C. & SREENIVASAN, K. R., The multifractal spectrum of the dissipation field in turbulent flows. *Nuclear Physics B* **2**, 49 (1987)

[54] MOFFATT, H.K., The degree of knottedness of tangled vortex lines. *J. Fluid Mech.* **35**, 117 (1969)

[55] MOFFATT, H.K., Developments in the theory of turbulence. *J. Fluid Mech.* **106**, 27 (1981)

[56] MOFFATT, H.K., Magnetostatic equilibria and analogous Euler flows of arbitrarily complex topology. *J. Fluid Mech.* **159**, 359 (1985)

[57] MOFFATT, H.K., Geophysical and astrophysical turbulence. *Advances in Turbulence*, eds. G. Comte-Bellot & J. Mathieu Springer Verlag (Berlin, 1987).

[58] MOFFATT, H.K., & TSINOBER, A., *Topological Fluid Mechanics.* Cambridge University Press (Cambridge, 1990)

[59] MOIN, P. *Studying turbulence using numerical simulation databases.* Proceedings of the 1987 Summer Program, Center for Turbulence Research, (1987)

[60] MOIN, P. *Studying turbulence using numerical simulation databases.* Proceedings of the 1988 Summer Program, Center for Turbulence Research, (1988)

[61] MONIN, A.S. & YAGLOM, A.M., *Statistical Fluid Mechanics.* MIT Press (1971,1975)

[62] MOREAU, J.J., Constantes d'un ilot tourbillonaire en fluide parfait barotrope. *C.R. Acad. Sci.*, **252**, 2810 (1961)

[63] ORSZAG, S.A., Analytical theories of turbulence, *J. Fluid Mech.* **41**, 363 (1970)

[64] ORSZAG, S.A., Numerical simulation of incompressible flows within simple boundaries. I. Galerkin (spectral) representations. *Stud. Appl. Math.* **L**, 293 (1971)

[65] ORSZAG, S.A., Lectures on the statistical theory of turbulence. *Fluid Dynamics*, eds. R. Balian & J.L. Peube, Gordon & Breach (London, 1977)

[66] PANDA, R., SONNAD, V., CLEMENTI, E., ORSZAG, S.A. & YAKHOT, V. Turbulence in a randomly stirred fluid. *Phys. Fluids A* **1**, 1045 (1989)

[67] PATTERSON, G.S. & ORSZAG, S.A., Spectral calculations of isotropic turbulence: Efficient removal of aliasing interactions. *Phys. Fluids* **14**, 2538 (1)971

[68] PELZ, R.B., YAKHOT,V., ORSZAG, S.A., SHTILMAN, L., & LEVICH, E., Velocity-vorticity patterns in turbulent flow. *Phys. Rev. Lett.* **54**, 2505 (1985)

[69] PELZ, R.B., SHTILMAN, L., & TSINOBER, A., The helical nature of unforced turbulent flows. *Phys. Fluids* **29**, 3506 (1986)

[70] POLIFKE, W. & LEVICH, E., Entangledness of vortex lines in turbulent flows. *Topological Fluid Mechanics.* eds. H.K. Moffatt & A. TSINOBER, Cambridge University Press (Cambridge, 1990)

[71] POLIFKE, W. & SHTILMAN, L., The dynamics of helical decaying turbulence. *Phys. Fluids A* **1**, 2025 (1989)

[72] POLIFKE, W. & SHTILMAN, L., Reduction of nonlinearity and energy cascade in helical and non-helical turbulent flows. *Topological Fluid Mechanics.* eds. H.K. Moffatt & A. Tsinober, Cambridge University Press (Cambridge, 1990)

[73] PRESS, W.H., FLANNERY, B.P., TEUKOLSKY, S.A., & VETTERLING, W.T., *Numerical Recipes.* Cambridge University Press (Cambridge, 1986)

[74] ROGALLO, R.S., Numerical Experiments in Homogeneous Turbulence. *NASA Technical Memorandum 81315* (1981)

[75] ROGALLO, R.S., private communication. (1988)

[76] ROGALLO, R.S., & MOIN, P., Numerical simulation of turbulent flows. *Ann. Rev. Fluid Mech.* **16**, 99 (1984)

[77] ROGERS,M.M., Ph.D. dissertation, Stanford University (1986)

[78] ROGERS, M.M. & MOIN, P., Helicity fluctuations in incompressible turbulent flows. *Phys. Fluids* **30**, 2662 (1987)

[79] SAGDEEV, R.Z. , MOISEEV, S.S. , TUR, A.V. & YANOVSKII. V.V., Theory of strong turbulence and topological solitons. in *Nonlinear Phenomena in Plasma Physics & Hydrodynamics* Mir (Moscow, 1986)

[80] SANTANGELO, P., BENZI, R., LEGRAS, B., The generation of vortices in high resolution two-dimensional decaying turbulence and the influence of initial conditions on the breaking of self-similarity. *Phys. Fluids A* **1**, 1027 (1989)

[81] SHE, Z.S., JACKSON,E., & ORSZAG, S.A., Intermittent Vortex Structures in homogeneous isotropic turbulence. to be published in *Nature* (1990)

[82] SHTILMAN, L., LEVICH, E., ORSZAG, S.A., PELZ, R.B., & TSINOBER A., On the role of helicity in complex fluid flows. *Phys. Lett. A* **113**, 32 (1985)

[83] SHTILMAN, L., PELZ, R.B., & TSINOBER, A., Numerical investigation of helicity in turbulent flows. *Computers in Fluids* **16**, (341)1988

[84] SHTILMAN, L. & POLIFKE, W., On the mechanism of the suppression of nonlinearity in the incompressible Navier-Stokes equation. *Phys. Fluids A* **1**, 778 (1989)

[85] SHTILMAN, L. & POLIFKE, W., Reduction of nonlinearity and energy cascade in helical an non-helical turbulent flows. *Topological Fluid Mechanics.* eds. H.K. Moffatt & A. Tsinober, Cambridge University Press (Cambridge, 1990)

[86] SPEZIALE, C.G., On helicity fluctuations in turbulence.
Quart. Appl. Math. **45**, 123 (1987)

[87] SPEZIALE, C.G., On helicity fluctuations and the energy cascade in turbulence. *Recent advances in engineering science*, Lecture notes in engineering ,**39**, 10, eds. S.L. Koh & C.G. Speziale (1989)

[88] STANIŠIĆ, M.M., *The mathematical theory of turbulence.*
2nd Edition, Springer Verlag (New York, 1988)

[89] TENNEKES, H. & LUMLEY, J.L. *A first course in turbulence.*
MIT Press (Cambridge, 1972)

[90] TENNEKES, H., Eulerian and Lagrangian time microscales in isotropic turbulence. *J. Fluid Mech.* **67**, 561 (1975)

[91] TSINOBER, A. & LEVICH, E. On the helical nature of three-dimensional coherent structures in turbulent flows. *Phys. Lett. A* **99**, 321 (1983)

[92] TSINOBER, A., On one property of the Lamb vector in isotropic turbulent flow. *Phys. Fluids A* **2**, 484 (1990)

[93] WALLACE, J. M., & BALINT, J. L., An experimental study of helicity and related properties in helical and non-helical turbulent flows. *Topological Fluid Mechanics.* eds. H.K. Moffatt & A. Tsinober, Cambridge University Press (Cambridge, 1990)